Quarterly Reviews of Biophysics **41**, 3/4 (2008), pp. 205–264. © 2008 Cambridge University Press
doi:10.1017/S003358350800472l Printed in the United States of America

Interactions of surfactants with lipid membranes

Heiko Heerklotz*

Leslie Dan Faculty of Pharmacy, University of Toronto, Toronto, ON, Canada M5S 3M2

Abstract. Surfactants are surface-active, amphiphilic compounds that are water-soluble in the micro- to millimolar range, and self-assemble to form micelles or other aggregates above a critical concentration. This definition comprises synthetic detergents as well as amphiphilic peptides and lipopeptides, bile salts and many other compounds. This paper reviews the biophysics of the interactions of surfactants with membranes of insoluble, naturally occurring lipids. It discusses structural, thermodynamic and kinetic aspects of membrane–water partitioning, changes in membrane properties induced by surfactants, membrane solubilisation to micelles and other phases formed by lipid–surfactant systems. Each section defines and derives key parameters, mentions experimental methods for their measurement and compiles and discusses published data. Additionally, a brief overview is given of surfactant-like effects in biological systems, technical applications of surfactants that involve membrane interactions, and surfactant-based protocols to study biological membranes.

1. Scope and introduction 206

2. Membrane–water partitioning 208
2.1 Partition coefficients and isotherms: overview 208
2.2 Ideal mixing 209
2.3 Non-ideal mixing 211
2.4 Electrostatic effects 214
2.5 Kinetic aspects 215
2.6 Methods for measuring partition coefficients 216
2.7 Experimental values of partition coefficients 217

3. Surfactant-induced changes in membrane properties 225
3.1 Bilayer couple concept of asymmetric bilayer expansion 225
3.2 Monolayer curvature strain 225
3.3 Surfactants forming complexes and mixing favourably with lipids 228
3.4 Surfactant-induced 'melting' of gel and ℓo phases 228
3.5 Detergent-induced formation or promotion of ℓo domains 230
3.6 Membrane permeabilisation 231

4. Solubilisation, reconstitution, non-lamellar phases 233
4.1 The three-stage model 233
4.2 Aggregate structures observed upon solubilisation and reconstitution of fluid membranes 233
4.3 Thermodynamics of fluid membrane solubilisation 235
4.4 Solubilisation in systems comprising multiple lipids or surfactants 237

* H. Heerklotz, Leslie Dan Faculty of Pharmacy, University of Toronto, 144 College St., Toronto, ON, Canada M5S 3M2.
Tel.: +1-416-978-1188; Fax: +1-416-978-8511; Email: heiko.heerklotz@utoronto.ca

https://doi.org/10.1017/S0033583508004721 Published online by Cambridge University Press

4.5 Direct solubilisation of gel and ℓo membranes 239
4.6 Kinetics of solubilisation and reconstitution 239
4.7 Methods of detecting solubilisation 240
4.8 Effects governing the solubilisation of fluid membranes 241
4.9 Transitions involving type II phases 242
4.10 Lyotropic phase behaviour 242
4.11 Lipid-induced transitions of micellar structures 243

5. Applications and biological relevance of surfactant–membrane interactions 244
5.1 Biological effects of surfactants on membranes 244
5.2 Medical and cosmetic applications of surfactants 246
5.3 Use of surfactants for the isolation and investigation of membrane proteins 247
5.4 Study of detergent-resistant membrane fractions 248

6. Prospects 249

7. Symbols and abbreviations 250

8. Acknowledgements 253

9. References 253

1. Scope and introduction

This paper is aimed at reviewing the knowledge of interactions of surfactants with lipid membranes. The term surfactant is used here for surface-active, soluble amphiphiles (Small, 1970). These are molecules reducing the surface tension of water by forming a monolayer at the air–water interface. They possess an aqueous solubility (critical micelle or aggregation concentration) in the micro- or millimolar range above which they self-associate to micelles, bilayer vesicles or other aggregates. Surfactants include synthetic detergents, physiological compounds such as bile salts, lysolipids and certain amphiphilic peptides and other amphiphiles. 'Lipids' here refers to virtually insoluble phospholipids found in biological membranes.

The interactions discussed in this paper play an important role in a vast field, including the regulation of cellular processes, the activity and delivery of drugs, biochemical techniques for membrane studies, digesting food and washing dishes. The main aim of this paper is to provide a general, yet detailed basis of the models and parameters describing such systems, filling also the gap between general physical chemistry textbooks and specific research articles.

Pioneering studies in the field of surfactant–lipid interactions (e.g. Helenius & Simons, 1975; Ribeiro & Dennis, 1975; Alonso *et al.* 1981; Kresheck & Nimsgern, 1983; Lichtenberg *et al.* 1983; Lichtenberg, 1985; Schurtenberger *et al.* 1985; Small, 1986; Ollivon *et al.* 1988) have provided a sound basis.

Details require some careful attention to physical chemistry, but it is amazing how much qualitative and even semi-quantitative insight can already be obtained according to the simple logics of a pizza service: Quasi-triangular slices come from round pizzas; slices from small pizzas are more conical and have a higher proportion of outer crust than large ones. Rectangular slices come from rectangular pizzas. From the effective shape of the surfactant, in particular the lateral area required by the head group and the volume filled by the chain, one can immediately make a qualified guess which aggregate structure it forms (Fig. 1); a quantitative expression is given by

https://doi.org/10.1017/S0033583508004721 Published online by Cambridge University Press

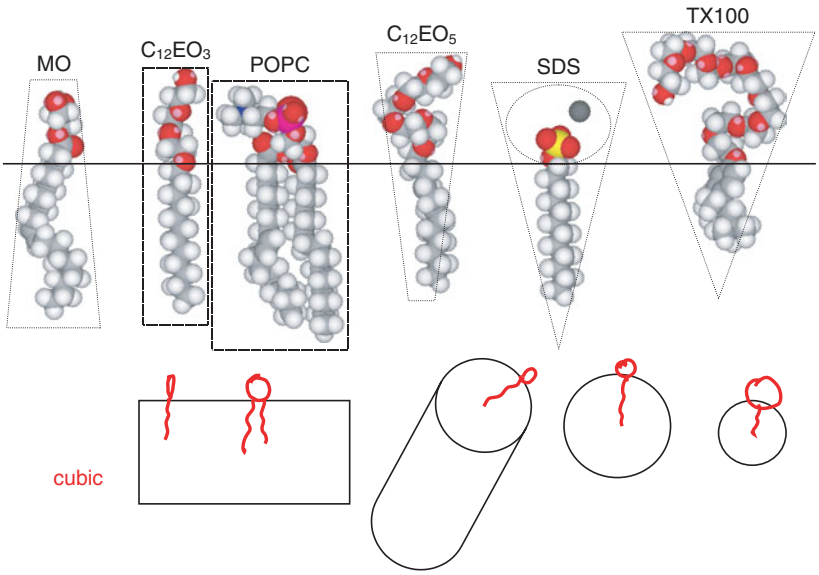

Fig. 1. Semi-schematic representations of the structures and 'effective shapes' of a series of surfactants and a lipid, POPC. From the left to the right, molecules have a negative (MO, monoolein), about zero ($C_{12}EO_3$, POPC) and increasingly positive spontaneous curvature at 25 °C. In accord with this, they form aggregates with increasingly positive curved surfaces: inverse hexagonal (no example shown), cubic, lamellar, cylindrical micellar and spherical micellar. See list of symbols for full names.

Israelachvili's (1991) simple, yet powerful concept of packing parameters. What goes beyond pizza logics is that the effective shape is not always obvious; an example shown in Fig. 1 is SDS, which has a small head group when van der Waals radii are concerned but a large effective head group size in pure SDS micelles because the negatively charged sulphates cannot be fully dehydrated and packed directly together. Hence, the effective shape of SDS depends also on salt concentration and, in mixtures, on the nature of the lipid or co-surfactant. Another problem is that there are effective shapes requiring a mean curvature that cannot be practically realised by any principal aggregate topology because there are gaps between the mean interfacial curvatures for stable spheres, cylinders, lamellae and cubic/inverse phases. Instead, the molecules have to undergo elastic deformations upon association (Helfrich, 1973; Andelman *et al.* 1994). This is considered by the concept of real *versus* spontaneous curvature (Section 3.2).

Another key concept of surfactant–lipid systems has been to treat different aggregate structures (and monomers in solution) as separate pseudo-phases. This provides the basis for the famous three-stage model (Helenius & Simons, 1975; Lichtenberg, 1985) comprising lamellar, lamellar + micellar and micellar ranges (aggregates are in equilibrium with surfactant monomers, respectively). Again, it is surprising how well this simple approximation describes the thermodynamic behaviour of many systems, and again, the challenge is in the detail: Which of the many structural intermediates and components belong to the lamellar and which to the micellar family (see Section 4)?

After Lasch's (1995) review and the excellent special journal issue edited by Alonso and Goñi (2000), the phenomenon of DRMs has arisen as one major new focus in lipid–detergent research. Generally, a major aim of recent and current investigations has been the extension of the established, quantitative models to more complex systems.

https://doi.org/10.1017/S0033583508004721 Published online by Cambridge University Press

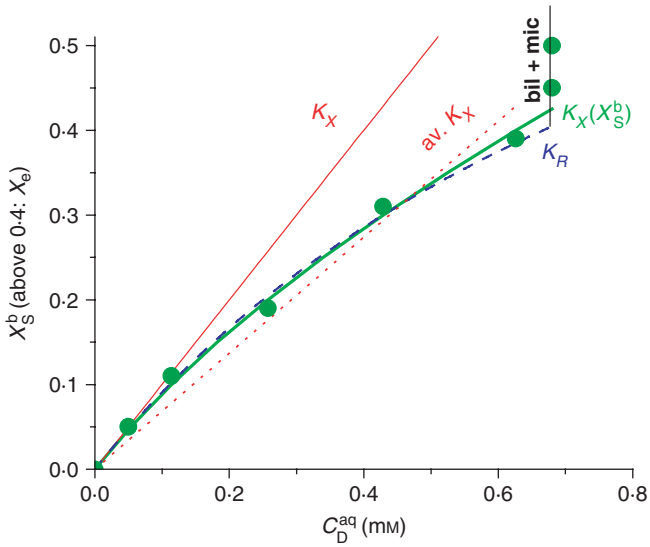

Fig. 2. Schematic illustration of a partitioning isotherm of a surfactant into lipid vesicles. The spheres represent arbitrary but typical data points, and the lines were generated with different models as follows: thin red line: $\tilde{K}_X = 1$ mM^{-1}, Eq. (6), identical with $K_X = 55\,500$, Eq. (5); red dotted line: average $\tilde{K}_X = 0{\cdot}68$ mM^{-1}; bold green line: $\tilde{K}_X(X_S^b)$ analogously to Eq. (21) with $\tilde{K}_X(0) = 1$ mM^{-1} and $\rho^0 = -0{\cdot}7RT$; dashed blue line: $K_R = 1$ mM^{-1} according to Eq. (10). The partitioning isotherms end at the onset of solubilisation at $C_{Saq,\,sat} = 0{\cdot}68$ mM, as implied by the vertical increase of the 'bound' mole fraction [that is now X_e, Eq. (34), and no longer X_S^b] at constant C_S^{aq} (see line marked 'bil + mic').

Nevertheless, substantial further efforts will be required to understand the functions of surfactant-like biomolecules and to optimise the numerous biomedical, cosmetic and technical applications of surfactants in a rational manner. Section 5 gives a superficial overview of some of these topics, each being a vast field in itself. Considerable progress in these scientifically, medically and economically highly important fields will depend crucially on understanding surfactant effects.

2. Membrane–water partitioning

2.1 Partition coefficients and isotherms: overview

Up to a certain surfactant concentration (for substantial lipid concentrations, this is well above the CMC), there are no micelles but the surfactant molecules partition between the membrane and the aqueous solution. Distinguishing surfactant molecules that are incorporated in a membrane from those in aqueous solution is a key requirement for virtually all surfactant–lipid studies, and data disregarding partitioning are very limited in their applicability. The large number of different definitions and models and different characteristics of pertinent methods might be confusing at first glance; Section 2 aims at shedding light on this issue.

One way to illustrate the membrane–water partitioning of a solute is to plot a partition isotherm showing the mole fraction of the solute in the membrane (X_S^b) as a function of the aqueous surfactant concentration (C_S^{aq}) that is in equilibrium with this mixed membrane at a given temperature. The isotherm is usually modelled in terms of a partition coefficient (and, if required, an activity coefficient). Let us, for the sake of illustration, consider the spheres in Fig. 2,

https://doi.org/10.1017/S0033583508004721 Published online by Cambridge University Press

which represent an artificial but characteristic membrane partitioning isotherm of a surfactant. Nernst's (1891) partitioning law stated that the ratio of the concentrations of *dilute* solutions in two equilibrated but macroscopically separated phases (solvents) is a constant, the partition coefficient. Dilute solutions show no solute-induced changes of the phases and virtually no solute–solute contacts; in our example, this regime applies approximately up to $X_S^b \sim 0{\cdot}1$. There, the partitioning can be equally well described by all the definitions, K_R, K_X, $\tilde{K}_X$, K_C mentioned here (see the following two sections); see also the lines in Fig. 2 except the red dotted one representing an average $\tilde{K}_X$.

At substantial solute concentration, the law of partitioning applies to the *activities* of the solute in the two phases, which agree with concentrations [relatively to standard state, such as X_S^b and X_S^{aq} or C_S^{aq}/C_S^{aq}(standard)] only if the solute mixes ideally with the solvent. The case of ideal mixing is illustrated by the thin, red solid line which assumes that K_X as obtained for dilute solutions applies also to high concentrations. However, this is not true for our example and most real lipid–surfactant systems. Instead, the apparent $\tilde{K}_X$ in Fig. 2 decreases from 1 mM^{-1} at low X_S^b to 0·62 mM^{-1} at $X_S^b = 0{\cdot}4$. Above this concentration, X_S^b increases almost vertically (with C_S^{aq} remaining constant) indicating that solubilisation has started; this range has to be excluded from membrane partitioning analysis. Fitting the whole isotherm (up to $X_S^b = 0{\cdot}4$) with a constant $\tilde{K}_X$ yields 0·68 mM^{-1} (red dotted line in Fig. 2), which is a poor fit and fails to provide the thermodynamically interesting value of $\tilde{K}_X$ for dilute solutions. It is therefore advisable to include a suitable term for a concentration-dependent activity coefficient in the partition model so that it describes the curve properly. This is achieved semi-empirically in many cases by using K_R (here, $K_R = 1$ mM^{-1} along the whole dashed curve) or by $\tilde{K}_X(X_S^b, \rho^0)$ (bold green curve), which fits the data by two physically meaningful parameters, $\tilde{K}_X(0) = 1$ mM^{-1} and the non-ideality parameter $\rho^0 = -0{\cdot}7RT$. Although both models base on different rationales and expressions, they yield practically indistinguishable isotherms up to $X_S^b \sim 0{\cdot}4$ (see Section 2.3 for details). The curves deviate at higher X_S^b, but most surfactants cannot be incorporated to such high amounts into membranes anyway. That means, for isotherms limited to $X_S^b < 0{\cdot}4$–$0{\cdot}5$, mathematical simplicity favours K_R over $K_X(X_S^b, -0{\cdot}7RT)$. $K_X(X_S^b)$ may be superior for isotherms reaching high surfactant concentrations and systems exhibiting a different non-ideality. This is clearly the case for isotherms approaching pure surfactant aggregates (for surfactants forming vesicles or, analogously, for partitioning into mixed micelles) because K_R is not defined for $X_S^b = 1$.

The derivations, detailed properties and conversion rules of the different partition coefficients are given below for ideal mixing (K_X, $\tilde{K}_X$, K_C; Section 2.2) and non-ideal mixing (K_R, $K_X(X_S^b$; Section 2.3).

2.2 Ideal mixing

Assuming ideal mixing, the chemical potential, μ_S^b, of a surfactant, S, in a membrane bilayer, b, can be written as:

$$\mu_S^b = \mu_S^{0,b} + RT \ln X_S^b, \tag{1}$$

with the activity of the surfactant in the membrane equal to the mole fraction:

$$X_S^b = \frac{n_S^b}{n_S^b + n_L^b}. \tag{2}$$

https://doi.org/10.1017/S0033583508004721 Published online by Cambridge University Press

The terms n_S^b and n_L^b denote the mole numbers of surfactant (S) and lipid (L) in the bilayer (b). The reference state with the standard chemical potential $\mu_S^{0,b}$ is that of a detergent in a hypothetic, pure detergent bilayer. R and T stand for the general gas constant and the absolute temperature, respectively, and the concentration-dependent term, $RT\ln X_S^b$, corresponds to the change in entropy of ideal mixing in the membrane upon addition of surfactant.

Considering membrane and water as two separate phases, equilibrium partitioning is reached when the chemical potential of the surfactant is equal in the bilayer (b) and aqueous (aq) phase, $\mu_S^b = \mu_S^{aq}$. Writing μ_S^{aq} analogously to μ_S^b [Eq. (1)], we obtain:

$$\mu_S^{0,b} + RT\ln X_S^b = \mu_S^{0,aq} + RT\ln X_S^{aq}, \tag{3}$$

and, in turn:

$$\Delta\mu_S^{0,aq\to b} = \mu_S^{0,b} - \mu_S^{0,aq} = -RT\ln\frac{X_S^b}{X_S^{aq}}. \tag{4}$$

That means that the ratio of the mole fractions in the two phases should be constant for ideal mixing. It represents the concentration gradient that can be caused by a given intrinsic preference of the surfactant for the membrane, given by $\Delta\mu_S^{0,aq\to b} < 0$, against the entropy of mixing. This ratio is defined as the *mole fraction partition coefficient* K_X (often also referred to as P) (Tanford, 1980):

$$K_X \equiv \frac{X_S^b}{X_S^{aq}} = \frac{n_S^b(n_S^{aq} + n_W)}{(n_S^b + n_L)n_S^{aq}} \approx \frac{X_S^b \cdot C_W}{C_S^{aq}}. \tag{5}$$

The concentration of lipid in water is neglected since membrane lipids have an extremely low solubility (typically $\leqslant 10^{-9}$ M). The concentration of molecules in the aqueous phase is virtually constant, $C_W + C_S^{aq} \approx C_W \approx 55{\cdot}5$ M.

Whether partitioning into a real lipid membrane is spontaneous or favourable depends on whether the current, non-equilibrium ratio X_S^b/X_S^{aq} is above or below K_X. It has nothing to do with $\Delta\mu^0$, which refers to the 'intrinsic preference' of the molecule for a certain, often merely hypothetic standard state chosen to eliminate the entropy of mixing. For example, $K_X = 10$ implies that the transfer of surfactant from a hypothetic liquid of pure ($X_S^{aq} = 1$) yet fully hydrated (a contradiction in itself in practical terms) surfactant into a pure surfactant membrane would be favoured by $\Delta\mu_S^{0,aq\to b} = -5{\cdot}7$ kJ mol^{-1}.

Some authors omit the constant C_W in their definition of the partition coefficient (Lichtenberg *et al.* 2000; Ollivon *et al.* 2000), yielding $\tilde{K}_X$:

$$\tilde{K}_X \equiv \frac{X_S^b}{C_S^{aq}}. \tag{6}$$

Other authors use a concentration-based partition coefficient, K_C, for membrane/water partitioning analogous to bulk phases (Nernst, 1891):

$$K_C \equiv \frac{n_S^b \cdot v_{aq}}{v_b \cdot n_S^{aq}}, \tag{7}$$

where v_{aq} and v_b denote the partial volumes of the water and membrane phases, respectively. A major problem in using this definition for membrane systems is that there is no homogeneous, isotropic membrane volume in which the solute is free to dissolve. Small solutes partition either

https://doi.org/10.1017/S0033583508004721 Published online by Cambridge University Press

into the core of the membrane or into the interfacial or head group region, and surfactants distribute two-dimensionally over the membrane interface. Thus, application of Eq. (7) requires a rather ambiguous assumption regarding the effective membrane volume per lipid; and K_C data are meaningless if the membrane volume they are based on is not specified. In most cases, the molar volume of the whole lipid, V_L, is used as obtained from the specific volume of the lipid, ~ 1 ml g^{-1}, and the formula weight of the dry lipid. With molecular volumes reported by Nagle & Tristam-Nagle (2000), one obtains $V_L = 0{\cdot}76$ l mol^{-1} for POPC, $0{\cdot}78$ l mol^{-1} for DOPC and $0{\cdot}66$ l mol^{-1} for DMPC. A lipid filling a cylinder with a cross section of 65 Å^2 and a length of 2·5 nm corresponds to $V_L = 0{\cdot}98$ l mol^{-1}.

K_C can be converted approximately into K_X according to:

$$K_X \approx K_C \cdot V_L \cdot C_W, \tag{8}$$

with $C_W = 55{\cdot}5$ M. Other definitions of partition coefficients are based on volume fractions or contain specific corrections (Sharp *et al.* 1991).

2.3 Non-ideal mixing

In fact, both the aqueous solution and the membrane mix non-ideally in most cases. For non-ideal mixing, we may generally write:

$$\mu = \mu^0 + RT \ln[X \cdot f(X)], \tag{9}$$

where $f(X)$ is the activity coefficient and μ^0 is the standard chemical potential.

Of course, the polar groups of dry surfactants bind water and hence, surfactants do not mix ideally with water in the strict sense. Nevertheless, surfactant monomers in dilute aqueous solution are described by a pseudo-ideal behaviour with $f(X) \approx 1$ (as always for dilute systems) and a constant $\mu_S^{0,aq}$, but the latter refers to the hypothetic standard state, $X_S \rightarrow 1$, of 'pure but fully hydrated surfactant' and includes the free energy of hydration.

For surfactants in bilayers, non-ideal mixing gives rise to composition-dependent K_X, indicating that $f(X) \neq 1$. Two approaches, empirical [Eq. (10)] or based on a statistical model [Eq. (21)], are possible to derive an expression for $f(X)$.

Empirically, it has been found that the free surfactant concentration C_s^{aq} is often proportional to the mole ratio of surfactant to lipid in the membrane, R_b, so that the *mole ratio partition coefficient*, K_R:

$$K_R \equiv \frac{n_S^b}{n_L^b C_S^{aq}} = \frac{R_b}{C_S^{aq}} \tag{10}$$

is constant (Schurtenberger *et al.* 1985; Almog *et al.* 1986; Almog & Lichtenberg, 1988; Wenk & Seelig, 1997b; Wenk *et al.* 1997; Heerklotz & Seelig, 2000a; Heerklotz, 2001; Heerklotz & Seelig, 2001; Heerklotz *et al.* 2003; see Fig. 2 for a schematic representation). Equations (5)–(6) and (10) yield the conversion rules:

$$\frac{K_X}{C_W} = \tilde{K}_X = K_R\left(1 - X_S^b\right) = K_R X_L = \frac{K_R}{1 + R_b}. \tag{11}$$

The standard chemical potential difference becomes with Eq. (9):

$$\Delta\mu_S^{0,aq\rightarrow b} = -RT \ln\left[K_X(X_S^b) \cdot f(X_S^b)\right] = -RT \ln K_X(0), \tag{12}$$

https://doi.org/10.1017/S0033583508004721 Published online by Cambridge University Press

with the second equality taking into account that the term in the rectangular bracket must be constant, including the case where $X_S^b \rightarrow 0$ and, by definition, $f(0)=1$.

If K_R is a constant, we find with (11) and (12) that

$$f(X) = \left(1 - X_S^b\right)^{-1} = \left(X_L^b\right)^{-1} \tag{13}$$

and, because $K_X(0) = K_R \cdot C_W$:

$$\Delta\mu_S^{0,\mathrm{aq}\rightarrow\mathrm{b}} = -RT\ln\left(K_R \cdot C_W\right). \tag{14}$$

That means, K_X decreases with increasing surfactant content in the membrane:

$$K_X(X_S^b) = K_X(0)\cdot\left(1 - X_S^b\right) = K_X(0)\cdot X_L^b, \tag{15}$$

proportionally to the decreasing probability that a neighbouring molecule of the surfactant is a lipid, X_L^b. Apparently, the affinity of the surfactant to the membrane is targeted only at the lipids, whereas a membrane-bound surfactant essentially does not attract another surfactant into the membrane. This is in line with the argument that the membrane loses its stability and is converted to the micellar state when surfactant/surfactant contacts become abundant (Ueno, 1989).

An alternative method of describing non-ideal mixing in bilayers is based on a quantitative model treating non-ideal interactions in the membrane by pair-interaction statistics (Heerklotz *et al.* 1994b; Keller *et al.* 1997), an approach used also in the model of regular solutions (Hildebrand, 1929; Guggenheim, 1952; Cevc & Marsh, 1985). To a first approximation, mixing can be described as the formation of lipid/surfactant (L/S) contacts at the expense of lipid/lipid and surfactant/surfactant contacts:

$$\mathrm{S/S} + \mathrm{L/L} \longrightarrow 2\mathrm{S/L}. \tag{16}$$

In case of non-ideal mixing, the mixing process is not only accompanied by the entropy of ideal mixing but also by an additional 'reaction energy' which contributes an 'excess free energy', g_E, to the energy of the mixture. The molar excess free energy, G_E, is defined as the difference between the true free energy of the mixture, $G(X_S^b)$, and the free energy of an ideally mixing system (the weighted sum of the standard chemical potentials plus the contribution from the entropy of ideal mixing):

$$\begin{aligned} G_E(X_S^b) &= G(\text{real system}) - G(\text{ideal mixture}) \\ &= G(X_S^b) - X_S^b \times \left[\mu_S^0 + RT\ln X_S^b\right] - X_L^0 \times \left[\mu_L + RT\ln X_L\right]. \end{aligned} \tag{17}$$

That means G_E is a measure for the effect of mixing the two components on the free energy of the system. To a first approximation, G_E can be related to S/L pair interactions by a non-ideality parameter ρ^0

$$G_E = \frac{g_E}{n_S^b + n_L^b} = X_S^b\left(1 - X_S^b\right)\rho^0. \tag{18}$$

The term $X_S^b(1 - X_S^b)$ corresponds to the probability of S/L contacts in a random mixture, because X_S^b is the abundance of surfactant molecules and $X_L^b = 1 - X_S^b$ that of lipids. G_E vanishes by definition for pure phases, $X_S^b \rightarrow 0$ and $\rightarrow 1$, and reaches a maximum of $\rho^0/4$ for a 1:1 mixture. Since the chemical potential μ_S is $\partial g/\partial n_S$, the term:

$$\frac{\partial g_E}{\partial n_S^b} = \rho^0\left(1 - X_S^b\right)^2 \tag{19}$$

https://doi.org/10.1017/S0033583508004721 Published online by Cambridge University Press

appears as another concentration-dependent contribution to the chemical potential of the surfactant in the bilayer [compare with (1)]:

$$\mu_S^b = \mu_S^{0,b} + RT \ \ln X_S^b + \rho^0 \left(1 - X_S^b\right)^2 \tag{20}$$

and the derivation of the partition coefficient leads to (Heerklotz *et al.* 1994b; Keller *et al.* 1997)

$$K_X(X_S^b) = K_X(0) \cdot \exp\left\{ -\frac{\rho^0}{RT}\left[\left(1 - X_S^b\right)^2 - 1\right]\right\}. \tag{21}$$

Partitioning studies of a series of detergents, $C_{12}EO_n$ with $n = 3$–8, into POPC vesicles were evaluated according to this model. Although these detergents have different properties and yield quite different partition coefficients $K_X(0)$, they share a common non-ideality parameter, $\rho^0 = -1{\cdot}7$ kJ mol^{-1} $= -0{\cdot}7RT$ (Heerklotz *et al.* 1994b). A similar behaviour but somewhat larger value was reported for C_8Gluc/DMPC (Keller *et al.* 1997).

An extension of the formalism to ternary systems comprising two different lipids, such as Chol and PC (at a mole ratio $R_{Chol/PC}$), and a surfactant (Tsamaloukas *et al.* 2006):

$$K(X_S^b, R_{Chol/PC}) = K_{PC}(X_S^b) \cdot \exp\left\{ -\frac{\left(1 - X_S^b\right)^2 R_{Chol/PC}}{RT\left(1 + R_{Chol/PC}\right)}\left[\rho^0_{Chol/S} - \rho^0_{PC/S} - \frac{\rho^0_{PC/Chol}}{1 + R_{Chol/PC}}\right]\right\} \tag{22}$$

comprises non-ideality parameters for all three pair interactions. It allowed for determining the substantially unfavourable pair interaction parameter of TX100 and cholesterol ($\rho^0_{Chol/S} \sim 10$ kJ mol^{-1}) in POPC–cholesterol membranes at 37 °C, whereas TX100 mixes essentially ideally with POPC and ESM at this temperature.

The derivation of Eqs. (18) and (21) follows the statistics of pair interactions in a random mixture as used by the model of regular solutions. However, the model of regular solutions was derived for small 'hard' solutes the entropy of which arises exclusively from their mixing with the solvent. Then, the assumption of random mixing implies that there is no excess entropy, $S_E = 0$, and the non-ideality is of exclusively enthalpic nature, i.e. $G_E = H_E$, and thus $\rho^0_H = \rho^0$:

$$H_E = H^b(X_S^b) - X_S^b H_S^b(1) - X_L^b H_L^b(0) = \rho^0_H X_S^b\left(1 - X_S^b\right); \tag{23}$$

compare with Eq. (18). This assumption is not generally fulfilled for lipid/surfactant systems. Direct calorimetric measurements yielded endothermic excess enthalpies with ρ^0_H increasing continuously with the size of the head group [$C_{12}EO_5$: $\rho^0_H = +3{\cdot}9$ kJ mol^{-1}; $C_{12}EO_6$: $+4{\cdot}6$ kJ mol^{-1} (Heerklotz *et al.* 1998); $C_{12}EO_8$: $+10$ kJ mol^{-1} (Heerklotz *et al.* 1996)]; in contrast to a virtually constant $\rho^0 = -1{\cdot}7$ kJ mol^{-1}. Since the good fit obtained on the basis of a random mixing suggests that the entropy of mixing of the molecules in the membrane is close to that for ideal mixing, there must be a gain in intra-molecular entropy (e.g. conformational and motional freedom of the acyl chains or 'bound' water molecules) favouring 2 S/L contacts compared to 1 L/L + 1 S/S contact. This effect increases with increasing head group size and overcompensates the increasingly endothermic H_E to the constant, slightly negative G_E discussed above.

The energy of a mixture can be described by the sum of pair interactions only to a first approximation (Redlich & Kister, 1948; Guggenheim, 1952). The interaction enthalpies may also show effects of multibody interactions. For example, H_E of POPC/$C_{12}EO_3$ (a surfactant

https://doi.org/10.1017/S0033583508004721 Published online by Cambridge University Press

forming bilayers at room temperature) could be well described according to (Heerklotz *et al.* 1998):

$$H_{\mathrm{E}} = X_{\mathrm{S}}^{\mathrm{b}}\left(1 - X_{\mathrm{S}}^{\mathrm{b}}\right)\left[\rho_{\mathrm{LLS}}\left(1 - X_{\mathrm{S}}^{\mathrm{b}}\right) + \rho_{\mathrm{LSS}} X_{\mathrm{S}}^{\mathrm{b}}\right] \tag{24}$$

illustrated by the green curve in Fig. 6. The parameters suggest that randomly occurring clusters containing one surfactant and two lipids (LLS) are favoured by $\rho_{\mathrm{LLS}} = -2{\cdot}3$ kJ mol^{-1}, whereas LSS clusters are unfavourable by $\rho_{\mathrm{LSS}} = +1{\cdot}1$ kJ mol^{-1}. Modelling the enthalpies of detergents such as $C_{12}EO_n$ with $n = 5$, 6 in the membrane required higher-order terms taking into account cooperative interactions in larger clusters.

Finally, it should be noted that non-ideal, composition-dependent partition coefficients might also arise from composition-dependent changes in membrane structure or substantial interactions between the molecules in the aqueous phase. For C_8Gluc, Ueno (2003) explained decreasing values of K_X with detergent-induced structural changes of the bilayer phase, such as the conversion of large to small vesicles.

2.4 Electrostatic effects

The effects discussed so far apply to non-ionic lipids and detergents, or to charged compounds after correction for electrostatic effects. If the membrane contains charged lipids or surfactants, it possesses a surface charge density σ:

$$\sigma = \frac{e_0 \cdot \sum_i X_i^{\mathrm{b}} z_i}{\sum_i X_i^{\mathrm{b}} A_i}, \tag{25}$$

where e_0 is the elementary charge, and X_i^{b}, z_i and A_i denote the mole fraction, signed charge number and lateral area, respectively, which are summed over all i components (lipids and surfactants).

This charge density gives rise to a surface potential, ψ_0, which results in a difference between the local concentration of charged molecules close to the surface, $C_{\mathrm{S}}^{\mathrm{aq,surf}}$, and the bulk surfactant concentration, $C_{\mathrm{S}}^{\mathrm{aq,bulk}}$ as described by Boltzmann's law:

$$C_{\mathrm{S}}^{\mathrm{aq,surf}} = C_{\mathrm{S}}^{\mathrm{aq,bulk}} \cdot \exp\left\{-\frac{z_{\mathrm{S}} e_0 N_{\mathrm{A}} \psi_0}{RT}\right\}. \tag{26}$$

It should be noted that a more complex behaviour is observed if the charge z_{S} changes upon membrane binding due to protonation/deprotonation reactions at the membrane surface (Beschiaschvili & Seelig, 1992; Seelig, 1997). The ratio $R_{\mathrm{b}}/C_{\mathrm{S}}^{\mathrm{aq,bulk}}$ corresponds to an apparent partition coefficient, K_R^{app}, whereas the intrinsic mole ratio partition coefficient is $K_R^0 \equiv R_{\mathrm{b}}/C_{\mathrm{S}}^{\mathrm{aq,surf}}$. With (26), one obtains

$$K_{\mathrm{R}}^{\mathrm{app}} = \frac{R_{\mathrm{b}}}{C_{\mathrm{S}}^{\mathrm{aq,bulk}}} = K_R^0 \cdot \exp\left\{-\frac{z_{\mathrm{S}} e_0 N_{\mathrm{A}} \psi_0}{RT}\right\}. \tag{27}$$

The exponential term vanishes for uncharged surfactants, $z_{\mathrm{S}} = 0$, and for uncharged membranes, $\psi_0 = 0$. It becomes >1 for electrostatic attraction (z_{S} and ψ_0 differ in sign) so that $K_R^{\mathrm{app}} > K_R^0$, and <1 for electrostatic repulsion. Since the potential ψ_0 depends on the amount of membrane-bound, charged surfactant, K_R^{app} is a function of R_{b}. For example, K_R^{app} of SDS partitioning into

https://doi.org/10.1017/S0033583508004721 Published online by Cambridge University Press

(previously uncharged) POPC vesicles in 110 mM salt decreases from $K_R^0 = 23\ \mathrm{mM}^{-1}$ at $R_b \to 0$ and $\psi_0 \to 0$ to $\approx 2\ \mathrm{mM}^{-1}$ in the range used for typical partitioning measurements and further to about $0{\cdot}5\ \mathrm{mM}^{-1}$ upon membrane saturation, $R_b \approx 0{\cdot}3$ (Tan *et al.* 2002). A model to fit $R_b(C_S^{aq,bulk})$ must take into account the unknown surface potential ψ_0 (Beschiaschvili & Seelig, 1992; Seelig, 1997; Hildebrand *et al.* 2002; Tan *et al.* 2002; Keller *et al.* 2006b). This can be achieved by a numerical optimisation of the parameters to fulfill two independent relations between R_b and ψ_0. One is given by Eq. (27) and a second is derived combining the Gouy–Chapman equation:

$$\sigma = \mathrm{sgn}(\psi_0)\sqrt{2000\varepsilon_0\varepsilon_r RT \sum_j C_j^{bulk} \cdot \left(\exp\left\{-\frac{z_j e_0 N_A \psi_0}{RT}\right\} - 1\right)} \tag{28}$$

with Eq. (25) and replacing X_S^b by $R_b/(1+R_b)$. Note that Eq. (28) sums over all j species of ions in solution, thus taking into account the screening of charges by ions. The symbols ε_0 and ε_r denote the permittivity of vacuum and the dielectric constant, respectively.

For key reviews, see McLaughlin (1989) on electrostatics of membrane binding, Seelig (1997) for the explicit consideration of electrostatics in evaluating titration calorimetry data and Record *et al.* (1978) for a comprehensive treatment of all possible salt effects on 'binding' equilibria.

2.5 Kinetic aspects

Establishing the partitioning equilibrium after addition of surfactant to the aqueous phase proceeds in three steps with sometimes very different kinetics:

1. Part of the added surfactant inserts into the outer membrane leaflet. This is usually fast for practical purposes, e.g. 50–500 ms for lysolecithin (Elamrani & Blume, 1982), ~100 ms for TX100 (Alonso *et al.* 1987) and 10–30 s for SDS into PC vesicles containing no, 5% of positively or 5% of negatively charged lipids (Cocera *et al.* 2004).
2. In a second step, the surfactant has to equilibrate between the outer and inner leaflet of the vesicles (or analogously, cell membrane). To this end, its polar head group has to cross the hydrophobic core by a flip-flop or another mechanism of permeation. $C_{12}EO_8$ (le Maire *et al.* 1987), $C_{12}EO_7$ (Heerklotz *et al.* 1999), Triton X100 (Heerklotz *et al.* 2003; Tsamaloukas *et al.* 2006) and C_8Gluc (Wenk *et al.* 1997) equilibrate with both leaflets of the membrane within a time window from milliseconds to some tens of seconds. Surfactants with larger or charged head groups may, however, require hours or days to cross the membrane, as shown for SDS at room temperature (Cocera *et al.* 1999; Keller *et al.* 2006a), C_{12}Malt (Kragh-Hansen *et al.* 1998), C_nMalt with $n = 12$, 13 and 14 (Heerklotz, 2001), C_{16}lyso-PC (Bhamidipati & Hamilton, 1995) and others. Note that weak acids and bases can translocate across membranes via their no-charged form followed by re-establishing the equilibrium on the *trans* side, an effect that can also be used for active loading of liposomes with drugs driven by a pH gradient (Cullis *et al.* 1997). This transport mechanism applies, at least under certain conditions, to fatty acids (half-time for many species was shown to be <1 s), deoxycholate ($t_{1/2} < 1$ s) and cholate (~ 20 s) but not to their taurine conjugates ($t_{1/2} > 1$ h, $pK_a \sim 1$) at pH 7·4 (Kamp *et al.* 1993). It should, however, be kept in mind that flip-flop is not a property of the surfactant species alone; the dynamics and barrier properties of membranes may depend substantially on lipid composition, surfactant content, membrane curvature, temperature, etc. For example,

https://doi.org/10.1017/S0033583508004721 Published online by Cambridge University Press

permeation of SDS through membranes is strongly enhanced by increasing temperature and occurs within some minutes at 65 °C (Keller *et al.* 2006a).
The surfactant leaving the outer leaflet by flipping to the inner is partially replaced by further uptake from the aqueous phase.

3. In a last step, the inner leaflet equilibrates with the *trans* aqueous compartment, e.g. the interior of the vesicle. In vesicle systems, the enclosed volume is usually so small that the surfactant fraction in the interior is negligible (Keller *et al.* 2006a).

Systems with fast uptake but slow translocation across the bilayer can often be studied and described, approximately, in terms of an equilibrium of the surfactant between aqueous phase and outer lipid monolayer, with the lipid in the inner monolayer being not accessible and disregarded upon data evaluation. Seelig and co-workers (see, e.g. Seelig, 1997) have, to this end, introduced a factor γ which will be referred to here as the accessibility factor (for permeable membranes, $\gamma = 1$; for impermeable membranes, $\gamma = 0{\cdot}5$ for LUV, 0·6 for SUV, $\ll 0{\cdot}5$ for MLV); it corrects the lipid concentration to represent only the fraction that actually equilibrates with the aqueous phase within the available time. If the inner leaflet contains surfactant as in the release protocol, γ applies also to membrane-bound surfactant (Heerklotz & Seelig, 2000b; Keller *et al.* 2006a; Tsamaloukas *et al.* 2007). It should, however, be noted that the asymmetric insertion or extraction may in certain cases give rise to bilayer couple effects (see Section 3.1), which change the thermodynamic parameters of binding (Heerklotz, 2001).

2.6 Methods for measuring partition coefficients

The most direct method to measure partition coefficients is a macroscopic separation of at least part of the water phase from the mixed vesicles by, e.g. equilibrium dialysis (Kragh-Hansen *et al.* 1998) or centrifugation. Then, the free surfactant concentration must be measured to determine the partition coefficient. This can utilise radio-labelled (le Maire *et al.* 1987) or fluorescent surfactants, surfactant-selective electrodes (Kadi *et al.* 2004) or surface tension measurements (Kaufmann *et al.* 2006).

A very potent technique to study membrane partitioning of solutes is ITC (cf. Heerklotz & Seelig, 2000b for a review). One major advantage of this method is that it yields not only the partition coefficient but also the enthalpy and entropy of binding by a single, automated run. Different assays to measure uptake (1) or release (2, 3) of surfactant into or from membranes are based on injections:

1. of lipid vesicles into a surfactant solution (uptake protocol, cf. e.g. Seelig & Ganz, 1991; Wenk *et al.* 1997 for cumulative model and Heerklotz *et al.* 1996; Keller *et al.* 1997; Heerklotz & Seelig, 2000b for differential model);
2. of mixed vesicles into buffer (release protocol) (Heerklotz *et al.* 1999; Heerklotz, 2001);
3. of buffer into mixed vesicles (Opatowski *et al.* 1997a); or
4. of mixed vesicles into surfactant solutions (Rowe *et al.* 1998; Tsamaloukas *et al.* 2006).

The instrument measures the heat associated with surfactant transfer assuming that the lipid is insoluble in the aqueous phase and, thus, not transferred. A combination of uptake and release protocols refines the results and establishes whether the system equilibrates completely during the experiment, thus providing an independent measurement of membrane permeability and accessibility, γ (see previous section). The protocol and fit routine for the ITC-based uptake and

https://doi.org/10.1017/S0033583508004721 Published online by Cambridge University Press

release assay are given by Tsamaloukas *et al.* (2007); the analogous fluorescence spectroscopic assay is described by Keller *et al.* (2007). Rowe's protocol (4) allows for a partitioning measurement at specific, defined membrane composition(s).

Another widely used approach is the partitioning assay based on the recognition of at least one characteristic membrane composition, R_b^*, in samples with different lipid and total surfactant concentrations (Encinas & Lissi, 1982). The evaluation uses the relationship:

$$C_S^* = R_b^* \cdot C_L + C_S^{aq*} \tag{29}$$

representing the fact that the total surfactant concentration C_S comprises the membrane-bound surfactant, $C_S^b = R_b C_L$, and the free surfactant, C_S^{aq}. Let us consider vesicle suspensions of different lipid concentrations, C_L, that share the same R_b^* as indicated by a characteristic, R_b-dependent property or phenomenon (indicated by *) such as a spectroscopic signal of a membrane probe, a certain leakage, etc. A characteristic, constant R_b^* implies also a constant aqueous concentration C_S^{aq*} (determined by the partition coefficient) so that (29) corresponds to a straight line. That means, if the total concentrations leading to this phenomenon, C_S^*, are plotted *versus* C_L, the corresponding membrane composition R_b^* and free concentration C_S^{aq*} are obtained as the slope and intercept of a linear regression. The partition coefficient at this membrane composition is $K_R^* = R_b^* / C_S^{aq*}$. Lichtenberg *et al.* (1985) and Schurtenberger *et al.* (1985) established the evaluation of the onset of solubilisation, C_S^{sat}, to determine R_b^{sat}, $C_S^{aq,sat}$ and $K(R_b^{sat})$ according to (29) as one of the most frequently used approaches in the field. The same approach has been used on the basis of detergent-induced changes in the fluorescence spectra of a membrane probe (Heerklotz *et al.* 1994a, b; Paternostre *et al.* 1995), characteristic degrees of dye efflux from vesicles (de la Maza & Parra, 1994b, 1997; de la Maza *et al.* 1998a; Heerklotz & Seelig, 2007) and other parameters.

Surfactants showing a membrane-sensitive, intrinsic fluorescence or those quenching membrane probes (such as SDBS and TX100 quenching anthroyloxy-FA; Marcelino *et al.* 2007) can be monitored quantitatively by fluorescence spectroscopy. An estimate of K can also be derived from the 'melting point depression' analogously to dilute solutions, but this approach is limited to certain lipids and assumptions (cf. Section 3.4 and Inoue *et al.* 1986).

2.7 Experimental values of partition coefficients

Membrane partitioning and self association of surfactants are both governed by the *hydrophobic effect*. Therefore, the respective gains in chemical potential differ by

$$\Delta\mu_s^{0,m\to b} = -RT \ln[K_R \cdot \mathrm{CMC}] \tag{30}$$

of a few kJ mol^{-1} only. That implies that

$$K_R \approx \frac{1}{\mathrm{CMC}} \tag{31}$$

(Heerklotz & Seelig, 2000a). Data of K_R for homologous series (see Fig. 3, left) imply that each methylene group contributes $\Delta\Delta\mu_s^{0,aq\to b} = -(3{\cdot}4 \pm 0{\cdot}5)$ kJ mol^{-1} CH_2 to the chemical potential of membrane partitioning, a value close to $-2{\cdot}8$ to $-3{\cdot}1$ kJ mol^{-1} CH_2 reported for micelle formation (Israelachvili, 1991; Heerklotz & Epand, 2001). The slightly larger incremental value for membranes, if significant at all, could arise from chain length-dependent changes in membrane curvature strain (cf. Section 3.2).

https://doi.org/10.1017/S0033583508004721 Published online by Cambridge University Press

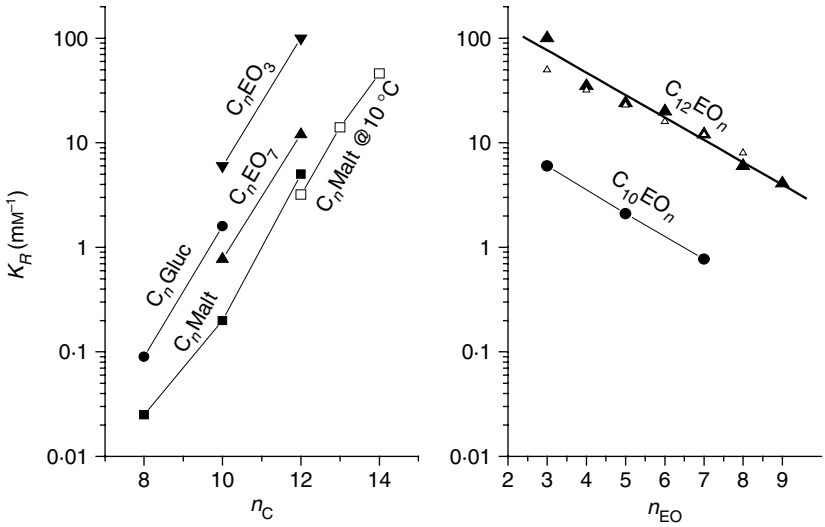

Fig. 3. Dependence of membrane/water partition coefficients (cf. Tables 1*a*–1*c*, typically for POPC at 25 °C) on the length of the alkyl chain (carbon number n_C, left panel) and on the length of the EO chain (detergent head group) (right panel). The slopes allow the estimation of group contributions of CH_2 and EO groups to the apparent standard free energy of transfer, $\Delta\mu_s^{0,\,aq\rightarrow b}$.

Let us consider the differences between self association and membrane partitioning that may render K_R somewhat different from 1/CMC. Trivially, mixed systems are favoured compared to pure ones by the entropy of mixing; this effect tends to increase $K_R \times$ CMC.

If surfactant or lipid is charged, *electrostatic interactions* have a major influence on partitioning, particularly at low salt. Partitioning of charged surfactants into neutral membranes is favoured over self-association by a reduction of unfavourable surfactant–surfactant interactions. Analogously, partitioning of neutral surfactants reduces repulsive interactions in a membrane made of charged lipids. And, of course, surfactant partitioning into membranes of oppositely charged lipid is enhanced. What applies to charges applies similarly, but with weaker influence on K_R, also to dipole–dipole interactions. Isolating lipid dipoles with non-dipolar detergents and *vice versa* as well as inserting detergents with reverse dipole orientations into membranes is favourable.

Another significant difference is that micelles show virtually no *curvature strain* (see Sections 0 and 0), since they can adapt their size and shape over a wide range of average interfacial curvatures. If already small amounts of a non-ionic surfactant induce curvature strain in a membrane (these were referred to as strong detergents), the strain diminishes K_R compared to 1/CMC so that $K_R \times \text{CMC} < 1$ (Heerklotz & Seelig, 2000a). These surfactants induce also membrane solubilisation at relatively low membrane content [see Eq. (41)]. Other surfactants, however, relax existing strains and favour membrane insertion over self-association, at least at low membrane contents (weak detergents; Heerklotz & Seelig, 2000a). They require high contents of more than one detergent per lipid in the membrane for solubilisation or form vesicles themselves (and do not solubilise membranes at all). Thermodynamic and structural origins and consequences of curvature strain are discussed below (Sections 3.1 and 3.2). The effect of curvature strain (or 'effective molecular shape' or packing parameter) is illustrated by comparing surfactants with different head groups sharing the same hydrophobic part and *vice versa* (Fig. 3). For example, K_R of surfactants $C_{12}EO_n$ with $n = 3$–8 decreases by a factor of $\approx 0{\cdot}6$ per EO group, i.e. the free

https://doi.org/10.1017/S0033583508004721 Published online by Cambridge University Press

energy gain is reduced by $\approx +1{\cdot}3$ kJ mol^{-1} EO. The fact that this arises from monolayer curvature strain and not, for example from solubility or hydrophilic–hydrophobic balance changes, is illustrated by the finding that this behaviour is not paralleled by the CMC so that $K_R \times$ CMC decreases continuously with n. The curvature model also explains that partition coefficients of strong detergents are, as a rule, higher into membranes of more unsaturated (more negative spontaneous curvature) lipids.

Let us compare pure lipid vesicles with biomembranes. Quantifying the partitioning of surfactants into, e.g. erythrocyte membranes requires a somewhat ambiguous definition of the effective lipid concentration of a cell suspension. Binford and Palm (1994) estimated the phospholipid concentration by a phosphate assay and assumed that the total lipid concentration (including cholesterol and glycolipids) is twice the phospholipid concentration. Pantaler *et al.* (2000) applied K_C [cf. Eq. (7)] to surfactant partitioning into erythrocytes, using the cell count of the suspension and a membrane volume of $0{\cdot}72$ μm^3 cell^{-1} (as computed from an area of ~ 140 μm^2 and a membrane thickness of ~ 5 nm). Generally, the resulting partition coefficients seem to be close to those for liquid–crystalline model vesicles (Tables 1*a*–1*c*), suggesting that there is no strong interference of the membrane proteins with surfactant uptake into the membrane.

The curvature of the bilayer seems to have only minor effects on the mean partition coefficient of amphiphiles although the thermodynamic effects governing membrane insertion are often substantially different between small and larger vesicles. The enthalpy of insertion of peptides and certain surfactants into small vesicles differs by a large, negative contribution from that obtained upon insertion into large vesicles (Seelig & Ganz, 1991). This exothermic contribution is temperature-independent (so that ΔC_p is virtually conserved) and almost perfectly compensated by a loss in entropy (so that $\Delta\mu_S^{0,\mathrm{aq}\to\mathrm{b}}$ is also essentially unchanged) (Wieprecht *et al.* 2002). The interpretation of this finding in terms of improved chain packing in the outer, positively curved lipid leaflet is supported by findings that the enthalpy of partitioning (but hardly $\Delta\mu_S^{0,\mathrm{aq}\to\mathrm{b}}$ and ΔC_p) depends crucially on chain alignment and ordering and differ, therefore, between bulk hydrocarbon and the core of micelles (Heerklotz & Epand, 2001) or bilayers (Wimley & White, 1993).

Lipids in the gel phase usually show a reduced affinity to surfactants. This is observed, for example for Triton partitioning into sphingomyelins and 1,2-dipalmitoyl-*sn*-glycero-3-phosphocholine (DPPC) (Nyholm & Slotte, 2001; Ollila & Slotte, 2002; Arnulphi *et al.* 2007; cf. Tables 1*a*–1*c*) or for various lyso-PCs into DPPC (Hoyrup *et al.* 2001). Given that the approximate validity of the general equation for freezing point depression suggests the detergents to be virtually immiscible with a gel phase (see Section 3.4), one would, however, expect even lower membrane–water partition coefficients below the melting temperature, T_m. A possible explanation is that a major part of the detergent sequesters into (and thus expands) relatively fluid defect regions between quasi-crystalline gel clusters rather than inserting into them directly (Patra *et al.* 1998, 1999; Sot *et al.* 2002). Interestingly, a much weaker reduction of K upon freezing is observed for fatty acids (C_{10} to C_{16}), which seem to fit into the gel lattice and show similar or slightly larger partition coefficients into DPPC at 20 °C compared to 50 °C (Hoyrup *et al.* 2001).

The temperature dependence of membrane partitioning can be described analogously to that of other 'equilibrium constants', K, in terms of van't Hoff's law:

$$\frac{\partial \ln K}{\partial T} = \frac{\Delta H}{RT^2} = \frac{\Delta C_p \times (T - T_0)}{RT^2}. \tag{32}$$

https://doi.org/10.1017/S0033583508004721 Published online by Cambridge University Press

Table 1a. *Ethylene oxide detergents*

Surfactant	Lipid	T (°C)	K_R (mM^{-1})	ΔH (kJ mol^{-1})	R_b^{sat}	R_b^{sol}	Reference
$C_{10}EO_3$	POPC	25	6	8	LAM		(Heerklotz & Seelig, 2000a)
$C_{10}EO_7$	POPC	25	0·77	27	0·6		(Heerklotz & Seelig, 2000a)
$C_{10}EO_8$	ESM	25	0·16	24			(Ollila & Slotte, 2002)
	DHSM	25	0·06	42			(Ollila & Slotte, 2002)
$C_{12}EO_3$	POPC	25	50		LAM		(Heerklotz *et al.* 1994b)
			100	6			(Heerklotz & Seelig, 2000a)
$C_{12}EO_4$	POPC	25	32		LAM		(Heerklotz *et al.* 1994b)
			35	12			(Heerklotz & Seelig, 2000a)
$C_{12}EO_5$	POPC	25	23				(Heerklotz *et al.* 1994b)
			24	16			(Heerklotz & Seelig, 2000a)
					3·1	7·3	(Heerklotz *et al.* 1997)
$C_{12}EO_6$	POPC	25	16				(Heerklotz *et al.* 1994b),
			20	20			(Heerklotz & Seelig, 2000a)
					1·2	4·9	(Heerklotz *et al.* 1997)
$C_{12}EO_7$	POPC	25	12				(Heerklotz *et al.* 1994b)
			12	20			(Heerklotz & Seelig, 2000a)
					0·7	2·6	(Heerklotz *et al.* 1997)
$C_{12}EO_8$	POPC	11			0·43	1·4	(Heerklotz *et al.* 1997)
	POPC	25	8				(Heerklotz *et al.* 1994b)
			6	32			(Heerklotz & Seelig, 2000a)
					0·57	1·9	(Heerklotz *et al.* 1997)
	EPC	25	9		0·62	2·3	(Edwards & Almgren, 1991)
	Sarc. ret. ves.		24–14		0·8		(Kragh-Hansen *et al.* 1998)
	POPC	50			1·0	2·7	(Heerklotz *et al.* 1997)
	Erythrocytes	37	16				(Pantaler *et al.* 2000)
$C_{12}EO_9$	POPC	25	4·1				(Heerklotz)
TX-100	POPC	25	3·0	15			(Heerklotz & Seelig, 2000a)
	EPC	25			0·8	2·9	(Partearroyo *et al.* 1996)
			2–4		0·64	2·6	(de la Maza & Parra, 1994b)
			3·4		0·64		(Paternostre *et al.* 1988)
	DOPC		12–10		1·4		(Kragh-Hansen *et al.* 1998)
	Sarc. ret. ves.		11–8		1·0		(Kragh-Hansen *et al.* 1998)
	Erythrocytes	37	2·4				(Pantaler *et al.* 2000)
	POPC	37	1·2	12	0·41		(Heerklotz *et al.* 2003)
	POPC-ESM-Cho	37	0·2	18	0·07		(Heerklotz *et al.* 2003)
	$C_{16}SM$	10	0·4	16			(Arnulphi *et al.* 2007)
	$C_{16}SM$	25	0·2	37	0·20		(Nyholm & Slotte, 2001)
	$C_{16}SM$	50	0·7	−21			(Arnulphi *et al.* 2007)
	DPPC	25	0·9	6	0·29		(Nyholm & Slotte, 2001)
	ESM	10	0·7	12			(Arnulphi *et al.* 2007)
	ESM	25	2	6·5			(Ollila & Slotte, 2002)
	ESM	50	1	−11			(Arnulphi *et al.* 2007)
	DHSM	25	0·6	13			(Ollila & Slotte, 2002)
TX100r	DOPE	25			2·2	100	(Johnsson & Bergstrand, 2004)
					1·5	16	(Johnsson & Bergstrand, 2004)
TX-114	EPC	25			0·9	4·5	(Partearroyo *et al.* 1996)
	POPC	25	3·5	8			

https://doi.org/10.1017/S0033583508004721 Published online by Cambridge University Press

Table 1b. *Other nonionic surfactants*

Surfactant	T (°C)	Lipid	K_R (mM^{-1})	ΔH (kJ mol^{-1})	R_b^{sat}	R_b^{sol}	Reference
C_8Gluc	25	EPC	0·08–0·10		1·4–1·7	2·4–3·1	(Walter *et al.* 2000)
			0·11		1·3	3·8	(Paternostre *et al.* 1988)
			0·11–0·08		1·3		(de la Maza & Parra, 1994a; de la Maza *et al.* 1998a)
			0·09				(Ueno, 1989)
	25	EPC/EPA	0·7–0·08		1·6	2·7	(Paternostre *et al.* 1995)
	27	SBPC	0·09	5·6	1·6	3·1	(Keller *et al.* 1997)
	27	DMPC	0·10	13	1·6	1·8	(Keller *et al.* 1997)
	28	POPC SUV	0·12	5·4			(Wenk *et al.* 1997)
					1·4	2·8	(Wenk & Seelig, 1997a)
	28	EPC	0·09		1·6	3·1	(Opatowski *et al.* 1997a)
				10			(Opatowski *et al.* 1997b)
	70	DMPC	0·07	9·0	1·7	2·6	(Keller *et al.* 1997)
	70	DPPC			1·5	1·9	(Keller *et al.* 1997)
C_9Gluc	25	EPC	0·4–0·3				(de la Maza *et al.* 1998a)
	20	DMPC	0·13				(Meister *et al.* 2004a)
C_{10}Gluc	25	POPC	1·6	4·9	LAM		(Heerklotz & Seelig, 2000a)
	25	EPC	1·2–1·0				(de la Maza *et al.* 1998a)
	37	Erythrocytes	1·1				(Pantaler *et al.* 2000)
C_{11}Gluc	25	EPC	5–4				(de la Maza *et al.* 1998a)
C_{12}Gluc	25	EPC	23–17				(de la Maza *et al.* 1998a)
C_8TGluc	28	POPC	0·24	4–8			(Wenk & Seelig, 1997b)
					1·5		(de la Maza & Parra, 1994a)
C_8Malt	25	POPC	0·025	10			(Heerklotz & Seelig, 2000a)
C_9Malt	25	POPC	0·1		0·48	1·45	(Beck *et al.* 2008)
C_{10}Malt	25	POPC	0·2	14			(Heerklotz & Seelig, 2000a)
	37	Erythrocytes	0·28				(Pantaler *et al.* 2000)
C_{12}Malt	10	POPC	3·2	15			(Heerklotz, 2001)
	25	POPC	5·0	4			(Heerklotz & Seelig, 2000a)
	25	POPC	6		0·7	1·44	(Beck *et al.* 2008)
	25	EPC	19–8		0·9		(de la Maza & Parra, 1997)
		Sarc. ret. ves.	27–11		1·0		(Kragh-Hansen *et al.* 1998)
	37	Erythrocytes	11				(Pantaler *et al.* 2000)
C_{13}Malt	10	POPC	14	8			(Heerklotz, 2001)
	25				0·87		(Heerklotz, 2001)
C_{14}Malt	10	POPC	46	3			(Heerklotz, 2001)
	25				0·94		(Heerklotz, 2001)
MEGA-8	~41	DPPC	0·01				(Inoue *et al.* 1986)
MEGA-9	~41	DPPC	0·3				(Inoue *et al.* 1986)
MEGA-10	~41	DPPC	0·1				(Inoue *et al.* 1986)

Membrane insertion, as a process driven by the hydrophobic effect, typically shows a virtually constant, negative heat capacity change. As a consequence, K exhibits a maximum at a characteristic isenthalpic temperature T_0 (there, $\Delta H = 0$). Non-ionic surfactants seem to show values of T_0 somewhat above room temperature, so that at room temperature, $\Delta H_S^{aq\rightarrow b}$ is endothermic and $K(T)$ increases (e.g. by $\approx$10–30% per 10 K for $\Delta H_S^{aq\rightarrow b} \approx +10$ to $+20$ kJ mol^{-1}). This is found for C_8Gluc partitioning into egg PC, with K_R increasing from $\approx$0·08 mM^{-1} (5 °C) to

https://doi.org/10.1017/S0033583508004721 Published online by Cambridge University Press

Table 1c. *Zwitterionic surfactants*

Surfactant	T (°C)	Lipid	K_R (mM^{-1})	ΔH (kJ mol^{-1})	R_b^{sat}	R_m^{sol}	Reference
CHAPS			0·4–0·5		0·77–1·5		(Schurholz, 1996)
			0·07		0·1/0·21	0·5	(Viriyaroj *et al.* 2005)
	25	POPC	0·06		0·09	0·4	(Beck *et al.* 2008)
D7PC	25	POPC	0·2	7	0·08		(Heerklotz & Seelig, 2000a)
FOSMEA	25	POPC	0·4				(Heerklotz)
C_{10}lysoPC	50	DPPC	1·7	−0·4			(Hoyrup *et al.* 2001)
C_{12}lysoPC			4·8	−1·0			
C_{14}lysoPC			12	−0·8			
C_{16}lysoPC			93	+0·4			
C_{12}lysoPC	20	DPPC	1·4	−1·0			(Hoyrup *et al.* 2001)
C_{14}lysoPC			2·2	−0·1			
C_{12}Bet	25	EPC	0·76				(de la Maza *et al.* 1998b)

For T-dependent CMC data of short-chain and lysolipids, cf. also Heerklotz & Epand (2001).

0·12 mM^{-1} (35 °C) (da Graca-Miguel *et al.* 1989). The heat capacity changes of binding and association were empirically related to changes in (apolar and polar) water accessible surface area (ASA) (Spolar *et al.* 1989; Baker & Murphy, 1998), but membrane binding often shows anomalously weak negative (or even positive) ΔC_p. This cannot be explained in terms of ASA, but implies effects of lipid chain packing on ΔC_p (Rowe *et al.* 1998; Heerklotz & Epand, 2001; Tsamaloukas *et al.* 2005). The T_0 of charged surfactants such as SDS (Tan *et al.* 2002; Keller *et al.* 2006a) and cholates (Hildebrand *et al.* 2003) is below room temperature so that experimental data refer usually to temperatures above T_0. Then, $\Delta H_S^{aq\to b}$ is exothermic and K_R decreases with increasing T.

Salt concentrations up to ≈0·1 M seem to have no strong effect on the K_R of non-ionic surfactants and on the intrinsic K_R^0 of charged surfactants. Partition coefficients of detergents $C_{12}EO_n$ into POPC vesicles from water (Heerklotz *et al.* 1994b) and from 10 mM Tris (pH 7·4), 100 mM NaCl (Heerklotz & Seelig, 2000a) show no systematic difference (cf. Table 1*a*–1*c*). High concentrations of co-solutes show the typical kosmotropic or chaotropic effect; NaCl and sucrose increase the energy of hydrophobic surfaces exposed to water and promote surfactant incorporation into membranes; urea has the opposite effect (cf. Table 2 for C_8Gluc; Walter *et al.* 2000). Of course, apparent partition coefficients [cf. Eq. (27)] of charged surfactants are greatly changed by salts (cf. data of Hildebrand *et al.* 2002 on cholate; Table 2), an effect that is even more pronounced for divalent ions (such as Ca^{2+}; Almog & Lichtenberg, 1988).

Meister *et al.* (2004a, b) have measured the partition coefficients of detergents into a lipid monolayer on the air/water interface by infrared reflection absorption spectroscopy; the results at the 'bilayer–monolayer equivalence pressure' of $\sim 32\times10^{-3}$ N m^{-1} agreed with those for vesicles.

Finally, it should be noted that many commercial surfactant brands (Triton, Lubrol, Tween, etc.) are, in fact, mixtures of surfactants with similar chemical structures. The apparent K_R of such a mixture may depend, in fundamental contrast to that for a pure system, strongly on lipid concentration (see Beck *et al.* 2008).

https://doi.org/10.1017/S0033583508004721 Published online by Cambridge University Press

https://doi.org/10.1017/S0033583508004721 Published online by Cambridge University Press

Table 2. *Properties of charged surfactants and salt effects on C_8Gluc*

Surfactant	T (°C)	Salt concentration (M)	Lipid	K_R^{app} (mM^{-1})	K_R^0 (mM^{-1})	ΔH (kJ mol^{-1})	R_b^{sat}	R_m^{sol}	Reference
C_8Gluc	25	0	EPC	0·09			1·5	2·6	(Walter *et al.* 2000)
		0·1 NaCl		0·10			1·7	3·1	
		1·5 NaCl		0·23			1·8	3·4	
		2 M sucrose		0·25			2·3	4·3	
		2 M urea		0·06			1·3	2·5	
C_{10}FA	20	0·01	DPPC	0·065		8·8			(Hoyrup *et al.* 2001)
C_{12}FA				0·74		−11			
C_{12}FA	37	KNPS pH 7·4	Erythrocytes	1·9					(Pantaler *et al.* 2000)
C_{10}FA	50	0·01	DPPC	0·052		−17			(Hoyrup *et al.* 2001)
C_{12}FA				0·5		−12			
C_{14}FA				7·9		−28			
NaC	25	0·13	EPC	0·13–0·11			0·3		(Paternostre *et al.* 1988)
		0·14	SPC				0·7	0·97	(Simes *et al.* 2004)
		0·13 NaCl		0·05			0·3	0·4	(Almog *et al.* 1986)
		0·13 NaCl + 0·03 $CaCl_2$		0·18				0·7	(Almog & Lichtenberg, 1988)
	25	0·1	POPC	0·7	51	−2·2	0·3	0·45	(Hildebrand *et al.* 2003)
	27		Erythrocytes	0·02			0·85		(Binford & Palm, 1994)
	60	0	DPPC	0·007			0·11	0·15	(Hildebrand *et al.* 2002)
		0·1		0·034			0·19	0·29	(Hildebrand *et al.* 2002)
	60	0	POPC	0·15	123	−1·5	0·39	0·57	(Hildebrand *et al.* 2003)
	60	0·1	DPPG	0·4	110	−4·4	0·28	0·4	(Hildebrand *et al.* 2004)
NaDC	30	0	DMPC	0·02			0·064	0·065	(Hildebrand *et al.* 2002)
	60	0	DPPC	0·033			0·21	0·23	
		0·1		0·14			0·20	0·39	
NaGC	20	0·15 NaCl	EPC	0·076					(Schurtenberger *et al.* 1985)
		0·5 NaCl		0·23					

Table 2 (*cont.*)

Surfactant	T (°C)	Salt concentration (M)	Lipid	K_R^{app} (mM^{-1})	K_R^0 (mM^{-1})	ΔH (kJ mol^{-1})	R_b^{sat}	R_m^{sol}	Reference
NaGCDC		0·15 NaCl	EPC	0·50					(Schurtenberger *et al.* 1985)
SDS	25	0·1	Sarcoplasmic reticulum	6–2			1·8		(Kragh-Hansen *et al.* 1998)
		0·13	Stratum corneum						(Lopez *et al.* 2000)
			30% Cer	2					
			50% Cer	4					
	25	0·164	POPC LUV		81	−19·5			(Keller *et al.* 2006a)
	28	0·11	POPC LUV	5–0·5	23	−21	0·28	2·2	(Tan *et al.* 2002)
			POPC SUV		60	−25			(Tan *et al.* 2002)
			POPC/POPG		60	−25			(Tan *et al.* 2002)
	37	KNPS	Erythrocytes	12					(Pantaler *et al.* 2000)
	50	0·11	POPC LUV		12·5	−26			(Tan *et al.* 2002)
			POPC SUV		30	−30			(Tan *et al.* 2002)
			POPC/POPG		45	−31			(Tan *et al.* 2002)
	30	0	DMPC	0·13			0·57	0·59	(Majhi & Blume, 2002)
	60	0		0·08			0·59	0·63	
		0·1					1·05	1·52	
	65	0·164	POPC LUV		25	−31·4			(Keller *et al.* 2006a)
	65	0·164	POPC LUV				1·5	2·7	(Keller *et al.* 2006b)
LDS	28	0·11	POPC SUV		40	−25			(Tan *et al.* 2002)
Surfactin	25	0·11	POPC	22		+38	0·22		(Heerklotz & Seelig, 2001)
	40			30		+7			
C_{16}TA Cl (CTAC)	25	0·025	POPC	9·5		−12			(Marcotte *et al.* 2005b)
C_{12}Pyr Cl	25	0·025	POPC	2·9		−0·06			(Marcotte *et al.* 2005b)
C_{16}Pyr Cl	25	0·025	POPC	15		−8·6			(Marcotte *et al.* 2005b)
C_{16}Pyr Cl	25	0·025	POPC/POPG	13		−15			(Marcotte *et al.* 2005a)
SDBS	25	0·1	EYPC	15					(Marcelino *et al.* 2007)
SLES	25	0·1	SBPC	50–10					(Cocera *et al.* 2002)

Rounded partition coefficients were obtained from references directly, by conversion of published values of K_X or K_C (in some cases, the corresponding R_b and v_L required for conversion into K_R had to be estimated) or on the basis of pairs of R_b and C_S^w according to (10). Please refer to original literature for detailed values and conditions and for information on additional systems.

https://doi.org/10.1017/S0033583508004721 Published online by Cambridge University Press

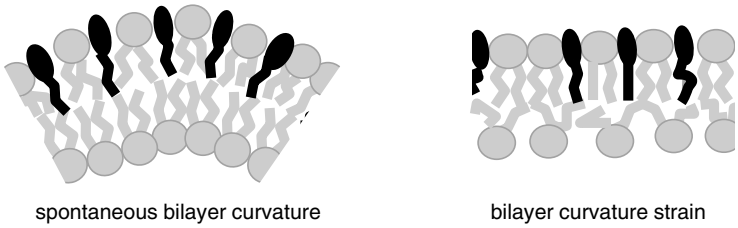

Fig. 4. Schematic representation of the bilayer couple concept. Insertion of molecules into a bilayer leads to an imbalance in area requirement between the two coupled lipid leaflets. If this cannot be relaxed via flip-flop of the molecules between the leaflets, it gives rise to a spontaneous bilayer curvature. In turn, the bilayer tends to bend locally (budding, shape transformations) and/or it develops a bilayer curvature strain which causes disorder (particularly in the low-pressure leaflet) and stores elastic energy.

3. Surfactant-induced changes in membrane properties

3.1 Bilayer couple concept of asymmetric bilayer expansion

Surfactants that insert, after addition to the external aqueous phase, quickly into the outer membrane monolayer but do not translocate to the inner monolayer (see Section 2.5) expand the bilayer asymmetrically. Sheetz and Singer (1974) compared this case to a bimetallic couple which tends to bend if the two leaflets expand differently (bilayer couple concept). Such effects may contribute to shape changes of vesicles (Mui *et al.* 1995) and erythrocytes as well as budding, ex- and invaginations, and endo- and exocytosis (see Section 5.1). If the bilayer is unable to bend to assume its spontaneous bilayer curvature, it develops a bilayer curvature strain by compressing the molecules in the overpopulated leaflet and/or expanding those in the underpopulated leaflet (Fig. 4). As a result, the partition coefficient from water into the overpopulated side of the vesicle (outside upon addition of surfactant to the suspension) decreases, whereas that into the under populated leaflet (outside upon surfactant extraction from pre-equilibrated vesicles) increases; the enthalpy of transfer depends also on the leaflet (Heerklotz, 2001). At a threshold value, bilayer curvature strain may also induce the transient rupture of the bilayer which anneals after translocation of some molecules to the underpopulated side (Heerklotz, 2001); see Section 3.6 on membrane leakage.

It should be noted that, in contrast to the bilayer couple effect, membrane permeant molecules can reduce the bending stiffness by moving to the stretched leaflet of a bent membrane.

3.2 Monolayer curvature strain

The previous section discussed that an imbalance *between* the optimum surface areas of the outer and the inner monolayer of a bilayer vesicle give rise to a bilayer curvature strain. The analogous effect occurs additionally *within* each monolayer.

In a relaxed, planar monolayer, the chains have to fill the volume determined by the lateral area needed by the head group and the thickness of the hydrophobic core. If the head group of a surfactant is too large or its hydrophobic part too small to fulfill this criterion, the ideal structure of the monolayer would be to assume a certain, convex (positive), so-called spontaneous or intrinsic curvature. However, this is impossible if the monolayer is part of a bilayer and competes with the opposite spontaneous curvature of the other leaflet (Fig. 5), because both are coupled with each other. Instead, the monolayers are 'bent straight' by an

https://doi.org/10.1017/S0033583508004721 Published online by Cambridge University Press

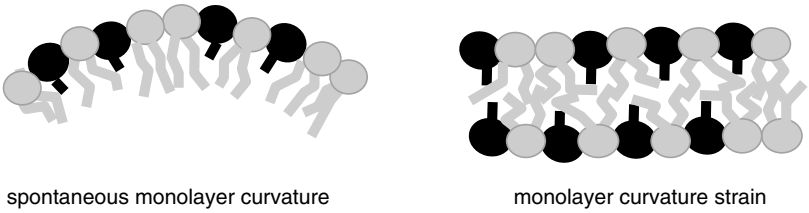

Fig. 5. Schematic representation of monolayer curvature effects. A relaxed lamellar packing requires that the hydrophobic part of the molecule fills the space that is determined by the area requirement of the head group and the thickness of the hydrophobic core. If the hydrophobic part is too small, the monolayer tends to bend outward (positive spontaneous curvature). Because such bending is incompatible with the other leaflet, it is compensated for by a disordering of the core, accompanied by a shrinking of its thickness.

elastic deformation giving rise to a monolayer curvature strain (Andelman *et al.* 1994; Epand & Epand, 1994).

Curvature strain can also be seen as the first moment of the lateral pressure profile of a membrane leaflet (Cantor, 1999; Van Den Brink-Van Der Laan *et al.* 2004).

It should be noted that the optimum lateral area of a head group depends not only on the molecular dimensions but also on order and mobility of moieties, hydration, hydrogen bonds, dipole- and electrostatic interactions. As a consequence, mixtures do not necessarily exhibit the average spontaneous curvature of their components. This is impressively illustrated by the fact that a mixture of anionic and cationic, micelle-forming surfactants can adopt a lamellar structure since head groups with different charge pack much closer together than equally charged ones in separate micelles (Meagher & Hatton, 1998). Equimolar mixtures of lysolipids and fatty acids (both micelle forming) can also form lamellar structures (Lemmich *et al.* 1998).

The major structural consequence of the curvature strain is a disordering of the chains. In turn, the membrane becomes thinner and more flexible. This is seen via deuterium NMR (Goni *et al.* 1986; Thurmond *et al.* 1994; Konig *et al.* 1997; Wenk *et al.* 1997; Heerklotz *et al.* 2004b), NMR relaxation studies (Otten *et al.* 2000), infrared spectroscopy (Goni *et al.* 1986; Binder & Klose, 2002; Meister & Blume, 2004), fluorescence spectroscopy (Lasch *et al.* 1990; Yegutkin, 1997), electron spin resonance (ESR) (Gallova *et al.* 1990), X-ray and neutron diffraction (Klose *et al.* 1996). The area per lipid increases. Data published by Karlovska *et al.* (2004) suggest that addition of, e.g. 10 mol% of C_nNO to EYPC increases the area per lipid by $\sim 4\%$ ($n = 18$) up to $\sim 6\%$ ($n = 8$).

Chain disordering is accompanied by changes in the interfacial and head group region of the membrane. These lead to spectral changes of probes (Gonzales-Manas *et al.* 1994; Heerklotz *et al.* 1994b) and tryptophan (Valpuesta *et al.* 1986) and altered affinity to 1-anilinonaphthalene-8-sulfonic acid binding (Alonso *et al.* 1982; Lasch *et al.* 1990). Strong detergents may also change the average orientation of the lipid head group to a slightly more 'upright' position (reducing the surface area requirement) (Otten *et al.* 1995; Heerklotz *et al.* 2004b) but no such effect was observed for C_8Gluc, a weak detergent (Wenk *et al.* 1997; Heerklotz *et al.* 2004b). The lateral area expansion of the membrane by detergents could be quantified by fluorescence resonance energy transfer (FRET) measurements (Lantzsch *et al.* 1996).

Surfactants with a positive spontaneous curvature tend to be enriched in membrane environments with positive real curvature, for example in the outer leaflet of small unilamellar vesicles

https://doi.org/10.1017/S0033583508004721 Published online by Cambridge University Press

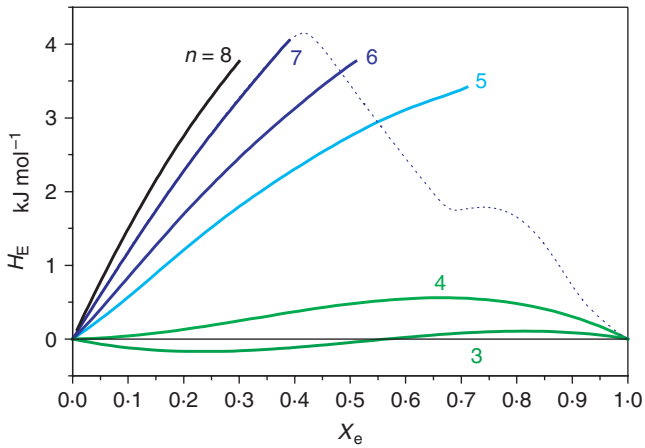

Fig. 6. Excess enthalpy functions of systems of POPC with detergents $C_{12}EO_n$ (n as indicated in the plot) at 25 °C. Bold solid lines correspond to exclusively lamellar phase ranges (i.e. the curves end at X_b^{sat}, in this range, $X_e = X_S^b$), the dotted line illustrates the typical behaviour of $H_E(X_e)$ in the coexistence and micellar phase ranges. The plot is compiled on the basis of data reported by Heerklotz *et al.* (1997, 1998). See discussion in Sections 3.2 and 4.3.

(enrichment of 3:1 for lyso-PC; Bhamidipati & Hamilton, 1995) or at the caps or the equator of prolate or oblate ellipsoid-shaped vesicles, respectively. This reduces the bending modulus of the membrane, can induce local shape changes that cannot be explained by bilayer couple effects (Hagerstrand *et al.* 2004) and can contribute to the formation of ultra-flexible liposomes (see applications discussed in Section 5.2).

Thermodynamically, monolayer curvature strain is governed by strong enthalpy–entropy compensation. The disturbance of intra- and intermolecular interactions causes a considerable endothermic excess enthalpy, H_E, but, at the same time, a gain in entropy due to increased motional and conformational freedom of the groups and molecules (Heerklotz *et al.* 1998). Figure 6 shows the excess enthalpies of surfactants $C_{12}EO_n$ and POPC, respectively, in the mixed membrane (i.e. sublytic) range (except for the dotted curve illustrating the effect of solubilisation). The excess enthalpies at a given X_e are the more positive the larger n becomes, i.e. the more positive the spontaneous curvature of the surfactant.

As outlined in Section 2.7, the free energy of curvature strain was discussed as the major reason rendering the product of $K_R \times$ CMC of non-ionic systems below 1. The lower this product, the stronger the membrane strains induced by a non-ionic surfactant appear to be (Heerklotz & Seelig, 2000a).

The intrinsic curvature of molecules is determined from lattice parameters of curvature-relaxed inverse hexagonal and other non-lamellar phases (Rand *et al.* 1998; Fuller & Rand, 2001). When it comes to curvature strain in a mixed membrane, it must, however, be kept in mind that the intrinsic curvature of a mixture is not necessarily the average of those of its components (cf. above). Other parameters that are related to the effect of membrane additives on monolayer curvature strain are shifts in the lamellar-to-inverse hexagonal transition temperature of a suitable lipid (e.g. POPE or DiPoPE) (Epand *et al.* 1988; Matsuzaki *et al.* 1998), the critical composition for the onset of solubilisation (R_b^{sat}) (Andelman *et al.* 1994) and changes in membrane area and thickness (Lantzsch *et al.* 1996).

https://doi.org/10.1017/S0033583508004721 Published online by Cambridge University Press

3.3 Surfactants forming complexes and mixing favourably with lipids

There are various effects by which surfactants may interact favourably with membrane lipids, such as the relaxation of a pre-existing curvature strain, direct interactions by hydrogen bonds or water bridges, electrostatic or dipole interactions. Mixtures of $C_{12}EO_3$ with fluid POPC show an exothermic enthalpy of mixing, H_E at low X_S^b (Heerklotz *et al.* 1998) (see Fig. 6). The composition dependence, $H_E(X_S^b)$, implies exothermic multibody interactions in statistically occurring arrangements of one lipid with two detergents in a largely random mixture [see Eq. (24)]. This enthalpic interaction, however, is largely compensated by an accompanying loss of entropy so that the free energy of formation of the arrangement is small compared to thermal energy. Similar effects but weaker and requiring larger multibodies were also found for $C_{12}EO_n$ with $n = 4$–6. A detailed MD study of a POPC/$C_{12}EO_4$ mixture (Schneider & Feller, 2001) revealed, in agreement with experimental data (Volke & Pampel, 1995; Klose *et al.* 1999) and Monte Carlo simulations (Klose & Levine, 2000), that the detergent is ordered upon insertion into the bilayer, the membrane becomes more densely packed and the lipid head group is gradually dehydrated. Both the chain length mismatch and the effective size of the head group are reduced. This means that there is a specific, well detectable interaction, but it does not seem to be appropriate to refer to it as a complex since its stability is marginal.

If inserted into a gel phase of DMPC or DPPC, $C_{12}EO_4$ and $C_{12}EO_5$ can form compound complexes with the lipid as implied by its phase behaviour (Madler *et al.* 1994, 1998; Pfeiffer *et al.* 2006). A de-mixing in the gel phase is also indicated by the splitting of DSC peaks of ESM mixed with TX100, $C_{10}EO_8$ and deoxycholate into a peak at $\sim T_m$ of the lipid and a second peak at $\sim$3–8 K lower temperature (Ollila & Slotte, 2002). The cubic and inverse hexagonal phase-forming surfactant $C_{12}EO_2$ (Funari *et al.* 1996) can stabilise the lipid gel phase (Binder & Klose, 2002), fatty acids with saturated chains form complexes with lipids in the gel phase and increase the melting temperature (Inoue *et al.* 2001). Some of these effects show some resemblance to the interactions of cholesterol with lipid membranes.

3.4 Surfactant-induced 'melting' of gel and ℓo phases

Most surfactants tend to shift the gel-to-liquid crystalline 'melting' transition temperature of lipids to lower values (Goni *et al.* 1986), i.e. their addition to a gel membrane may 'melt' lipids (depending on concentration and temperature). Interestingly, this effect is (in contrast to many others) not proportional to the spontaneous curvature. Instead, the interaction of surfactants with gel and liquid ordered (ℓo) phases (Ipsen *et al.* 1987, 1989) is widely governed by the very weak miscibility of surfactants with the tightly packed, ordered phase. The presence of the surfactant renders a phase more favourable for the lipid because it reduces its activity, approximately expressed by the mole fraction X_L, and hence its chemical potential, $\mu_L = \mu_L^0 + RT \ln X_L$, in this phase. This is equivalent with the statement that the addition of surfactant stabilises a membrane phase by $RT \ln X_L$ due to the entropy of mixing. Hence, preferential insertion into the fluid phase shifts the gel–fluid equilibrium in favour of the fluid phase. The effect of a certain preference of a surfactant for the fluid over an ordered phase was modelled by Keller *et al.* (2005b). In the extreme case, when the detergent mixes ideally with the fluid phase but is completely excluded from the gel, the T_m shift would be described by the general equation for the freezing point depression (Inoue *et al.* 1986):

$$T_m(X_S^b) - T_m(0) = -\frac{RT_m^2}{\Delta H} X_S^b. \tag{33}$$

https://doi.org/10.1017/S0033583508004721 Published online by Cambridge University Press

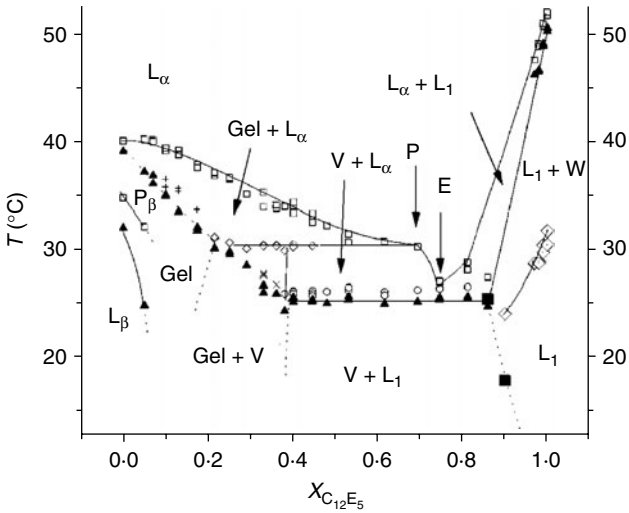

Fig. 7. Pseudo-binary phase diagram of DPPC–$C_{12}EO_5$ reported by Pfeiffer *et al.* (2006) and reproduced with permission, copyright Elsevier (2006). It comprises the following phases: liquid–crystalline (L_α), different, not fully characterised gel phases (Gel, L_β), gel complex (V), ripple ($P_{\beta'}$), micellar (L_1) and micellar 'clouded' (L_1+W) and a eutectic (E) and a peritectic (P) point.

Equation (33) implies that the shift in the melting temperature, T_m, is independent of the specific properties of the surfactant (as long as the ΔH of melting is not strongly affected) and proportional to its mole fraction in the membrane, X_S^b, with a proportionality constant corresponding to ~ -24 K (i.e. 10 mol% of surfactant decrease T_m by 2·4 K) for DPPC ($\Delta H = 34$ kJ mol^{-1}, $T_m \sim 314$ K) and ~ -33 K for DMPC ($\Delta H = 25$ kJ mol^{-1}, $T_m \sim 297$ K).

This is essentially in line with experimental data on DMPC–$C_{12}EO_4$ (Madler *et al.* 1998), DPPC–$C_{12}EO_5$ and DMPC–$C_{12}EO_5$ (Pfeiffer *et al.* 2006) and DPPC–C_{12}Gluc (Carion-Taravella *et al.* 2002). For DPPC–C_{12}Malt (Carion-Taravella *et al.* 2002) and DPPC–$C_{12}EO_4$ (Madler *et al.* 1994), the range of surfactant-induced melting is limited by gel phase complexes/demixing and peritectics and the initial slope dT_m/dX_S^b seems slightly less steep.

The range of linear T_m shifts with increasing X_S^b is typically limited by the occurrence of eutectic or peritectic points and, finally, membrane solubilisation at higher X_S^b (cf. also Fig. 7). However, the minimum T_m (at any X_S^b) seems to increase with increasing spontaneous curvature of the detergent, reflecting the lower capacity of stronger perturbants to be incorporated. For DPPC (T_m corresponds to 41 °C), it reaches down to below 25 °C for the lamellar phase-forming C_{12}Gluc (Carion-Taravella *et al.* 2002), $\sim$25 °C for $C_{12}EO_5$ (Madler *et al.* 1998) and to $\sim$29 °C for $C_{10}EO_5$, to $\sim$35 °C for $C_{10}EO_6$ (Inoue *et al.* 1994b) and C_{12}Malt (Carion-Taravella *et al.* 2002), and 38 °C for $C_{10}EO_7$ (Inoue *et al.* 1994b).

As discussed above, even low amounts of perturbants in a gel phase may be sequestered from ordered clusters into lattice defects surrounding them, as shown for pyrene by Galla and Sackmann (1974) and discussed also for surfactants (Inoue *et al.* 1994a; Arnulphi *et al.* 2007). The partitioning of lipids into the fluid clusters may play a role in kinetic and mechanistic aspects of surfactant-induced melting. Ultrasonic measurements have shown that the addition of $C_{12}EO_5$ increased the relaxation time of the melting transition of DPPC (Pfeiffer *et al.* 2006).

https://doi.org/10.1017/S0033583508004721 Published online by Cambridge University Press

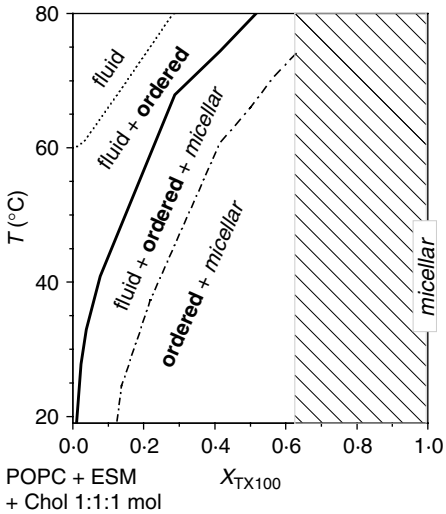

Fig. 8. Pseudo-binary phase diagram of a lipid mixture capable of forming a ℓo phase, POPC–ESM–Chol (ratio fixed at 1:1:1 mol) interacting with TX100. With increasing mole fraction of TX100, X_{TX} ($\sim X^{b}_{TX}$ in this case) and decreasing temperature, the system forms fluid, ordered and micellar phases. The range shaded in grey was not investigated. Plotted based on data from Heerklotz (2002).

3.5 Detergent-induced formation or promotion of ℓo domains

Taking into account the phenomenon of surfactant-induced melting as discussed in the previous section, it may be surprising that the phase behaviour of a so-called 'lipid raft' mixture (POPC/ESM/Chol 1:1:1 mol with varying concentrations of TX100) implied that the addition of TX100 promotes ordered domains rather than dissolving them (Heerklotz, 2002) (see Fig. 8).

Thermodynamic equilibrium simulations revealed that the induction of ordered domains by a membrane-disordering surfactant requires a mixture of two or more lipids and a non-ideal, unfavourable interaction of the surfactant with one of these lipids (Keller *et al.* 2005b). Measurements of such pair-interaction energies in the quaternary system have indeed revealed a strong 'repulsive' interaction between TX100 and Chol in fluid membranes (Tsamaloukas *et al.* 2006) (and a favourable interaction between ESM and Chol). If the free energy penalty from Chol–TX100 contacts in a mixed fluid phase overcompensates for the effect of the entropy of mixing, the system tends to avoid these contacts by partially separating Chol (along with ESM) and TX100 (along with POPC) into different domains.

This concept of detergent-induced domain formation is similar to the promotion of ordered domains by addition of highly flexible lipids with highly unsaturated chains (Wassall *et al.* 2004; Bakht *et al.* 2007).

Nicolini *et al.* (2004) concluded from SANS experiments that TX100 reduces the abundance of small domains in a POPC/SM/Chol (1:1:1 mol) mixture; this finding alone could be explained either by a growth or coalescence of small (ordered) domains or by their disintegration. Garner *et al.* (2008) (see their Fig. S4, supplement) showed via atomic force microscopy that different detergents differ in their suitability to selectively solubilise ℓd domains in supported bilayers with pre-formed domains. Starting, however, with a homogeneous ℓd lipid mixture, the addition of Triton was monitored to induce the formation of ℓo domains prior to selective solubilisation of the ℓd phase. Detergent-induced domain formation was also detected *in vivo* (van Rheenen *et al.*

https://doi.org/10.1017/S0033583508004721 Published online by Cambridge University Press

2005). These findings challenge the assumption that DRM fractions resemble *in vivo* membrane domains (rafts); see Section 5.4.

3.6 Membrane permeabilisation

Surfactants may enhance the flip-flop of lipids and amphiphilic compounds and the passive diffusion of solutes across the membrane. Pantaler *et al.* (2000) studied the surfactant-induced flip-flop of a NBD-labelled lipid across erythrocyte membranes and observed that strong detergents undergoing a fast flip-flop themselves (such as Triton or $C_{12}EO_8$) are most active, reaching, e.g. a lipid flip rate of 0·002 min^{-1} at $R_b \approx 0{\cdot}01$. The same effect seems to require larger amounts of weak detergents (e.g. $R_b \approx 0{\cdot}2$ for $C_{12}Gluc$, 0·1 for $C_{12}EO_3$) or detergents with a slow flip-flop (e.g. $R_b \approx 0{\cdot}07$–0·3 for $C_{12}Malt$, $C_{12}TAB$, SDS and $C_{11}FA$). Demina *et al.* (2005) measured a relative increase of the flip rates of NBD-PE proportional to the concentration of Brij30 (main component $C_{12}EO_4$) with a slope of 0·01 μM^{-1}. Hagerstrand *et al.* (1998) studied the effect of surfactants of different charge on the translocation of PS across erythrocyte membranes by monitoring FITC–annexin V binding. Surfactants may enhance both flip-flop and passive diffusion by chain disordering (increasing diffusion and possibly partition coefficients) and membrane thinning.

At higher concentration, surfactants may induce membrane leakage. This is usually detected by entrapping water-soluble probes of a certain size within vesicles, where their fluorescence is quenched (Ruiz *et al.* 1988). Examples for self-quenching probes are carboxyfluorescein (CF) (de la Maza & Parra, 1994b), calcein (Wieprecht *et al.* 1999) and fluorescent dextran (Ladokhin & White, 2001), and a frequently used dye-quencher pair is ANTS–DPX (Duzgunes *et al.* 1985; Ladokhin *et al.* 1995). Probe molecules that can pass through the membrane via a leak are greatly diluted in the solution outside the vesicle and show fluorescence. Leakage is easily detected but the fluorescence intensity is not proportional to the released fraction of dye and a detailed quantitative evaluation is not trivial (Ladokhin *et al.* 1995). An alternative approach has been described entrapping solid particles of γ-Fe_2O_3 with a size of 8 nm within vesicles (Lesieur *et al.* 2003). The entrapped iron particles are visible on cryo-TEM pictures. The results of leakage experiments are best expressed in terms of the partition coefficient of the surfactant and the surfactant content in the membrane, e.g. R_b, causing a certain percentage of de-quenching after a certain time (or a characteristic rate by which dequenching increases); such results require considering data collected at varying lipid concentration, C_L (e.g. de la Maza *et al.* 1998a; Heerklotz & Seelig, 2007). Results obtained at a single C_L are valid only at this C_L.

Surfactants can increase the membrane permeability to aqueous solutes by a variety of mechanisms. Bilayer curvature strain caused by asymmetric insertion of, e.g. surfactants or peptides into a bilayer (cf. Section 3.1) may lead to mechanical failure of the membrane, allowing for the relaxation of the imbalance followed by the annealing of the membrane. This is a possible explanation for transient leakage that stops after reaching a characteristic, partial release of entrapped dye; see Lesieur *et al.* (2003) and Heerklotz & Seelig (2007) and peptide studies discussed in Section 5.1.

Monolayer curvature strain is another possible reason for membrane leakage, since it can be partially relaxed by the sequestering of surfactants into highly curved rims covering the hydrophobic edges of toroidal pores or leaks (cf. Fig. 9). Karatekin *et al.* (2003) measured line tensions of tension-induced pores in giant liposomes in viscous medium; 0·6 mM of Tween reduced the line tension along pore edges in DOPC from 8 to 0·2 pN, giving rise to long lifetimes of the

https://doi.org/10.1017/S0033583508004721 Published online by Cambridge University Press

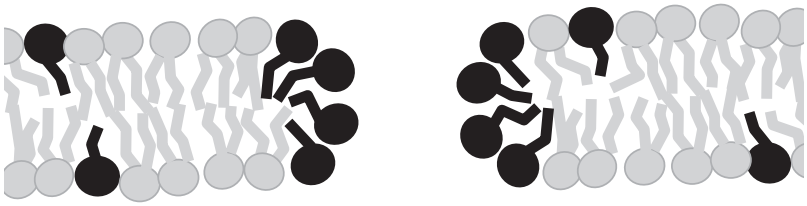

Fig. 9. Schematic representation of a toroidal membrane pore induced by a surfactant. The hydrophobic edges of the pore are covered with a highly curved, surfactant-rich rim.

pores. The same effect may account for the observation that non-cytotoxic concentrations of $C_{12}EO_8$ render cell membranes more sensitive to electroporation (Kanduser *et al.* 2003). Above critical surfactant content, leaks appear spontaneously so that de-quenching tends toward 100% after a sufficient period.

The size of the pores as illustrated by Fig. 9 must be considered to depend on concentration of the surfactant, the spontaneous curvatures of the molecules and the bending and splay elasticity of the membrane. Note that the molecules in the pore experience a positive curvature in one dimension (normal to the membrane) but a negative one in the other (top view of the pore). The threshold concentration of forming such pores is thus expected to correspond to their minimum size, which might account for channel-like quantisation of the conductivity and a selectivity regarding the size of permeants. Hence, such findings alone should not be interpreted as compelling evidence of the formation of specific channel-forming oligomers (see Section 5.1). Whether these pores increase in size or in number with increasing surfactant concentration should depend on the interplay between line tension and mixing entropy. A growth in pore size may give rise to cup-shaped vesicles (Saitoh *et al.* 1998) or even essentially flat bilayer sheets (see also next section).

Octyl glucoside (C_8Gluc) induces a strong increase in membrane permeability for chloride above $R_b \geqslant 0{\cdot}4$, which is explained in terms of locally destabilising detergent-detergent contacts in the membrane that become abundant at this concentration (Ueno, 1989). The detergent-per-lipid mole ratio in the membrane giving rise to 50% dequenching of entrapped carboxyfluorescein after 30 min is $R_b(50\%\ \mathrm{CF}) \approx 1{\cdot}0$ for C_8- and C_{10}Gluc (de la Maza *et al.* 1998a). Strongly curvature-active detergents are far more active in membrane permeabilisation. $C_{12}EO_8$ and TX100 cause a practically instantaneous, complete leakage of EPC vesicles at $R_b \approx 0{\cdot}4$; smaller detergent concentrations cause leakage at slower, measurable rates (Edwards & Almgren, 1990) for TX100, $R_b(50\%\ \mathrm{CF}) \approx 0{\cdot}15$ (de la Maza & Parra, 1994b). The permeabilisation of vesicles of stratum corneum lipids by SDS decreases continuously with increasing ceramide concentration from $R_b(50\%\ \mathrm{CF}) \approx 0{\cdot}1$ (30% ceramide) to $\approx 0{\cdot}4$ (50%) (Cocera *et al.* 1999). Permeabilisation of EYPC vesicles by C_{12}Malt requires $R_b(50\%\ \mathrm{CF}) \approx 0{\cdot}53$, showing slower and more complex kinetics since this detergent shows a slow flip-flop across the membrane (de la Maza & Parra, 1997).

The permeabilising activity of certain antimicrobial peptides (Prenner *et al.* 2001) and surfactants (e.g. SDS; Apel-Paz *et al.* 2005) is reduced or inhibited by cholesterol. Cholesterol acts both by reducing the partition coefficient and by mechanically stabilising the membrane, thus increasing the R_b causing a certain leakage signal (Cocera *et al.* 2003). Vesicles in the ℓo phase are more resistant against permeabilisation by Triton but not by C_8Gluc (Tamba *et al.* 2004), a fact that is in line with the resistance of membrane fragments against solubilisation by TX100 but not C_8Gluc (see Section 5.4).

https://doi.org/10.1017/S0033583508004721 Published online by Cambridge University Press

4. Solubilisation, reconstitution, non-lamellar phases

4.1 The three-stage model

An excellent, still almost generally used description of membrane solubilisation is the 'three-stage model' proposed by Helenius and Simons (1975) in their legendary review. They denote stage I as 'detergent binding'; micelles dissolve and surfactants partition into the membrane. Stage II is 'lamellar–micellar phase transition'; it starts when the membrane is saturated with surfactant and lipid-saturated micelles appear in coexistence. In stage II, only the proportions between lamellae and micelles change but their internal compositions (e.g. expressed as the surfactant-to-lipid mole ratios R_b^{sat} and R_m^{sol}, respectively) are constant. When only micelles are left, the system enters stage III, denoted 'size decrease of mixed micelles'. In this stage, no lamellar structures are left and the size of the mixed micelles decreases, typically with decreasing relative lipid content.

Hence, the three-stage model explicitly distinguishes three characteristic types of aggregates, lamellar, large micellar and small micellar, plus surfactant monomers in solution. The transition from lamellar structures to large micelles often resembles, to a good approximation, a first-order phase transition as indicated by the coexistence of lamellae and micelles of fixed composition (Section 4.3). The discussion of structural pathways given below (Section 4.2), however, will show that such a pseudo-phase may comprise a number of structurally diverse yet thermodynamically similar types of aggregates or local molecular arrangements.

The transition from large (typically cylindrical, see Section 4.2) to small spherical micelles may, in general, also involve a coexistence but it cannot usually be described reasonably well as a true phase transition (see Section 4.11).

4.2 Aggregate structures observed upon solubilisation and reconstitution of fluid membranes

The fact that the three-stage model distinguishes between three characteristic states does not rule out that each of these 'states' may comprise a variety of specific local and principal structures and does not provide a specific description of intermediates or kinetic pathways. Let us discuss three pathways that show some similarity but differ from each other in some respects.

(i) *Coexistence of extended lamellae and cylindrical micelles.* One solubilisation pathway describes the solubilisation to cylindrical micelles involving a series of stages and possible intermediate structures encountered with increasing surfactant concentration as explained in the following (cf. Fig. 10). At low concentrations, the surfactant molecules partition between the vesicles and the aqueous phase. They perturb membrane packing gradually and may lead to a growth of small vesicles to sizes of the order of 100 nm. At higher concentrations, the surfactant starts to form membrane leaks or pores by stabilising the hydrophobic edges with a surfactant-rich rim (cf. Fig. 9). These pores may grow in size and/or number with increasing R_b and lead to open, cup-shaped vesicles or quasi-planar bilayer sheets. When the membrane is saturated with surfactant ($R_b = R_b^{sat}$), long, flexible cylindrical micelles (also referred to as worm-, rod- or thread-like) appear in coexistence. The proportion of the lamellar structures decreases until only cylindrical micelles are left. With increasing surfactant concentration, these decrease in length and are ultimately transformed into spherical micelles. Comparing this sequence with the three-stage model, lamellar sheets seem to still belong to stage 1 (although their edges may also show some micelle-like properties) and the 'large micelles' are cylindrical.

https://doi.org/10.1017/S0033583508004721 Published online by Cambridge University Press

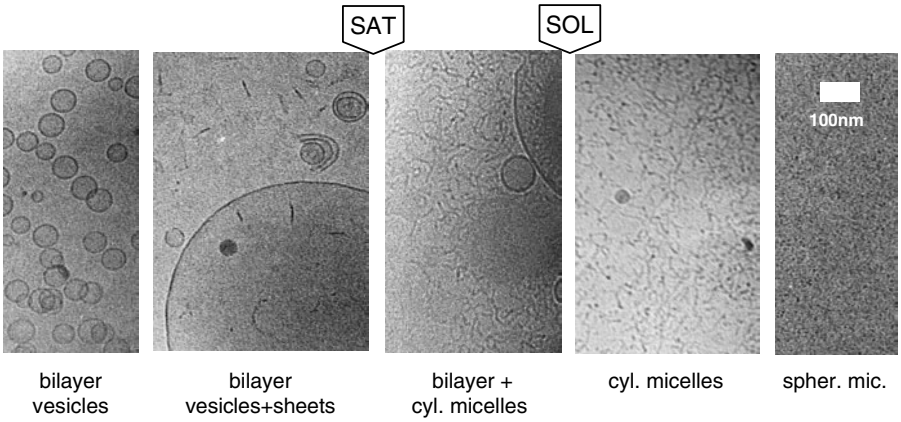

Fig. 10. Cryo-TEM images of mixtures of sodium cholate and EPC with increasing R_e from left to right. Adapted from Walter *et al.* (1991), courtesy of the American Biophysical Society.

This solubilisation scenario via cylindrical micelles applies to cholate (Walter *et al.* 1991) and other bile salts (Hjelm *et al.* 1992; Long *et al.* 1994; Moschetta *et al.* 2002), $C_{12}EO_8$ (Edwards & Almgren, 1991; Gutberlet *et al.* 2000), C_8Gluc (Vinson *et al.* 1989), $C_{12}EO_6$ (Gutberlet *et al.* 2000) and TX100 (Edwards *et al.* 1989). Similar structures were also found in systems of bile salts with EYPC, sphingomyelin and cholesterol (Nibbering *et al.* 2002).

(ii) *Coexistence of micellar and lamellar microenvironments in perforated vesicles.* A second pathway involving networks of cylindrical micelles arising from perforations was described particularly for charged surfactants. Addition of surfactant gives rise to perforated vesicles or stomatosomes. The detergent-rich rims covering the edges of the perforations resemble 'half-cylindrical micelles'. Increasing detergent concentration increases the number of pores until the pores touch each other and only the rims are left as a network of entangled, branched, interconnected cylindrical micelles. Addition of further surfactant leads to rather linear cylindrical, then (potentially) oblate discoidal and finally to spherical micelles (Gustafsson *et al.* 1997; Almgren, 2007). Kadi *et al.* (2004) describe such a behaviour for glycerol monooleate vesicles upon addition of C_{16}TAC. Although this pathway involves the same principal topologies, lamellar, cylindrical, spherical, it differs from pathway (i) in a number of respects.

(iii) *Solubilisation by continuous shrinking of lamellar sheets to disc micelles.* A third, at least formally possible pathway proceeds via leaky to open vesicles, and further to lamellar sheets which shrink to discoidal or oblate-shaped micelles and transform, finally, into spherical micelles. The concept goes back to the mixed disc model by Mazer *et al.* (1980). Originally, this pathway was believed to apply generally, but this suggestion was ruled out by cryo-TEM and neutron scattering results for many (if not all) systems. Walter *et al.* (1991) have reviewed the observations of cylinders and discs in detail, and Kozlov *et al.* (1997) provided a theoretical analysis of the two alternative structures.

Mixtures that form discoidal micelles are, for example, those of DMPC with short-chain lipids such as dihexanoyl-PC (D7PC) (so-called bicelles; cf. below) (Luchette *et al.* 2001) and with PEG-grafted lipids (Johnsson & Edwards, 2003). The mere existence of discs, however, is no

https://doi.org/10.1017/S0033583508004721 Published online by Cambridge University Press

proof for pathway (iii) to apply; Van Dam *et al.* (2004) also show cylindrical micelles for DMPC–D7PC and suggest that discoidal micelles are formed at intermediate D7PC concentrations between cylinders and small spheres. Furthermore, discs may also play a role as metastable intermediates, particularly upon reconstitution (see next section).

Addition of substantial but still sub-solubilising amounts of C_8Gluc to LUV was shown to induce the formation of small vesicles termed SUV* (Ueno *et al.* 2003).

4.3 Thermodynamics of fluid membrane solubilisation

The key to the understanding of solubilisation is monolayer curvature strain as explained in Section 3.2. The dotted line in Fig. 6 illustrates that curvature strain as represented by the excess enthalpy H_E reaches its maximum at X_b^{sat}, and is then relaxed upon solubilisation to rod-like (cylindrical) micelles and further by the rod-to-sphere transition. Note that here H_E is defined analogously to (17) but as a function of X_e [see Eq. (34) below], and is thus not specific to bilayers but as a mean value for all existing aggregates. The figure also implies a critical value of H_E that is related to the maximum curvature strain that can be accommodated by a POPC membrane. All systems shown in the figure start solubilisation when H_E reaches ~ 4 kJ mol^{-1}; the larger the head group, the steeper is the H_E curve and the less detergent is needed to reach the critical value.

The state of a lipid–surfactant–water system at a given composition, temperature (T) and pressure (p) is represented by a phase diagram. A ternary system at constant T, p is usually represented by a phase triangle with the pure components at the corners (see Section 4.10); taking into account the effect of temperature expands the triangle to a prism. Different strategies lead to a much more convenient, two-dimensional plot depending on the aim of the study. A way to eliminate monomers and partitioning effects is to introduce an effective mole fraction X_e:

$$X_e \equiv \frac{C_S - C_S^{aq}}{(C_S - C_S^{aq}) + C_L} \tag{34}$$

or, analogously, the mole ratio (Lichtenberg, 1985; Lichtenberg *et al.* 2000)

$$R_e \equiv \frac{C_S - C_S^{aq}}{C_L}. \tag{35}$$

When virtually all surfactant resides in aggregates (lamellae, micelles or others), the total $X_S = X_e$. Hence, a pseudo-binary, $T(X_e)$, phase diagram refers to the average surfactant content of all coexisting aggregates and assumes the surfactant to be fully hydrated but excludes surfactant monomers. The state of the surfactant–lipid phases is fully determined by X_e (abscissa) and T (ordinate) for a given pressure (see, for example Figs 7 and 8).

If the total lipid and surfactant concentrations (not explicitly specified) are not large enough to render aqueous monomers negligible, additional information on partitioning is required to calculate X_e and read the corresponding phase state from the diagram. The latter problem is avoided by a rectangular, pseudo-binary $C_S(C_L)$ diagram sacrificing the temperature axis (Fig. 11) (Lichtenberg, 1985; Lichtenberg *et al.* 2000).

It should be emphasised that phases in the strict sense are macroscopically separate volume ranges, such as those formed by octanol/water or oil/water. To a certain approximation, coexisting types of microenvironments in a colloidal dispersion can, however, be treated as pseudo-phases. Two different pseudo-phases must show a different topology so that a transition

https://doi.org/10.1017/S0033583508004721 Published online by Cambridge University Press

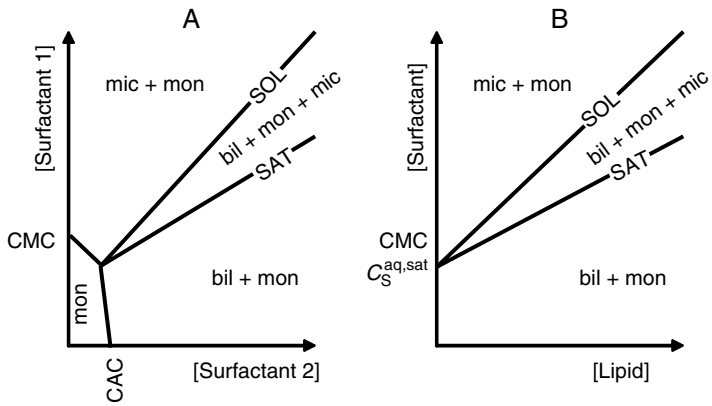

Fig. 11. Models for surfactant–lipid phase diagrams. Schematic illustration of ideal phase diagrams for a surfactant mixture (no 'lipid', *a*) and a binary lipid/surfactant mixture (CAC of lipid ≈ 0, *b*).

proceeds via phase coexistence and cannot be realised as a gradual transformation. For the solubilisation pathway involving cylindrical micelles, there is only one transition that fulfills this requirement well: the step from a lamellar to a cylindrical geometry. Hence, in spite of the complexity of the structures involved, a corresponding lipid/surfactant phase diagram distinguishes only three pseudo-phases: the aqueous solution of monomers (mon), the lamellar or bilayer (bil) phase (regardless of whether vesicles or lamellar sheets are concerned) and the micellar (mic) phase (cylindrical or spherical, see Section 4.11). For the solubilisation pathways via discoidal micelles or via networks of cylindrical micelles, there is no principal discontinuity in topology from one type of particle to another, and one may expect no pseudo-phase transition to occur. There is, however, a topological step between lamellar membrane patches and the curved rims of pores or discs. Since the rims are also enriched in detergent compared to the bulk bilayer, perforated bilayers, lamellar sheets and discs may actually resemble a coexistence of two phases, rim and planar, although these structures are combined in one type of particle (Kadi *et al.* 2004). Then, thermodynamics may refer to the onset of membrane perforation as the beginning of solubilisation, whereas most structural methods (including light scattering) would assign the onset of solubilisation to the situation when the gradually shrinking sheets, discs or networks reach a certain size.

Let us illustrate the principal features of a $C_S(C_L)$ diagram by first considering the ideal phase behaviour of a mixture of a micelle-forming surfactant (S1) and a bilayer-forming surfactant (S2) in dilute solution (Fig. 11*a*). At very low concentrations, monomers of S1 and S2 are dissolved in water. Pure S1 starts to self-associate to micelles at the CMC(1), and pure S2 aggregates to bilayers at the critical aggregation concentration, CAC(2). Small amounts of S1 promote the aggregation of S2 and *vice versa*, so that the phase boundary to the micellar phase decreases with increasing concentration of S2. A transition from the monomer range to a coexistence of monomers, micelles and bilayers is possible only at a single point with the coordinates $C_{S1} = C_{S1}^{aq,sat}$ and $C_{S2} = C_{S2}^{aq,sat}$, since the monomer concentrations in the whole three-phase range are constant, $C_{S1}^{aq,sat}$ and $C_{S2}^{aq,sat}$. This is a requirement of Gibbs' phase rule (Cevc & Marsh, 1985), which implies that there is no degree of freedom for a three-phase coexistence of a three-component system at a given p and T. The constant slopes of the sat and sol boundaries represent the mole ratios of the surfactants in the micelles and bilayers, which must also be constant within the three-phase range, $R_b = R_b^{sat}$ and $R_m = R_m^{sol}$.

https://doi.org/10.1017/S0033583508004721 Published online by Cambridge University Press

Membrane lipids show an extremely low solubility, so that CAC$\approx$0 and the ideal phase diagram in the experimentally accessible concentration range is simplified as illustrated in Fig. 11*b* (Lichtenberg, 1985; Lichtenberg *et al.* 2000). The point of intersection of the boundaries shifts to the ordinate but remains below the CMC. The boundaries obey Eq. (29) with the slopes R_b^{sat} and R_m^{sol}, respectively, and a common intercept of $C_S^{aq,sat} = C_S^{aq,sol}$.

Hence, the 'extent of solubilisation', α, can be written as:

$$\alpha \equiv \frac{C_L^m}{C_L} = \frac{R_e - R_b^{sat}}{R_m^{sol} - R_b^{sat}} \tag{36}$$

and runs from 0 at the onset to 1 at the completion of solubilisation. If detergent or lipid is added to the mixture so that the system crosses the coexistence range, only α varies but the composition of the mixed membranes and micelles remains constant. Experimental parameters representing the state of the system should be a linear function of α within the coexistence range (Ollivon *et al.* 2000), and partial molar enthalpies of a titrant (lipid or surfactant) measured by ITC correspond to the derivative of the state function and should therefore be constant in the three-phase range (Heerklotz *et al.* 1996). As mentioned, the aqueous surfactant concentration should be constant as well (Heerklotz *et al.* 1994b; Paternostre *et al.* 1995; le Maire *et al.* 2000), see also vertical increase of the partitioning isotherm (Fig. 2).

This ideal behaviour is only approximately found for the pseudo-phase transition in colloidal systems. Micelles differ from a real, macroscopically separate phase by (1) a large interface between micelles and water, (2) the entropy of mixing of the micelles with water and (3) inter-micellar interactions. Then, the chemical potential no longer depends only on the composition of the micelles (R_m^{sol}) but also on their abundance, which increases in the course of solubilisation. The same applies to bilayer particles. It has been shown (Roth *et al.* 2000) that such effects account for the fact that the phase boundaries do not exactly share the same intercept with the ordinate, $C_S^{aq,sat} \neq C_S^{aq,sol}$ (Lichtenberg, 1993; Paternostre *et al.* 1995; Keller *et al.* 1997; Lichtenberg *et al.* 2000) and that the phase boundaries become non-linear in very dilute systems ($R_b^{sat} \neq$ const. for $C_L \rightarrow 0$).

Major deviations from the three-stage model were found for CHAPS (Viriyaroj *et al.* 2005), which shows a binding isotherm with two subsequent transitions indicated by steep increases of $X_e(C_S^{aq})$ (cf. Fig. 2) at $X_e \sim 0{\cdot}1$ and 0·21. As a result, literature values on R_b^{sat} and K depend strongly on the method and specific sample conditions used (see comparison in Beck *et al.* 2008). Lipid–cholate mixtures in pure water show a very unusual behaviour. The limiting compositions of coexisting bilayers and micelles are virtually the same ($R_b^{sat} \approx R_m^{sol}$) so that surfactant molecules added to the bilayer–micelle system partition almost exclusively into the aqueous phase ($C_S^{aq,sat} < C_S^{aq,sol}$) (Hildebrand *et al.* 2002). Note that this system shows comparatively strong, electrostatic inter-micellar interactions since the micelles are small (and thus many) and the charges are not screened by extra salt. Solubilisation, i.e. an increasing number of micelles, will increase this unfavourable contribution to $\mu_S^{0,m}$. If R_m is unchanged, μ_S^m increases and, to retain equilibrium, μ_S^{aq} and thus C_S^{aq} (and possibly R_b) will increase as well.

4.4 Solubilisation in systems comprising multiple lipids or surfactants

Homogeneous fluid mixed lipid membranes such as those of egg, brain or soy bean PC seem to behave very similar to one-component membranes and were not found to exhibit any qualitatively different solubilisation behaviour from one-component membranes. In fact, the values of K,

https://doi.org/10.1017/S0033583508004721 Published online by Cambridge University Press

R_b^{sat} and R_m^{sol} of egg yolk PC are very close to those reported for its major component, POPC (see Tables 1*a*–1*c* and 2). A much more complex behaviour, however, is encountered if the different lipids are capable of forming different membrane phases or domains. Even if the membrane is homogeneous and fluid at the onset of solubilisation (the other case is discussed in Section 4.5), the lipids will partition between coexisting membranes and micelles differently, so that those that are more compatible with a disordered environment are selectively solubilised whereas order-preferring lipids become enriched in the membrane. This effect was predicted to induce, under suitable conditions, a (re)appearance of ordered domains in membranes upon solubilisation (Keller *et al.* 2005b). Apel-Paz *et al.* (2005) showed that high surfactant concentrations (leading to the presence of micelles) rendered cholesterol-rich vesicles resistant against surfactant-induced leakage by selective solubilisation, whereas lower concentrations caused leakage. Their result also implies that, in contrast to what has been described for gel or fluid phases, ℓo phases can form stable, non-leaky vesicles in coexistence with mixed micelles. The local enhancement of sterol concentrations by selective solubilisation of PC from PC–sterol vesicles was also shown by FRET and discussed in relation to gallstone formation (Wrenn *et al.* 2001).

Systems of a lipid interacting with a mixture of surfactants (at fixed ratio) show pseudo-binary phase diagrams with curved boundaries. If the surfactants mix ideally, the reciprocal of the total surfactant concentration required for the onset of solubilisation in this case, C_S^{sat}, is the weighted sum of the reciprocals of the concentrations of the individual detergents alone that would be needed for solubilisation, C_{Si}^{sat} (Beck *et al.* 2008). The weighting is given in terms of the fraction of surfactant *i*, referred to as the sum of all surfactant concentrations, ξ_i:

$$\frac{1}{C_S^{sat}} = \sum \frac{\xi_i}{C_{Si}^{sat}} = \sum_i \frac{\xi_i K_i}{R_{bi}^{sat}(1 + K_i C_L)}. \tag{37}$$

The solubilising concentration of a single surfactant (C_{Si}^{sat}) can be expressed in terms of the lipid concentration (C_L) and the mole-ratio partition coefficient of surfactant *i* (K_i) and its critical mole ratio in the membrane, R_{bi}^{sat}, yielding the second equality in Eq. (37). The 'sat' phase boundary, $C_S^{sat}(C_L)$, for a system of two surfactants and one lipid is obtained from Eq. (37) as:

$$C_D^{sat} = \frac{R_{b1}^{sat}(K_1 C_L + 1) \cdot R_{b2}^{sat}(K_2 C_L + 1)}{\xi_1 K_1 R_{b2}^{sat}(K_2 C_L + 1) + \xi_2 K_2 R_{b1}^{sat}(K_1 C_L + 1)}. \tag{38}$$

Analogously, the 'sol' phase boundary obeys for ideal mixing:

$$\frac{1}{C_D^{sol}} = \sum_i \frac{\xi_i}{R_{mi}^{sol}\left(C_L + \dfrac{CMC_i}{1 + R_{mi}^{sol}}\right)} \tag{39}$$

yielding for a two-surfactant system:

$$C_D^{sol} = \frac{R_{m1}^{sol}\left(C_L + \dfrac{CMC_1}{1 + R_{m1}^{sol}}\right) R_{m2}^{sol}\left(C_L + \dfrac{CMC_2}{1 + R_{m2}^{sol}}\right)}{\xi_1 R_{m2}^{sol}\left(C_L + \dfrac{CMC_2}{1 + R_{m2}^{sol}}\right) + \xi_2 R_{m1}^{sol}\left(CC_L + \dfrac{CMC_1}{1 + R_{m1}^{sol}}\right)}. \tag{40}$$

The phase boundaries in such a system become non-linear and the compositions of the membranes and micelles are not constant throughout the coexistence range. The apparent (overall) partition coefficient and the critical mole ratio of all surfactant to lipid within the membrane for

https://doi.org/10.1017/S0033583508004721 Published online by Cambridge University Press

saturation, R_b^{sat}, of a surfactant mixture vary as a function of the lipid concentration. It should be noted at this point that many industrial (e.g. Triton, Lubrol, Tween series) as well as biological (e.g. surfactin) surfactants are actually mixtures of chemically related, but not identical, substances and may, under certain conditions, show such lipid-dependent variations of their key parameters.

4.5 Direct solubilisation of gel and ℓo membranes

Not too far below the melting temperature of the lipid, gel phases are typically molten by added detergent (Section 3.4) before, at higher surfactant concentration, the fluid membrane is solubilised. However, below a certain temperature ($\sim$25 °C in Fig. 7), the gel phase is converted directly into micelles without an intermediate fluid membrane.

If the surfactant-rich defects in a gel membrane do not acquire sufficient lipid, they will ultimately turn into a strongly curved, micelle-like state. Hence, the gel clusters break apart forming gel-like, surfactant-depleted (or virtually surfactant-free) lamellar sheets or discs surrounded by a surfactant-rich rim (Inoue *et al.* 1994a; Funari *et al.* 2001; Carion-Taravella *et al.* 2002). The sequestering of the surfactant to high local concentrations in defects accounts for the very low average values of R_b^{sat} observed for ordered phase membranes (Patra *et al.* 1998, 1999; Nyholm & Slotte, 2001; Heerklotz, 2002; Ollila & Slotte, 2002; Sot *et al.* 2002). With increasing surfactant concentration, the sheets may shrink (increasing the rim-to-core ratio) or coexisting, detergent-rich micelles might form. Carion-Taravella *et al.* (2002) distinguish between liquid and solid micelles. The surfactant content that is required to convert the whole system into a liquid micellar state, where all chains are disordered and the molecules mix, is governed by the affinity of the lipid to these micelles (Keller *et al.* 2005b).

It is not straightforward to define and detect the phase ranges in such a system. The core and perimeter of gel-like membrane particles with their characteristic compositions and packing properties may be well approximated as two coexisting phases, although they are combined within one type of particle (see also Section 4.3). Techniques revealing the molecular structure such as ESR (Inoue *et al.* 1994a), wide angle X-ray diffraction or other methods (Funari *et al.* 2001; Carion-Taravella *et al.* 2002) allow operators to distinguish gel particles from regular micelles. However, methods detecting the size of the particles such as turbidity and centrifugation assays fail to distinguish 'solid micelles' (small gel particles) from regular, 'liquid' micelles.

Galla and Sackmann's (1974) finding that cholesterol anneals defect structures between gel clusters in membranes suggest a different scenario for cholesterol-rich, ℓo phases. Indeed, cholesterol-rich membranes differ from both gel and fluid (Chol-free) membranes in requiring higher surfactant concentrations and more time to reduce turbidity to low values characteristic of small particles (Saez-Cirion *et al.* 2000). In contrast to gel membranes, they do not break apart into very small pieces upon addition of surfactant, but form much larger 'resistant' particles and can even form leakage- and solubilisation-resistant vesicles coexisting with detergent micelles (Apel-Paz *et al.* 2005).

4.6 Kinetics of solubilisation and reconstitution

Different kinetic mechanisms have been described for solubilisation and reconstitution processes (for a review, see Gradzielski, 2004). Reconstitution of vesicles from mixed micelles with bile

https://doi.org/10.1017/S0033583508004721 Published online by Cambridge University Press

salts was shown to proceed via the formation of metastable, discoidal structures that close themselves to vesicles driven by the line tension along the perimeter (Leng *et al.* 2003). The size of the vesicles is determined by the kinetics of their formation rather than the equilibrium state. Mechanistic aspects of the transition between bicelles and (perforated) lamellae were studied by time-resolved SANS (Wang *et al.* 2003).

Solubilisation could proceed via the reverse process, as described for a sequence of equilibrium structures in Section 4.2, pathway (iii), or involving metastable discoidal intermediates. However, Vinson *et al.* (1989) saw 'strings', most probably cylindrical OG/PC micelles, emerging directly from vesicles in cryo-TEM images. The '*in situ*' formation of micelles in the membrane followed by their separation from the vesicle was also described by Lopez *et al.* (1998). Cocera *et al.* (2004) measured fast relaxation times of 2 s or less for the desorption of mixed micelles from neutral or somewhat negatively charged vesicles super-saturated with SDS. The disintegration of pure detergent micelles is also relatively fast; pure SDS micelles were detected only for 10–30 s after (super-saturating) addition to vesicles (Cocera *et al.* 2004). However, since this '*in situ* micellisation' process requires the localisation of the detergent in both membrane leaflets, membrane permeation may become the rate-limiting step and the completion of solubilisation primarily by 'impermeant' detergents may require many hours or days as shown for SDS at room temperature (Cocera *et al.* 2004). Solubilisation is also slowed down by low temperatures (Schnitzer *et al.* 2005; Keller *et al.* 2006b) and highly ordered membranes such as purple membrane (Viguera *et al.* 1994) and vesicles of lipids containing saturated chains and/or substantial amounts of cholesterol (Schnitzer *et al.* 2005). It should be noted that the application of standard protocols to isolate DRM fractions (cf. Section 5.4) does not distinguish between thermodynamic and kinetic resistance.

4.7 Methods of detecting solubilisation

A variety of methods has been used to detect surfactant-induced transitions of lipid vesicles. An excellent method to detect phase boundaries or critical R_e values for transformations is ITC (Heerklotz *et al.* 1995, 1996, 1997; Keller *et al.* 1997; Wenk & Seelig, 1997a; Heerklotz, 2001, 2002; cf. Heerklotz & Seelig, 2000b for a review). To explore the composition-dependent mixing behaviour, vesicles can be titrated with surfactant micelles (solubilisation experiment) or *vice versa* (reconstitution experiment). The great sensitivity for transitions arises from the fact that the heat of injection does not primarily report on the state of the system (the existence of the first few micelles is hardly detectable) but on the process induced by the injection (the formation of micelles). Therefore, the heat usually changes its sign at the 'sat' boundary when injected surfactant is no longer transferred from micelles into the membrane but additional surfactant (and lipid) is solubilised from membranes to micelles.

For non-ionic detergents with high partition coefficients, the ITC experiments also yield a complete set of transfer enthalpies of detergent and lipid between membranes and micelles (Heerklotz *et al.* 1996) as well as the composition-dependent excess enthalpy function of the mixed aggregates (Heerklotz *et al.* 1998) in a rather straightforward manner. In the general case, a complete modelling of ITC solubilisation and reconstitution curves has to further take into account effects of membrane–water (re)partitioning and, for ionics, electrostatic interactions and composition-dependent changes in counter ion binding (see Keller *et al.* 2006b).

Micelles and lamellar structures in highly concentrated samples (typically 50 wt% of water) give rise to different solid-state ^{31}P NMR spectra (Jackson *et al.* 1982; Goni *et al.* 1986;

https://doi.org/10.1017/S0033583508004721 Published online by Cambridge University Press

Paternostre *et al.* 1988; Otten *et al.* 1995; Wenk & Seelig, 1997a; Heerklotz, 2002). This technique is particularly sensitive for lipids in micelles with their narrow, quasi-isotropic signal and thus for identifying R_m^{sol} (Lichtenberg *et al.* 2000).

Static light scattering and turbidity experiments reveal the value of R_e above which only small ellipsoidal or spherical micelles are present (Vinson *et al.* 1989), but do not allow a reliable differentiation between vesicles, lamellar sheets and cylindrical micelles, which may all scatter light to a considerable extent so that micelles may be present already at concentrations below that, giving rise to the maximum turbidity of the sample (Vinson *et al.* 1989; Walter *et al.* 1991; Long *et al.* 1994). Cylindrical micelles may also show hydrodynamic radii that cannot clearly be distinguished from vesicles or bilayer particles by dynamic light scattering (e.g. Garidel *et al.* 2007). This must be taken into account when R_b^{sat} or R_m^{sol} are to be estimated on the basis of light scattering measurements.

FRET between donor and acceptor probes attached to the lipids (Ollivon *et al.* 1988; da Graca-Miguel *et al.* 1989; Walter *et al.* 2000) or dehydroergosterol (as a donor to dansyl) (Wrenn *et al.* 2001) can be used to detect solubilisation. It is reduced in micelles since fewer lipids (potentially carrying an acceptor) are close to a donor in a cylindrical (one-dimensional) than in a lamellar (two-dimensional) geometry. Separation of donors from acceptors into different small micelles makes FRET impossible. Excimer formation of pyrene is enhanced right above R_b^{sat} (Ceu Rei *et al.* 2004), obviously due to a tendency of the dye to sequester in the (small fraction of) micelles. Fourier transform infrared measurements revealed the changes in chain order of surfactants and lipids upon solubilisation (Meister & Blume, 2004).

Partitioning isotherms, i.e. plots of R_e or X_e as a function of the aqueous concentration, C_S^{aq}, depend on the free energy of the surfactant in the membrane. Structural transitions may give rise to break points in the isotherm; a pseudo-phase coexistence can be identified as a range in R_e that corresponds to an almost constant C_S^{aq} (cf. Fig. 2) (Heerklotz *et al.* 1994b; Paternostre *et al.* 1995; Kragh-Hansen *et al.* 1998).

Cryo-TEM (Vinson *et al.* 1989; Walter *et al.* 1990; Edwards & Almgren, 1991; Almgren, 2000) (cf. Fig. 10) and SANS (Hjelm *et al.* 1992) are superior methods of identifying abundant aggregate structures within a certain range, but considerable expertise is essential to avoid artefacts. Suggestions from light and X-ray scattering and negative-staining electron microscopy have led to misinterpretations in the past.

4.8 Effects governing the solubilisation of fluid membranes

The fact that $C_S^{aq,sat}$ is usually only somewhat smaller than the CMC (since micelles are slightly stabilised by small available amounts of lipid) shows a direct relationship between membrane perturbation at low concentration (quantified in terms of $K_R \times \mathrm{CMC}$; cf. Section 2.7) and the onset of solubilisation:

$$R_b^{sat} \approx K_R \times \mathrm{CMC} \tag{41}$$

derived with (10) and $C_S^{aq,sat} \approx \mathrm{CMC}$ (Heerklotz & Seelig, 2000a, 2001).

The lowest R_b^{sat} published seems to be 0·012 for the synthetic lipopeptide P2A2 ($R_m^{sol} = 0{\cdot}13$, both values for POPC at 25 °C; Keller *et al.* 2005a); very strong membrane solubilisers also include the lipopeptide surfactin ($R_b^{sat} = 0{\cdot}2$; Heerklotz & Seelig, 2001, 2007), steroid-like surfactants such as bile salts (e.g. Hildebrand *et al.* 2002) and the short-chain diacyl lipid D7PC. All these compounds share a common trait in that they are anchored by more than a single alkyl

https://doi.org/10.1017/S0033583508004721 Published online by Cambridge University Press

chain to the membrane so that they can impose strong perturbations without being 'squeezed out' to a less perturbing position (see Heerklotz *et al.* 2004b). Strong 'polar head and alkyl tail' detergents exhibit typical R_b^{sat} values of $\sim 0{\cdot}5$; weak detergents initiate solubilisation only at concentrations when more than half of the molecules in the membrane are detergents ($R_b^{sat} > 1$), and others do not solubilise the membrane at all but form lamellar aggregates themselves (see Tables 1*a*–1*c* and 2).

Since solubilisation is governed by the net spontaneous curvature of the lipid/surfactant system, it is promoted with increasing positive spontaneous curvature of the surfactant and with less negative/more positive spontaneous curvature of the lipid. This is observed for surfactants with larger head groups or smaller hydrophobic parts (Partearroyo *et al.* 1996; Heerklotz *et al.* 1997) or for lipids with longer chains (increasing the mismatch) (Keller *et al.* 1997) (cf. Table 1*a*). The total concentration of TX100 required for solubilisation (at 1 mM lipid) was found to increase for lipids with lower order (probably related to more negative spontaneous curvature), caused by the addition of *cis* double bonds or changing the position of these *cis* bonds; ether and ester lipids showed no major difference (Ahyayauch *et al.* 2006). Solubilisation of DOPE, a lipid with a strong negative spontaneous curvature, requires extremely high amounts of detergent to be solubilised (e.g. $R_b^{sat} = 2{\cdot}2$ of reduced TX100; Johnsson & Bergstrand, 2004).

An increase in temperature tends to render spontaneous curvature less positive or more negative and increases R_b^{sat} typically (Otten *et al.* 1995; Heerklotz *et al.* 1997; Keller *et al.* 1997; Heerklotz, 2002). If this effect is not (over)compensated by a stronger partitioning of the surfactant into the membrane with increasing temperature (da Graca-Miguel *et al.* 1989), membrane reconstitution can also be observed as a thermotropic transition (Majhi & Blume, 2001, 2002; Heerklotz, 2002).

4.9 Transitions involving type II phases

Surfactants with a positive spontaneous curvature can convert cubic or hexagonal phases formed by type II lipids into lamellar (vesicle) systems. This has been demonstrated, for example, for the addition of reduced Triton (Johnsson & Bergstrand, 2004) and C_8Gluc (Angelov *et al.* 1999) to DOPE. Surfactants with a negative spontaneous curvature (such as $C_{12}EO_2$, Funari *et al.* 1996; and fatty acids, Winter *et al.* 1999) can convert lipid membranes into different cubic or inverse phases. The transition to inverse phases is promoted by reduced hydration (see next section) and increased temperature (Gutberlet *et al.* 1998).

4.10 Lyotropic phase behaviour

So far, lipid–surfactant systems have been treated as pseudo-binary systems, assuming that there is an excess of water and all exposed groups are fully hydrated. It is important to note that the dispersion in water is the reason that lipids and surfactants self-assemble to membranes and micelles in the first place. A complete description of the ternary system (surfactant, lipid, water) at a given temperature and pressure is possible by a triangular phase diagram. Published examples are the system $C_{12}EO_4$–POPC–D_2O (Klose *et al.* 1995), TX100–lecithin–water (Sadaghiani *et al.* 1989) and EPC–C_{16}TAC–brine and EPC–C_{12}TAC–brine (Gustafsson *et al.* 1997). Very detailed studies on water sorption to $C_{12}EO_n$ detergents are available; at 97% relative humidity, the number of water molecules adsorbed from vapour increases linearly with a slope of $\sim 2{\cdot}3$ water per EO unit between at least $n = 2$ and 7 and over a broad range of detergent contents in the

https://doi.org/10.1017/S0033583508004721 Published online by Cambridge University Press

membrane (Konig *et al.* 1997). The fact that the intercept ($n \rightarrow 0$) of ~ 8 waters/lipid is well below the value for pure POPC under these conditions, 13 water molecules per lipid, implies that the detergent causes a lower hydration of the lipid.

A number of lyotropic transitions typically occur upon dehydration. The lack of excess water tends to pack previously dispersed aggregates closer together, such as vesicles to multilamellar systems, rod-like micelles to hexagonal phases and spherical micelles to isotropic phases. Furthermore, dehydration reduces the size of the polar head groups and renders the spontaneous curvature of the molecules less positive/more negative. As a result, dehydration may freeze a fluid membrane into a gel phase, shift the boundaries of the lamellar-to-micelle transition in favour of the lamellar phase and promote inverse (type II) phases (with a negative real curvature). For example, at 97% relative humidity, POPC containing $R_e = 2$ of, e.g. $C_{12}EO_7$ and $C_{12}EO_8$ was found to be exclusively lamellar (Konig *et al.* 1997), whereas at excess water these systems would start forming micelles already at $R_e^{sat} = 0{\cdot}43$ and $0{\cdot}35$, respectively.

Even in an excess of water, the insertion of detergents into the membrane may partially dehydrate lipid head group region (Volke & Pampel, 1995; Rieber *et al.* 2007). This may be due to the increased lateral pressure in the head group region accompanying positive curvature strain (see Section 3.2) or the formation of hydrogen bonds between lipid and surfactant that replace bonds to water. Furthermore, experimental data (Volke & Pampel, 1995) and MD simulations (Schneider & Feller, 2001) implied that the EO units of $C_{12}EO_4$ in POPC membranes are partially dehydrated and localised in the hydrocarbon core. Dehydration phenomena may also contribute to the excess enthalpy of lipid–surfactant systems (Heerklotz *et al.* 1998; Schneider & Feller, 2001; Barriocanal *et al.* 2005) and the formation of compound complexes (Madler *et al.* 1994, 1998) (see Section 3.3). It is noteworthy that all these references deal with detergents including EO units.

4.11 Lipid-induced transitions of micellar structures

Because the cylinder-to-sphere transition of mixed micelles is also governed by curvature effects, lipid-saturated mixed micelles are also typically cylindrical if the pure surfactant forms spherical micelles (see Sections 0 and 0). For example, $C_{12}EO_8$ forms spherical micelles that transform to cylinders at a lipid content of about 24 mol% (Heerklotz *et al.* 1996). For $C_{12}EO_7$, 12 mol% of POPC suffice for forming cylinders (Heerklotz *et al.* 1998) and $C_{12}EO_5$ forms cylindrical micelles at room temperature even in the absence of lipid (Nilsson *et al.* 1983). The cylinder-to-sphere transition relaxes curvature strain as indicated by the quasi-sigmoidal decrease of H_E (Fig. 6, see dotted curve at $X_e \sim 0{\cdot}88$). Cylindrical micelles of lipid and bile salt were shown to decrease in length with increasing detergent content (thus increasing the proportion of the detergent-rich end caps) but keep their radius (and local composition in the body) constant (Long *et al.* 1994). It should be noted that cylindrical micelles may exhibit a minimum length so that they cannot shrink gradually to prolates and spheres but show a transition involving a cylinder–sphere co-existence. This seems to be in conflict with the traditional model of a cylinder with half-spherical end caps, but could be explained by a peanut-like shape so that end caps (and coexisting spheres) have a larger radius than the quasi-cylindrical part; for data and theory on one-component micelles, see Heerklotz *et al.* (2004a) and May & Ben-Shaul (2001).

There are also systems involving no cylindrical micelles, for example DOPE/reduced TX100; this might result from the fact that only extremely low amounts (1–6 mol% depending on pH) of DOPE can be accommodated in micelles (Johnsson & Bergstrand, 2004). The agreement of the

https://doi.org/10.1017/S0033583508004721 Published online by Cambridge University Press

lamellar–micellar phase boundaries detected by ITC with the break points of the light scattering curve for SDS–POPC mixtures suggested that 'large' (cylindrical) micelles seem to play no significant role in this system also (Keller *et al.* 2006b).

Finally, it should be noted that insertion of lipids into surfactant micelles may reduce the cloud point, i.e. the temperature above which the micellar dispersion splits into two separate phases. In Fig. 7, this is depicted by open diamonds separating L_1 and $L_1 + W$ at about 25–30 °C and high X. For a detailed study, cf. Kresheck and Mihelich (2003). The formation of small droplets of the second phase leads to a strong, transient increase in turbidity (clouding) but, typically after some hours, these droplets coalesce to form a macroscopically separate, transparent phase.

5. Applications and biological relevance of surfactant–membrane interactions

5.1 Biological effects of surfactants on membranes

Surfactants and molecules with surfactant-like properties play a role in an enormous variety of biological systems and processes, and this review can only mention a few particularly prominent examples. Classical biosurfactants are saponins (sapo is latin for soap; for a review, see Francis *et al.* 2002); they are produced by many plants and considered, possibly among other functions, part of their defence system against microbes, insects etc. They impose a variety of effects on cells and organisms, including membrane permeabilisation and complexation of cholesterol; these biological activities of saponins (e.g. digitonin) are also utilised for technical and pharmaceutical applications.

Nibbering *et al.* (2002) and references therein have discussed the relevance of mixed vesicle and micelle formation of bile salts with glycerolipids, sphingomyelins and cholesterol for proper digestion and for gallstone formation. Cholesterol nucleation for gallstone formation was related to the selective solubilisation of lecithin from lecithin–cholesterol vesicles by bile salts (Wrenn *et al.* 2001). Emulsification of lipids by bile salts may be followed by their hydrolysis by pancreatic lipase which is inhibited by lysolecithin (Tsuzuki *et al.* 2004), another biological surfactant. For recent reviews on bile salts, see Garidel *et al.* (2007) and the other articles in this special issue of 'molecules'.

Pulmonary surfactant forms highly flexible monolayers on the surface of alveoli which are a prerequisite for their surface area changes upon breathing (see Seifert *et al.* 2007 and references therein). Micro-organisms synthesise a variety of surfactants, such as glycolipids, lipopeptides and others. Such molecules could act as bioemulsifiers, increasing the bioavailability of water-insoluble substrates or regulating the attachment–detachment of micro-organisms to and from surfaces (Rosenberg & Ron, 1999).

Most antimicrobial peptides are commonly believed to act by permeabilising the membrane of the target organism. The specific mechanisms are still debated, but a detergent-like behaviour must be taken into account as one, possibly crucial effect in certain cases (Ladokhin & White, 2001; Hallock *et al.* 2003; Bechinger & Lohner, 2006; Heerklotz & Seelig, 2007). Graded leakage followed by an annealing of the membranes can be explained in terms of being induced by an asymmetric localisation of the peptide (causing, e.g. bilayer curvature strain). This has been found, for example, for transportan (Yandek *et al.* 2007), PGLa (Wieprecht *et al.* 2000) or surfactin (Heerklotz & Seelig, 2007), whereas cecropin was shown to exhibit an all-or-none leakage (Gregory *et al.* 2008). Magainin induces dye efflux from vesicles that seems to be proportional to R_b, suggesting a non-cooperative mode of action (Wieprecht *et al.* 1999). A magainin analogue,

https://doi.org/10.1017/S0033583508004721 Published online by Cambridge University Press

MSI-78, has been suggested to perturb membranes by inducing positive curvature strain (Hallock *et al.* 2003). Mellitin causes vesicle leakage at $R_b \approx 0{\cdot}02$ (Ladokhin *et al.* 1997; Ladokhin & White, 2001). Experiments using entrapped dyes of different size revealed that mellitin forms small pores in POPC membranes (Ladokhin *et al.* 1997) but larger or unspecific leaks are formed in POPC/POPG mixtures (Ladokhin & White, 2001).

Some ambiguity is caused in the literature by the fact that the term *detergent-like effects of antibiotic activity* is not clearly defined. Detergents are *not* known to form supermolecular arrangements with a fixed three-dimensional structure as expected for the barrel-stave model (Matsuzaki *et al.* 1996). A toroidal pore formed by peptides (Yang *et al.* 2001) may be formed by a specific number of peptide molecules and thus be more specific than a detergent-induced pore; both agree, however, in the topology of the pore and its formation by a molecule covering and stabilising, along with lipid, the hydrophobic edges. Virtually all other phenomena of membrane permeabilisation can possibly be induced by detergents. This includes membrane thinning and decreased mechanical stability (making the membrane vulnerable to other perturbations), bilayer couple effects, toroidal pores (line tension and monolayer curvature effects) and membrane lysis (micellisation). These phenomena may give rise to transient or steady, graded or all-or-none leakage, and possibly size selectivity and channel-like behaviour (see Section 3.6).

Some bacterial lipopeptide surfactants such as surfactin or polymyxin show also inhibitory activity against parasitic mollicutes (Beven & Wroblewski, 1997). Surfactin forms micelles, partitions into lipid vesicles and destabilises them strongly (Heerklotz & Seelig, 2001); unlike typical detergents, however, its peptide 'head group' is also partially hydrophobic so that it inserts partially into the hydrophobic core of the membrane, which may be the reason for its high activity and specific, chain-tilting effects on membrane order (Heerklotz *et al.* 2004b). A detergent-like mechanism was also proposed for the catalytic endotoxin Cyt1A (Manceva *et al.* 2005).

Whereas high concentrations of surfactants are haemolytic, low concentrations may be antihaemolytic, i.e. they inhibit hypotonic haemolysis (Isomaa *et al.* 1986; Sanchez *et al.* 2007).

Examples of other biologically relevant surfactants include lysolipids, fatty acids and acyl glycerols. An unspecific mechanism by which these and other surfactants may interfere with membrane function is the alteration of the spontaneous monolayer curvature. Biological membranes contain a variety of non-bilayer (negative spontaneous curvature) lipids that may have a variety of biological functions (for classical reviews, see Cullis & de Kruijff, 1979; Epand, 1998a, b). It was shown that different organisms regulate the spontaneous curvature of their membrane leaflets to a characteristic, negative value (Wieslander *et al.* 1980; Gruner, 1985; Bhakoo & McElhaney, 1988; Rietveld *et al.* 1994). Proteins such as protein kinase C (Giorgione *et al.* 1995) and cytidyl transferase (Davies *et al.* 2001) are activated by membranes with a negative spontaneous curvature. Kluge *et al.* (1987) showed that lysolecithin inhibits the infectivity of red clover mottle virus. LysoPC arrests exocytosis and membrane fusion (Vogel *et al.* 1993). Chernomordik *et al.* (1997, 1993) used and explained the effects of lysolipid and oleic acid on specific fusion intermediates in detail in terms of spontaneous monolayer curvature. Lysolipids also modify the mode of fusion peptide insertion into the membrane (Martin *et al.* 1993). Farge (1994) and Rauch & Farge (2000) suggested that endocytosis can be biologically regulated via the creation of a bilayer curvature strain by lipid flipases. Shape changes and vesiculation from erythrocytes upon addition of surfactants can also often be interpreted in terms of the bilayer couple model and curvature-inducing inclusions in the monolayers (Hagerstrand *et al.* 1998; Schwarz *et al.* 1999; Pantaler *et al.* 2000). Finally, curvature strains can facilitate or inhibit conformational changes in membrane proteins that change the 'effective shape' of the protein;

https://doi.org/10.1017/S0033583508004721 Published online by Cambridge University Press

examples are the photoactivation (Alves *et al.* 2005) and oligomerisation (Botelho *et al.* 2006) of rhodopsin.

Given all these biological functions that are facilitated by curvature strains and thus regulated or at least affected by biological surfactants, one should expect that organisms tend to counteract curvature effects imposed by extrinsic surfactants. This has indeed been shown impressively already by Wieslander *et al.* (1986), who demonstrated in *Acholeplasma laidlawii* that the ratio between the main negative curvature lipid, MGDG, to the positive curvature lipid, DGDG, systematically increases with increasing positive curvature of detergents (C_mEO_n with m = 12, 16 and $n = 3 - 12$) added to their medium. Lactobacilli grown in bile salt containing medium showed a strongly enhanced content of lipids with unsaturated acyl chains (Taranto *et al.* 2003), another way of relaxing positive curvature strain.

5.2 Medical and cosmetic applications of surfactants

The surfactant-like properties of antibiotic peptides were discussed in the previous section. The membrane-permeabilising activity of synthetic detergents such as nonoxynol-9, BZK and SDS are used in spermicides and topical microbicides for preventing sexually transmitted diseases (Apel-Paz *et al.* 2005). Cationic surfactants, including arginine-based lipoamino acids, show antimicrobial activity in the micromolar range which was found to be correlated with their activity to insert into lipid membranes (Castillo *et al.* 2004). Alkylphosphatidylcholines are anti-cancer agents and oral medication with $C_{16}PC$ (brand name, Miltefosine) was shown to cure leishmaniasis (see Rakotomanga *et al.* 2004 and references therein). Other drugs such as the antipsychotic chlorpromazine or the antidepressant imipramine show surfactant-like behaviour including, for instance membrane permeabilisation (see Ahyayauch *et al.* 2002 and references therein).

Of course, topical applications of surfactants have to consider the potential toxic effects of surfactants on the skin. Wei *et al.* (2006) determined the inhibitory concentrations of several technically relevant surfactants on keratinocytes. They also showed that the application of surfactants may alter the expression levels for enzymes involved in the biosynthesis of membrane components such as cholesterol, ceramides and fatty acids. A number of studies have addressed the specific properties of stratum corneum lipids interacting with surfactants (see, e.g. Cocera *et al.* 1999).

Reconstitution from mixed micelles has been a standard method for producing unilamellar vesicles of a desired size (Schubert, 2003), now primarily competing with extrusion techniques. The size of the vesicles may be chosen by adjusting the speed of detergent removal. This technique has also been used for entrapping compounds in liposomes. Lipid vesicles with a sub-solubilising content of bile salts were shown to retain an enzyme, *Micrococcus luteus* polynucleotide phosphorylase, but proved to be permeable to nucleotides (Treyer *et al.* 2002). Bile salts were used to facilitate the loading of drugs into pre-formed liposomes (Schubert *et al.* 1991).

Surfactants are also directly used in drug formulations to solubilise the drug and aid its transport across barriers. Like other membrane-active compounds, surfactants may act unspecifically as transdermal penetration enhancers (Williams & Barry, 2004). Furthermore, surfactants are an essential component of ultra-deformable liposomes (Transfersomes™) that overcome permeability barriers (such as human skin) driven by hydration energy and allow the administration of drugs into sub-dermal tissue or blood (for a review, see Cevc, 2004). Surfactants can also facilitate the transport of drugs or DNA across cell membranes. Aside from unspecific membrane permeabilisation, they may also enhance the net uptake of drugs by

https://doi.org/10.1017/S0033583508004721 Published online by Cambridge University Press

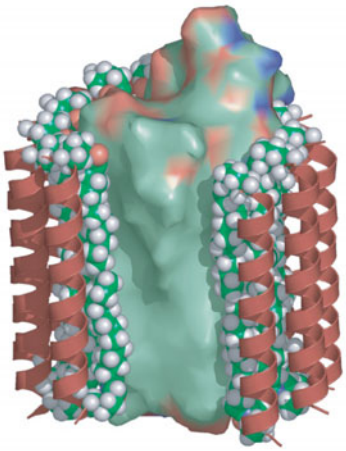

Fig. 12. Lipopeptides comprising an alpha helix with two alkyl chains attached to its ends as designed for membrane protein isolation by Privé and co-workers. Reproduced with permission from Macmillan Publishers Ltd, *Nature Biotechnology* (McGregor *et al.*), copyright 2003.

inhibiting multidrug resistance proteins (Alqawi & Georges, 2003; Seelig & Gerebtzoff, 2006). Positively charged surfactants form complexes with DNA which have lamellar or inverse hexagonal structures and can be used as vectors in gene therapy (Radler *et al.* 1997; Koltover *et al.* 1998). The dipalmitylated cationic peptide P2A2 is a specifically tailored surfactant comprising an arginine-rich, cell-penetrating peptide as a head group; it forms micellar aggregates which are internalised into living cells and solubilises lipid membranes extremely efficiently (Keller *et al.* 2005a).

5.3 Use of surfactants for the isolation and investigation of membrane proteins

The isolation and investigation of membrane proteins is an extremely complex task that requires optimisation of the protocol to the protein, to the source membrane and to the method that is to be used to study the protein. So far, only relatively few, rather empirically optimised solutions were found for specific systems.

Membrane protein studies constitute a vast field and much of it is outside the scope of this review (see instead Gohon & Popot, 2003; Rigaud & Levy, 2003; Prive, 2007). Understanding the interactions of surfactants with lipid membranes, however, is one of the prerequisites for a more rational approach. Given the complexity of the task, typical solubilisation buffers often contain not only a single surfactant but co-surfactants, co-solvents and other components that stabilise the protein. For instance, neurotensin (Grisshammer *et al.* 2005) and cannabinoid (Yeliseev *et al.* 2005) receptors can be isolated from *Escherichia coli* membranes by a buffer containing specific amounts of C_{12}Malt, CHAPS, glycerol, Tris, NaCl and cholesteryl hemisuccinate. Other approaches are based on completely new types of surfactants. McGregor *et al.* (2003) introduced lipopeptides comprising an alpha helix with two alkyl chains grafted to its ends. These specifically tailored 'surfactants' mimic quite closely the conditions of a protein in a membrane: the peptides form an oligomeric bundle surrounding the relatively ordered hydrocarbon chains (Kelly *et al.* 2005) (and, if present, the protein), the thickness of the hydrophobic part is well defined and the overall geometry is cylindrical with a minimum concentration of 'surfactant' and minimum size of the protein 'micelle' (Fig. 12). Gohon and Popot (2003) provide a brief, yet

https://doi.org/10.1017/S0033583508004721 Published online by Cambridge University Press

impressive overview over the concepts of using amphipathic peptides (peptidergents), polymers (amphipols), tripod detergents and hemifluorinated surfactants. PEG-grafted cholesterol acts as a detergent but can be enzymatically cleaved into cholesterol, a physiological membrane component, and water-soluble ethylene glycol, thus inducing reconstitution (Chopineau *et al.* 1998).

A number of the interactions of surfactants with lipid membranes discussed here belong, further to surfactant–protein interactions, to the criteria relevant to membrane protein studies (see also Lichtenberg *et al.* 2000; Ollivon *et al.* 2000). Partition coefficients and kinetics (usually governed by membrane permeability) are critical for surfactant removal. R_b^{sat} and R_m^{sol} affect the amount of surfactant needed and the amount of lipid retained in the micelles. Reconstitution of the protein into proteoliposomes can, for example be achieved by surfactant extraction (bio beads, dialysis, gel filtration), dilution or temperature changes. Membrane leakage induced by a membrane permeant co-surfactant can facilitate the complete removal of an impermeant surfactant from vesicles. Both kinetics and the affinity of the protein for micelles *versus* membranes control the homogeneity of the distribution of proteins between liposomes formed upon reconstitution. The speed of reconstitution also controls the size of the vesicles. The crystallisation of membrane proteins that are highly enriched in a certain membrane can be induced by selective solubilisation of other membrane components (Vanderkooi *et al.* 1972; Corless *et al.* 1982). Bacteriorhodopsin was crystallised upon expulsion from a cubic phase (Landau & Rosenbusch, 1996).

NMR studies suffer from the problem that the distribution of molecular orientations causes a broadening of the signals. There are two strategies to overcome this problem, isotropic averaging and macroscopic orientation, and both have been pursued using detergents. Membrane proteins that are solubilised in small micelles rotate much faster, thus giving rise to a narrower signal. A specific, macroscopic orientation is possible using so-called bicelle systems (Sanders & Landis, 1995; Sanders & Oxenoid, 2000), which are dispersions of discoidal micelles or detergent-stabilised bilayer fragments. They are made of a mixture of a bilayer-forming lipid, such as DMPC, and a detergent, typically the micelle-forming, short-chain lipid D7PC. The surfactant forms a rim around the edge of the bilayer fragment, thus screening the hydrophobic part of the bilayer from water. Comprehensive studies using a large variety of methods have supported and refined this picture (Glover *et al.* 2001; Luchette *et al.* 2001). What makes bicelles so useful is their property to align in a magnetic field (mostly with the bilayer normal preferentially perpendicular to the field). By choosing another composition (Loudet *et al.* 2005) or by addition of lanthanides, bicelles can be oriented with their bilayer normal parallel to the field. Membrane proteins inserted into such bicelles will share essentially the same orientation with respect to the field, thus yielding rather well-resolved NMR signals.

5.4 Study of detergent-resistant membrane fractions

Yu *et al.* (1973) have described already that membrane constituents could be selectively solubilised using cold TX100. Later, the hypothesis (Simons & Ikonen, 1997) that biological membranes contain lipid-based, cholesterol-dependent functional domains (referred to as 'lipid rafts') that could be isolated as the DRM fraction by cold Triton has stimulated enormous interest and research efforts. The results and models on rafts are still not fully consistent and partially controversial; they are reviewed in detail by many authors (Edidin, 2003; Munro, 2003; McMullen *et al.* 2004; Simons & Vaz, 2004; Lichtenberg *et al.* 2005; London, 2005; Jacobson *et al.* 2007) and shall not be discussed here.

https://doi.org/10.1017/S0033583508004721 Published online by Cambridge University Press

A thermodynamic background of 'detergent resistance' is that lipids preferring gel or ordered phases show a very weak partitioning into micelles so that extremely high surfactant concentrations are required to solubilise them (see Section 3.5). Whether DRMs are really obtained from a certain membrane, however, also depends on kinetic and technical aspects. Gel-like particles obtained from pure gel phases are too small to be recognised as 'resistant' by centrifugation or turbidity assays; these membranes are therefore referred to as 'not resistant'. One may hypothesise that the specific role of cholesterol (or, alternatively, ceramide; Sot *et al.* 2006) for DRM formation is not primarily to induce resistance but to render the resistant particles large enough for their detection and separation (Keller *et al.* 2005b).

It seems widely accepted now that detergent resistance should not be considered a definition or strict evidence for *in vivo* rafts (see, e.g. the new definition published by Pike, 2006) for a number of reasons. (1) It has been shown that detergents and other membrane-disordering molecules or moieties may induce domain formation in model membranes (see Section 3.5) which has also been observed in life cells (van Rheenen *et al.* 2005). The latter authors showed that the addition of 0·0025% of TX100 to HEK cells did not kill or solubilise the cells but induced the clustering of previously randomly distributed PIP_2, which has been considered a raft marker. (2) Preferential solubilisation of fluid phase-preferring lipids enhances the concentration of order-preferring lipids in the remaining unsolubilised membrane, which can induce domain formation (see Section 4.4). (3) Domains are altered if the temperature of isolation differs from the physiologically relevant temperature. (4) Lipids that are separated into different leaflets and membranes *in vivo* become mixed upon solubilisation, thus changing the structural preferences. (5) Surfactant-induced changes in line tension may induce the stabilisation and growth of critical membrane density fluctuations (which may be too short-lived to function as rafts) to macroscopic domains or 'phases'.

Some of these problems upon isolating pre-existing domains could be avoided technically if a sudden addition of detergent at high concentration separates the domains so fast that there is no time for equilibration involving a re-sorting of molecules between domains and their reorganisation (London, 2005; Staneva *et al.* 2005). This may be approximately achieved where pre-existing, macroscopic domains are concerned (as in certain model systems), but does not apply to the case when no or only nanoscopic domains are present in the respective membrane *in vivo*.

Hence, DRM isolation cannot detect the existence, size and dynamics of domains *in vivo*. It can, however, yield important information on the preferences of membrane constituents for (artificial) ordered, cholesterol-rich (cholesterol has many more effects than just ordering lipid chains) *versus* disordered domains. This means that *if* there are rafts in biological membranes that are governed by similar parameters and show similar behaviour as liquid ordered domains in model membranes, *then* DRM extraction is a method for estimating their possible contents.

6. Prospects

In spite of all the progress made in the past decades, there are many issues that remain unsolved today. New surfactants have become available that are not characterised yet. Dynamics may be crucial for applications but has been rather neglected compared to structural or thermodynamic studies so far. Thus, there is a need for ongoing fundamental work.

A major focus will be on functions and applications. After solving minor issues such as the human genome and the structure of about a thousand soluble proteins, a key task for bio-medical research has become to understand the structure, dynamics and function of membrane proteins.

https://doi.org/10.1017/S0033583508004721 Published online by Cambridge University Press

A broad, systematic and reasonably efficient tackling of this problem, however, suffers from the lack of rules for a rational choice of the optimum detergents, co-solutes and conditions for isolating a specific protein from a specific membrane environment to study the subject by a specific method. In other words, the field of surfactant–membrane interactions (which includes surfactant–lipid interactions and much more) is just turning from an exercise for pioneers and specialists into a rate-limiting step of biomedical and pharmacological progress.

Other challenges are applications of surfactant-like compounds as antimicrobial agents for topical and systemic application or the delivery of hydrophobic drugs to their target tissue. The regulation of proteins and biological processes by surfactant-induced changes in membrane properties will very likely become a much more acknowledged topic in the future, when bio-membrane studies become more feasible.

All these promising goals will warrant and stimulate substantial research efforts in the future and will require new approaches, techniques and theories. They will have to consider complex systems of surfactants, lipids, proteins and other components, and their success may depend on being truly interdisciplinary. We will learn many new things; knowing the basics might be useful anyway.

7. Symbols and abbreviations

A	area per molecule
ANS	1-anilinonaphthalene-8-sulfonic acid
ANTS	8-aminonaphthalene-1,3,6-trisulfonic acid
ASA	(water-) accessible surface area
Bet	betaine
BZK	benzalkonium chloride
C	molar concentration
C_{10}	decyl
C_{11}	undecyl
C_{12}	dodecyl
C_{12}TAB	dodecyl trimethylammoniumbromide
C_{16}SM	palmitoyl sphingomyelin
C_8-	octyl-
CAC	critical association concentration
Cer	ceramide
CF	carboxyfluorescein
Chol	cholesterol
CMC	critical micelle concentration
C_nEO_m	Oligo ethylene oxide alkyl ether, $CH_3(CH_2)_{m-1}$ $(O\text{-}CH_2\text{-}CH_2)_nOH$
C_nNO	alkyl dimethylaminoxides
C_p	heat capacity at constant p
cryo-TEM	cryo transmission electron microscopy
D7PC	diheptanoylphosphatidyl-choline
DC	deoxycholate
DHSM	dihydrosphingomyelin
DiPoPE	dipalmitoleoyl PC
DMPC	1,2-dimyristoyl-*sn*-glycero-3-phosphocholine

https://doi.org/10.1017/S0033583508004721 Published online by Cambridge University Press

DOPC	1,2-dioleoyl-*sn*-glycero-3-phosphocholine
DOPE	1,2-dioleoyl-*sn*-glycero-3-phosphoethanolamine
DPPC	1,2-dipalmitoyl-*sn*-glycero-3-phosphocholine
DPX	*p*-xylene-bis-pyridinium bromide
DRM	detergent-resistant membrane
DSC	differential scanning calorimetry
e_0	elementary charge
EO	ethylene oxide
EPC	egg yolk phosphatidylcholine
ESM	egg sphingomyelin
f	activity coefficient, see Eq. (9)
FA	fatty acid
FOSMEA	dodecyl phospho-n-methylethanolamine
G	molar Gibbs free energy
g	Gibbs free energy
GC	glycocholate
Gluc	β-glycopyranoside
H	molar enthalpy
ITC	isothermal titration calorimetry
K	partition coefficient or equilibrium constant in general
K_C	concentration-based partition coefficient, cf. Eq. (7)
K_R	mole ratio partition coefficient, Eq. (10)
K_R^{app}	apparent partition coefficient, Eq. (27)
K_X	mole fraction partition coefficient, Eq. (5)
LAM	forms lamellar phase
LUV	large unilamellar vesicles
lyso-PC	lysophosphatidylcholine
Malt	maltopyranoside
MD	molecular dynamics
n	mole number
n	number of groups such as EO, CH_2
N_A	Avogadro's constant
NaC	sodium cholate
NBD-PE	(N-(7-nitrobenz-2-oxa-1,3-diazol-4-yl)-1,2-dihexadecanoyl-*sn*-glycero-3-phosphoethanolamine
NMR	nuclear magnetic resonance
p	pressure
PC	(diacyl)phosphatidylcholine
PEG-DSPC	polyethyleneglycol-distearoylphosphatidylcholine
POPC	1-palmitoyl-2-oleoyl-*sn*-glycero-3-phosphocholine
POPE	1-palmitoyl-2-oleoyl-*sn*-glycero-3-phosphoethanolamine
POPG	1-palmitoyl-2-oleoyl-*sn*-glycero-3-[phospho-rac-(1-glycerol)]
PS	(diacyl) phosphatidylserine
PyrC	pyridinium chloride
R	general gas constant, 8·31 J/(mol K)

https://doi.org/10.1017/S0033583508004721 Published online by Cambridge University Press

R_m, R_b, R_e	mole ratio of surfactant to lipid in micelles (m), bilayers (b) or aggregates in general [e, cf. Eq. (34)]
S	in acronyms for detergents: sulphate
SANS	small-angle neutron scattering
sarc. ret. ves.	sarcoplasmatic reticulum vesicles
SBPC	soy bean phosphatidylcholine
SDS	sodium dodecyl sulphate
SDBS	dodecyl benzene sulfonate
strat. corn.	mixture of typical stratum corneum lipids
SUV	small unilamellar vesicles
T	temperature
TAC	trimethyl ammonium chloride
TGluc	Thioglycopyranoside
TX100	Triton X-100
TX114	Triton X-114
v	volume
V	molar volume
X	mole fraction
z	signed charge number
Ψ_0	surface potential
Δ	difference
α	degree of solubilisation, Eq. (36)
γ	accessibility parameter (see Section 2.5)
ε_0	permittivity of vacuum
ε_r	dielectric constant
μ	chemical potential
μ^0	standard chemical potential
ρ^0	non-ideality parameter, cf. Eq. (18)
ρ^0_H	non-ideality parameter for enthalpy, Eq. (23)
σ	surface charge density

Indices and superscripts

aq	in aqueous phase
b	in the bilayer
cyl	cylindrical micelles
E	excess
L	lipid
m	in micelles
S	surfactant
sat	at the onset of solubilisation, boundary between bilayer and bil + mic range
sol	at completion of solubilisation, boundary between bil + mic coexistence and micellar range
sph	spherical micelles
W	of water
→	of transfer, e.g. $\Delta H_S^{w\to b}$ is the molar enthalpy of transfer of surfactant from the water into the bilayer

https://doi.org/10.1017/S0033583508004721 Published online by Cambridge University Press

8. Acknowledgements

I dedicate this publication to the memory of Michel Ollivon, a great expert in lipid–detergent systems and most pleasant colleague who passed away much too soon. For valuable comments on the science and style of this manuscript, I am very much indebted to Felix Goñi, Sandro Keller, Gil Prive, Nardin Samuel and Alekos Tsamaloukas.

9. References

Ahyayauch, H., Larijani, B., Alonso, A. & Goni, F. M. (2006). Detergent solubilization of phosphatidylcholine bilayers in the fluid state: influence of the acyl chain structure. *Biochimica et Biophysica Acta – Biomembranes* **1758**, 190–196.

Ahyayauch, H., Requero, M. A., Alonso, A., Bennouna, M. & Goni, F. M. (2002). Surfactant effects of chlorpromazine and imipramine on lipid bilayers containing sphingomyelin and cholesterol. *Journal of Colloid and Interface Science* **256**, 284–289.

Almgren, M. (2000). Mixed micelles and other structures in the solubilization of bilayer lipid membranes by surfactants. *Biochimica et Biophysica Acta* **1508**, 146–163.

Almgren, M. (2007). Vesicle Transformations resulting from curvature tuning in systems with micellar, lamellar, and bicontinuous cubic phases. *Journal of Dispersion Science and Technology* **28**, 43–54.

Almog, S., Kushnir, T., Nir, S. & Lichtenberg, D. (1986). Kinetic and structural aspects of reconstitution of phosphatidylcholine vesicles by dilution of phosphatidylcholine–sodium cholate mixed micelles. *Biochemistry* **25**, 2597–2605.

Almog, S. & Lichtenberg, D. (1988). Effect of calcium on kinetic and structural aspects of dilution-induced micellar to lamellar phase transformation in phosphatidylcholine–cholate mixtures. *Biochemistry* **27**, 873–880.

Alonso, A. & Goni, F. M. (2000). Detergents in biomembrane studies. *Biochimica et Biophysica Acta* **1508**, 1–256.

Alonso, A., Saez, R. & Goni, F. M. (1982). The interaction of detergents with phospholipid vesicles: a spectrofluorimetric study. *FEBS Letters* **137**, 141–145.

Alonso, A., Urbaneja, M. A., Goni, F. M., Carmona, F. G., Cánovas, F. G. & Gómez-Fernández, J. C. (1987). Kinetic studies on the interaction of phosphatidylcholine liposomes with Triton X-100. *Biochimica et Biophysica Acta* **902**, 237–246.

Alonso, A., Villena, A. & Goni, F. M. (1981). Lysis and reassembly of sonicated lecithin vesicles in the presence of Triton X-100. *FEBS Letters* **123**, 200–204.

Alqawi, O. & Georges, E. (2003). The multidrug resistance protein ABCC1 drug-binding domains show selective sensitivity to mild detergents. *Biochemical and Biophysical Research Communications* **303**, 1135–1141.

Alves, I. D., Salgado, G. F. J., Salamon, Z., Brown, M. F., Tollin, G. & Hruby, V. J. (2005). Phosphatidylethanolamine enhances rhodopsin photoactivation and transducin binding in a solid supported lipid bilayer as determined using plasmon-waveguide resonance spectroscopy. *Biophysical Journal* **88**, 198–210.

Andelman, D., Kozlov, M. M. & Helfrich, W. (1994). Phase-transitions between vesicles and micelles driven by competing curvatures. *Europhysics Letters* **25**, 231–236.

Angelov, B., Ollivon, M. & Angelova, A. (1999). X-ray diffraction study of the effect of the detergent octyl glucoside on the structure of lamellar and nonlamellar lipid/water phases of use for membrane protein reconstitution. *Langmuir* **15**, 8225–8234.

Apel-Paz, M., Doncel, G. F. & Vanderlick, T. K. (2005). Impact of membrane cholesterol content on the resistance of vesicles to surfactant attack. *Langmuir* **21**, 9843–9849.

Arnulphi, C., Sot, J., García-Pacios, M., Arrondo, J.-L. R., Alonso, A. & Goñi, F. M. (2007). Triton X-100 partitioning into sphingomyelin bilayers at subsolubilizing detergent concentrations. Effect of lipid phase and a comparison with dipalmitoylphosphatidylcholine. *Biophysical Journal* **93**, 3504–3514.

Baker, B. M. & Murphy, K. P. (1998). Prediction of binding energetics from structure using empirical parametrization. *Methods Enzymology* **295**, 294–314.

Bakht, O., Pathak, P. & London, E. (2007). Effect of the structure of lipids favoring disordered domain formation on the stability of cholesterol-containing ordered domains (lipid rafts): identification of multiple raft-stabilization mechanisms. *Biophysical Journal* **93**, 4307–4318.

Barriocanal, L., Taylor, K. M. G. & Buckton, G. (2005). Bilayer to micelle transition of DMPC and alcohol ethoxylate surfactants as studied by isoperibol calorimetry. *Journal of Pharmaceutical Sciences* **94**, 1747–1755.

Bechinger, B. & Lohner, K. (2006). Detergent-like actions of linear amphipathic cationic antimicrobial peptides. *Biochimica et Biophysica Acta – Biomembranes* **1758**, 1529–1539.

Beck, A., Tsamaloukas, A., Jurcevic, P. & Heerklotz, H. (2008). Additive action of two or more solutes on lipid membranes. *Langmuir* 24, 8833–8840.

Beschiaschvili, G. & Seelig, J. (1992). Peptide binding to lipid bilayers. Nonclassical hydrophobic effect and

https://doi.org/10.1017/S0033583508004721 Published online by Cambridge University Press

membrane-induced p*K* shifts. *Biochemistry* **31**, 10044–10053.

Beven, L. & Wroblewski, H. (1997). Effect of natural amphipathic peptides on viability, membrane potential, cell shape and motility of mollicutes. *Research in Microbiology* **148**, 163–175.

Bhakoo, M. & McElhaney, R. N. (1988). The effect of variations in growth temperature, fatty acid composition and cholesterol content on the lipid polar head-group composition of *Acholeplasma laidlawii* B membranes. *Biochimica et Biophysica Acta* **945**, 307–314.

Bhamidipati, S. P. & Hamilton, J. A. (1995). Interactions of lyso 1-palmitoylphosphatidylcholine with phospholipids: a ^{13}C and ^{31}P NMR study. *Biochemistry* **34**, 5666–5677.

Binder, H. & Klose, G. (2002). Lyotropic phase behavior and structure of mixed lipid (POPC)–detergent ($C_{12}E_n$, $n=2$, 4, 6) assemblies: insights from hydration-tuning infrared spectroscopy. *Journal of Physical Chemistry B* **106**, 10991–11001.

Binford Jr., J. S. & Palm, W. H. (1994). Absorption of surfactants by membranes: erythrocytes *versus* synthetic vesicles. *Biophysical Journal* **66**, 2024–2028.

Botelho, A. V., Huber, T., Sakmar, T. P. & Brown, M. F. (2006). Curvature and hydrophobic forces drive oligomerization and modulate activity of rhodopsin in membranes. *Biophysical Journal* **91**, 4464–4477.

Cantor, R. S. (1999). The influence of membrane lateral pressures on simple geometric models of protein conformational equilibria. *Chemistry and Physics of Lipids* **101**, 45–56.

Carion-Taravella, B., Lesieur, S., Chopineau, J., Lesieur, P. & Ollivon, M. (2002). Phase behavior of mixed aqueous dispersions of dipalmitoylphosphatidylcholine and dodecyl glycosides: a differential scanning calorimetry and X-ray diffraction investigation. *Langmuir* **18**, 325–335.

Castillo, J. A., Pinazo, A., Carilla, J., Infante, M. R., Alsina, M. A., Haro, I. & Clapés, P. (2004). Interaction of antimicrobial arginine-based cationic surfactants with liposomes and lipid monolayers. *Langmuir* **20**, 3379–3387.

Ceu Rei, M., Coutinho, P. J. G., Castanheira, E. M. S. & Real Oliveira, M. E. C. D. (2004). $C_{12}E_7$–DPPC mixed systems studied by pyrene fluorescence emission. *Progress in Colloid and Polymer Science* **123**, 83–87.

Cevc, G. (2004). Lipid vesicles and other colloids as drug carriers on the skin. *Advanced Drug Delivery Reviews* **56**, 675–711.

Cevc, G. & Marsh, D. (1985). *Phospholipid Bilayers*. John Wiley and Sons, New York.

Chernomordik, L. V., Leikina, E., Frolov, V., Bronk, P. & Zimmerberg, J. (1997). An early stage of membrane fusion mediated by the low pH conformation of influenza hemagglutinin depends upon membrane lipids. *Journal of Cell Biology* **136**, 81–93.

Chernomordik, L. V., Vogel, S. S., Sokoloff, A., Onaran, H. O., Leikina, E. A. & Zimmerberg, J. (1993). Lysolipids reversibly inhibit Ca(2+)-, GTP- and pH-dependent fusion of biological membranes. *FEBS Letters* **318**, 71–76.

Chopineau, J., Lesieur, S., Carion-Taravella, B. & Ollivon, M. (1998). Self-evolving microstructured systems upon enzymatic catalysis. *Biochimie* **80**, 421–435.

Cocera, M., Lopez, O., Coderch, L., Parra, J. L. & de la Maza, A. (1999). Influence of the level of ceramides on the permeability of stratum corneum lipid liposomes caused by a C_{12}-betaine/sodium dodecyl sulfate mixture. *International Journal of Pharmaceutics* **183**, 165–173.

Cocera, M., Lopez, O., Coderch, L., Parra, J. L. & De La Maza, A. (2003). Permeability investigations of phospholipid liposomes by adding cholesterol. *Colloids and Surfaces A: Physicochemical and Engineering Aspects* **221**, 9–17.

Cocera, M., Lopez, O., Estelrich, J., Parra, J. L. & De la Maza, A. (2002). Adsorption of sodium lauryl ether sulfate on liposomes by means of a fluorescent probe: effect of the ethylene oxide groups. *Langmuir* **18**, 8250–8254.

Cocera, M., Lopez, O., Pons, R., Amenitsch, H. & De La Maza, A. (2004). Effect of the electrostatic charge on the mechanism inducing liposome solubilization: a kinetic study by synchrotron radiation SAXS. *Langmuir* **20**, 3074–3079.

Corless, J. M., McCaslin, D. R. & Scott, B. L. (1982). Two-dimensional rhodopsin crystals from disk membranes of frog retinal rod outer segments. *Proceedings of the National Academy of Sciences USA* **79**, 1116–1120.

Cullis, P. R. & de Kruijff, B. (1979). Lipid polymorphism and the functional roles of lipids in biological membranes. *Biochimica et Biophysica Acta* **559**, 399–420.

Cullis, P. R., Hope, M. J., Bally, M. B., Madden, T. D., Mayer, L. D. & Fenske, D. B. (1997). Influence of pH gradients on the transbilayer transport of drugs, lipids, peptides and metal ions into large unilamellar vesicles. *Biochimica et Biophysica Acta – Reviews on Biomembranes* **1331**, 187–211.

da Graca-Miguel, M., Eidelman, O., Ollivon, M. & Walter, A. (1989). Temperature dependence of the vesicle–micelle transition of egg phosphatidylcholine and octyl glucoside. *Biochemistry* **28**, 8921–8928.

Davies, S. M., Epand, R. M., Kraayenhof, R. & Cornell, R. B. (2001). Regulation of CTP: phosphocholine cytidylyltransferase activity by the physical properties of lipid membranes: an important role for stored curvature strain energy. *Biochemistry* **40**, 10522–10531.

de la Maza, A., Coderch, L., Gonzalez, P. & Parra, J. L. (1998a). Subsolubilizing alterations caused by alkyl glucosides in phosphatidylcholine liposomes. *Journal of Controlled Release* **52**, 159–168.

de la Maza, A., Lopez, O., Coderch, L. & Parra, J. L. (1998b). Solubilization of phosphatidylcholine

https://doi.org/10.1017/S0033583508004721 Published online by Cambridge University Press

liposomes by the amphoteric surfactant dodecyl betaine. *Chemistry and Physics of Lipids* **94**, 71–79.

de la Maza, A. & Parra, J. L. (1994a). Structural phase transitions involved in the interaction of phospholipid bilayers with octyl glucoside. *European Journal of Biochemistry* **226**, 1029–1038.

de la Maza, A. & Parra, J. L. (1994b). Vesicle–micelle structural transition of phosphatidylcholine bilayers and Triton X-100. *Biochemical Journal* **303**, 907–914.

de la Maza, A. & Parra, J. L. (1997). Solubilizing effects caused by the nonionic surfactant dodecylmaltoside in phosphatidylcholine liposomes. *Biophysical Journal* **72**, 1668–1675.

Demina, T., Grozdova, I., Krylova, O., Zhirnov, A., Istratov, V., Frey, H., Kautz, H. & Melik-Nubarov, N. (2005). Relationship between the structure of amphiphilic copolymers and their ability to disturb lipid bilayers. *Biochemistry* **44**, 4042–4054.

Duzgunes, N., Straubinger, R. M., Baldwin, P. A., Friend, D. S. & Papahadjopoulos, D. (1985). Proton-induced fusion of oleic acid–phosphatidylethanolamine liposomes. *Biochemistry* **24**, 3091–3098.

Edidin, M. (2003). The state of lipid rafts: from model membranes to cells. *Annual Review of Biophysics and Biomolecular Structures* **16**, 257–283.

Edwards, K. & Almgren, M. (1990). Kinetics of surfactant-induced leakage and growth of unilamellar vesicles. *Progress in Colloid and Polymer Science* **82**, 190–197.

Edwards, K. & Almgren, M. (1991). Solubilization of lecithin vesicles by $C_{12}E_8$ – structural transitions and temperature effects. *Journal of Colloid and Interface Science* **147**, 1–21.

Edwards, K., Almgren, M., Bellare, J. & Brown, W. (1989). Effects of Triton X-100 on sonicated lecithin vesicles. *Langmuir* **5**, 473–478.

Elamrani, K. & Blume, A. (1982). Incorporation kinetics of lysolecithin into lecithin vesicles. Kinetics of lysolecithin-induced vesicle fusion. *Biochemistry* **21**, 521–526.

Encinas, M. & Lissi, E. (1982). Evaluation of partition constants in compartmentalized systems from fluorescence quenching data. *Chemical Physics Letters* **91**, 55–57.

Epand, R. M. (1998a). Lipid polymorphism and membrane properties. In *Current Topics in Membranes*, vol. 44. San Diego, CA: Academic Press.

Epand, R. M. (1998b). Lipid polymorphism and protein–lipid interactions. *Biochimica et Biophysica Acta – Reviews on Biomembranes* **1376**, 353–368.

Epand, R. M. & Epand, R. F. (1994). Calorimetric detection of curvature strain in phospholipid bilayers. *Biophysical Journal* **66**, 1450–1456.

Epand, R. M., Epand, R. F. & Lancaster, C. R. (1988). Modulation of the bilayer to hexagonal phase transition of phosphatidylethanolamines by acylglycerols. *Biochimica et Biophysica Acta* **945**, 161–166.

Farge, E. (1994). Scale-dependent elastic response of closed phospholipid-bilayers to transmembrane molecular pumping activity – a key for exo-endocytosis physiological process. *Nuovo Cimento Della Societa Italiana Di Fisica D-Condensed Matter Atomic Molecular and Chemical Physics Fluids Plasmas Biophysics* **16**, 1457–1470.

Francis, G., Kerem, Z., Makkar, H. P. S. & Becker, K. (2002). The biological action of saponins in animal systems: a review. *British Journal of Nutrition* **88**, 587–605.

Fuller, N. & Rand, P. (2001). The influence of lysolipids on the intrinsic curvature and bending elasticity of phospholipid membranes. *Biophysical Journal* **80**, 2357.

Funari, S. S., Madler, B. & Rapp, G. (1996). Cubic topology in surfactant and lipid mixtures. *European Biophysics Journal* **24**, 293–299.

Funari, S. S., Nuscher, B., Rapp, G. & Beyer, K. (2001). Detergent–phospholipid mixed micelles with a crystalline phospholipid core. *Proceedings of the National Academy of Sciences USA* **98**, 8938–8943.

Galla, H. J. & Sackmann, E. (1974). Lateral diffusion in the hydrophobic region of membranes: use of pyrene excimers as optical probes. *Biochimica et Biophysica Acta* **339**, 103–115.

Gallova, J., Devinsky, F. & Balgavy, P. (1990). Interaction of surfactants with model and biological membranes. II. Effect of *N*-alkyl-*N*,*N*,*N*-trimethylammonium ions on phosphatidylcholine bilayers as studied by spin probe ESR. *Chemistry and Physics of Lipids* **53**, 231–241.

Garidel, P., Hildebrand, A., Knauf, K. & Blume, A. (2007). Membranolytic activity of bile salts: influence of biological membrane properties and composition. *Molecules* **12**, 2292–2326.

Garner, A. E., Smith, D. A. & Hooper, N. M. (2008). Visualization of detergent solubilization of membranes: implications for the isolation of rafts. *Biophysical Journal* **94**, 1326–1340.

Giorgione, J., Epand, R. M., Buda, C. & Farkas, T. (1995). Role of phospholipids containing docosahexaenoyl chains in modulating the activity of protein kinase C. *Proceedings of the National Academy of Sciences USA* **92**, 9767–9770.

Glover, K. J., Whiles, J. A., Wu, G., Yu, N., Deems, R., Struppe, J. O., Stark, R. E., Komives, E. A. & Vold, R. R. (2001). Structural evaluation of phospholipid bicelles for solution-state studies of membrane-associated biomolecules. *Biophysical Journal* **81**, 2163–2171.

Gohon, Y. & Popot, J. L. (2003). Membrane protein–surfactant complexes. *Current Opinion in Colloid and Interface Science* **8**, 15–22.

Goni, F. M., Urbaneja, M. A., Arrondo, J. L., Alonso, A., Durrani, A. A. & Chapman, D. (1986). The interaction of phosphatidylcholine bilayers with triton X-100. *European Journal of Biochemistry* **160**, 659–665.

Gonzales-Manas, J. M., Kaschny, P. & Goni, F. M. (1994). Use of Merocyanine 540 as an optical probe in

https://doi.org/10.1017/S0033583508004721 Published online by Cambridge University Press

the study of membrane–surfactant interactions. *Journal of Physical Chemistry* **98**, 10650–10654.

Gradzielski, M. (2004). Investigations of the dynamics of morphological transitions in amphiphilic systems. *Current Opinion in Colloid and Interface Science* **9**, 256–263.

Gregory, S. M., Cavenaugh, A., Journigan, V., Pokorny, A. & Almeida, P. F. (2008). A quantitative model for the all-or-none permeabilization of phospholipid vesicles by the antimicrobial peptide cecropin A. *Biophysical Journal* **94**, 1667–1680.

Grisshammer, R., White, J. F., Trinh, L. B. & Shiloach, J. (2005). Large-scale expression and purification of a G-protein-coupled receptor for structure determination – an overview. *Journal of Structural and Functional Genomics* **6**, 159–163.

Gruner, S. M. (1985). Intrinsic curvature hypothesis for biomembrane lipid composition: a role for nonbilayer lipids. *Proceedings of the National Academy of Sciences USA* **82**, 3665–3669.

Guggenheim, E. A. (1952). *Mixtures. The Theory of the Equilibrium Properties of Some Simple Classes of Mixtures, Solutions, and Alloys*. Oxford: Clarendon Press.

Gustafsson, J., Oradd, G. & Almgren, M. (1997). Disintegration of the lecithin lamellar phase by cationic surfactants. *Langmuir* **13**, 6956–6963.

Gutberlet, T., Dietrich, U., Klose, G. & Rapp, G. (1998). X-ray diffraction study of the lamellar–hexagonal phase transition in phospholipid/surfactant mixtures. *Journal of Colloid and Interface Science* **203**, 317–327.

Gutberlet, T., Kiselev, M., Heerklotz, H. & Klose, G. (2000). SANS study of mixed POPC/$C_{12}E_n$ aggregates. *Physica B* **276**, 381–383.

Hagerstrand, H., Holmstrom, T. H., Bobrowska-Hagerstrand, M., Eriksson, J. E. & Isomaa, B. (1998). Amphiphile-induced phosphatidylserine exposure in human erythrocytes. *Molecular Membrane Biology* **15**, 89–95.

Hagerstrand, H., Kralj-Iglic, V., Fosnaric, M., Bobrowska-Hagerstrand, M., Wrobel, A., Mrowczynska, L., Soderstrom, T. & Iglic, A. (2004). Endovesicle formation and membrane perturbation induced by polyoxyethyleneglycolalkylethers in human erythrocytes. *Biochimica et Biophysica Acta – Biomembranes* **1665**, 191–200.

Hallock, K. J., Lee, D. K. & Ramamoorthy, A. (2003). MSI-78, an analogue of the magainin antimicrobial peptides, disrupts lipid bilayer structure via positive curvature strain. *Biophysical Journal* **84**, 3052–3060.

Heerklotz, H. (unpublished data).

Heerklotz, H. (2001). Membrane stress and permeabilization induced by asymmetric incorporation of compounds. *Biophysical Journal* **81**, 184–195.

Heerklotz, H. (2002). Triton promotes domain formation in lipid raft mixtures. *Biophysical Journal* **83**, 2693–2701.

Heerklotz, H., Binder, H. & Lantzsch, G. (1994a). Determination of the partition coefficients of the nonionic detergent $C_{12}E_7$ between lipid-detergent mixed membranes and water by means of laurdan fluorescence spectroscopy. *Journal of Fluorescence* **4**, 349–352.

Heerklotz, H., Binder, H., Lantzsch, G. & Klose, G. (1994b). Membrane/water partition of oligo(ethylene oxide) dodecyl ethers and its relevance for solubilization. *Biochimica et Biophysica Acta* **1196**, 114–122.

Heerklotz, H., Binder, H., Lantzsch, G., Klose, G. & Blume, A. (1997). Lipid/detergent interaction thermodynamics as a function of molecular shape. *Journal of Physical Chemistry B* **101**, 639–645.

Heerklotz, H. & Epand, R. M. (2001). The enthalpy of acyl chain packing and the apparent water-accessible apolar surface area of phospholipids. *Biophysical Journal* **80**, 271–279.

Heerklotz, H., Lantzsch, G., Binder, H., Klose, G. & Blume, A. (1995). Application of isothermal titration calorimetry for detecting lipid membrane solubilization. *Chemical Physics Letters* **235**, 517–520.

Heerklotz, H., Lantzsch, G., Binder, H., Klose, G. & Blume, A. (1996). Thermodynamic characterization of dilute aqueous lipid/detergent mixtures of POPC and $C_{12}EO_8$ by means of isothermal titration calorimetry. *Journal of Physical Chemistry* **100**, 6764–6774.

Heerklotz, H. & Seelig, J. (2000a). Correlation of the membrane/water partition coefficients of detergents with the critical micelle concentration. *Biophysical Journal* **78**, 2435–2440.

Heerklotz, H. & Seelig, J. (2000b). Titration calorimetry of surfactant–membrane partitioning and membrane solubilization. *Biochimica et Biophysica Acta* **1508**, 69–85.

Heerklotz, H. & Seelig, J. (2001). Detergent-like action of the antibiotic peptide surfactin on lipid membranes. *Biophysical Journal* **81**, 1547–1554.

Heerklotz, H. & Seelig, J. (2007). Leakage and lysis of lipid membranes induced by the lipopeptide surfactin. *European Biophysics Journal* **36**, 305–314.

Heerklotz, H., Szadkowska, H., Anderson, T. & Seelig, J. (2003). The sensitivity of lipid domains to small perturbations demonstrated by the effect of triton. *Journal of Molecular Biology* **329**, 793–799.

Heerklotz, H., Tsamaloukas, A., Kita-Tokarczyk, K., Strunz, P. & Gutberlet, T. (2004a). Structural, volumetric, and thermodynamic characterization of a micellar sphere-to-rod transition. *Journal of the American Chemical Society* **126**, 16544–16552.

Heerklotz, H., Wieprecht, T. & Seelig, J. (2004b). Membrane perturbation by the lipopeptide surfactin and detergents as studied by deuterium NMR. *Journal of Physical Chemistry B* **108**, 4909–4915.

Heerklotz, H. H., Binder, H. & Epand, R. M. (1999). A 'release' protocol for isothermal titration calorimetry. *Biophysical Journal* **76**, 2606–2613.

https://doi.org/10.1017/S0033583508004721 Published online by Cambridge University Press

Heerklotz, H. H., Binder, H. & Schmiedel, H. (1998). Excess enthalpies of mixing in phospholipid-additive membranes. *Journal of Physical Chemistry B* **102**, 5363–5368.

Helenius, A. & Simons, K. (1975). Solubilization of membranes by detergents. *Biochimica et Biophysica Acta* **415**, 29–79.

Helfrich, W. (1973). Elastic properties of lipid bilayers – theory and possible experiments. *Zeitschrift fur Naturforschung C* **28**, 693–703.

Hildebrand, A., Beyer, K., Neubert, R., Garidel, P. & Blume, A. (2003). Temperature dependence of the interaction of cholate and deoxycholate with fluid model membranes and their solubilization into mixed micelles. *Colloids and Surfaces B: Biointerfaces* **32**, 335–351.

Hildebrand, A., Beyer, K., Neubert, R., Garidel, P. & Blume, A. (2004). Solubilization of negatively charged DPPC/DPPG liposomes by bile salts. *Journal of Colloid and Interface Science* **279**, 559–571.

Hildebrand, A., Neubert, R., Garidel, P. & Blume, A. (2002). Bile salt induced solubilization of synthetic phosphatidylcholine vesicles studied by isothermal titration calorimetry. *Langmuir* **18**, 2836–2847.

Hildebrand, J. H. (1929). Solubility. XII. Regular solutions. *Journal of the American Chemical Society* **51**, 66.

Hjelm, R. P., Thiyagarajan, P. & Alkanonyuksel, H. (1992). Organization of phosphatidylcholine and bile-salt in rodlike mixed micelles. *Journal of Physical Chemistry* **96**, 8653–8661.

Hoyrup, P., Davidsen, J. & Jorgensen, K. (2001). Lipid membrane partitioning of lysolipids and fatty acids: effects of membrane phase structure and detergent chain length. *Journal of Physical Chemistry B* **105**, 2649–2657.

Inoue, T., Kawamura, H., Okukado, S. & Shimozawa, R. (1994a). Characterization of molecular assemblies formed in aqueous C(10)E(7)/DPPC mixture by spin-label and fluorescence probe techniques and mechanism of micelle-to-vesicle transformation. *Journal of Colloid and Interface Science* **168**, 94–102.

Inoue, T., Miyakawa, K. & Shimozawa, R. (1986). Interaction of surfactants with vesicle membrane of dipalmitoylphosphatidylcholine – effect on gel-to-liquid-crystalline phase-transition of lipid bilayer. *Chemistry and Physics of Lipids* **42**, 261–270.

Inoue, T., Motoyama, R., Totoki, M., Miyakawa, K. & Shimozawa, R. (1994b). Molecular aggregates formed in aqueous mixtures of Poe type nonionic surfactants and phosphatidylcholines. *Journal of Colloid and Interface Science* **164**, 318–324.

Inoue, T., Yanagihara, S., Misono, Y. & Suzuki, M. (2001). Effect of fatty acids on phase behavior of hydrated dipalmitoylphosphatidylcholine bilayer: saturated *versus* unsaturated fatty acids. *Chemistry and Physics of Lipids* **109**, 117–133.

Ipsen, J. H., Karlstrom, G., Mouritsen, O. G., Wennerstrom, H. & Zuckermann, M. J. (1987). Phase equilibria in the phosphatidylcholine–cholesterol system. *Biochimica et Biophysica Acta* **905**, 162–172.

Ipsen, J. H., Mouritsen, O. G. & Zuckermann, M. J. (1989). Theory of thermal anomalies in the specific heat of lipid bilayers containing cholesterol. *Biophysical Journal* **56**, 661–667.

Isomaa, B., Hagerstrand, H., Paatero, G. & Engblom, A. C. (1986). Permeability alterations and anti-haemolysis induced by amphiphiles in human erythrocytes. *Biochimica et Biophysica Acta* **860**, 510–524.

Israelachvili, J. N. (1991). *Intermolecular and Surface Forces*, 2nd edn. London: Academic Press.

Jackson, M. L., Schmidt, C. F., Lichtenberg, D., Litman, B. J. & Albert, A. D. (1982). Solubilization of phosphatidylcholine bilayers by octyl glucoside. *Biochemistry* **21**, 4576–4582.

Jacobson, K., Mouritsen, O. G. & Anderson, R. G. W. (2007). Lipid rafts: at a crossroad between cell biology and physics. *Nature Cell Biology* **9**, 7–14.

Johnsson, M. & Bergstrand, N. (2004). Phase behavior of DOPE/TritonX100 (reduced) in dilute aqueous solution: aggregate structure and pH-dependence. *Colloids and Surfaces B: Biointerfaces* **34**, 69–76.

Johnsson, M. & Edwards, K. (2003). Liposomes, disks, and spherical micelles: aggregate structure in mixtures of gel phase phosphatidylcholines and poly(ethylene glycol)-phospholipids. *Biophysical Journal* **85**, 3839–3847.

Kadi, M., Hansson, P. & Almgren, M. (2004). Determination of isotherms for binding of surfactants to vesicles using a surfactant-selective electrode. *Journal of Physical Chemistry B* **108**, 7344–7351.

Kamp, F., Westerhoff, H. V. & Hamilton, J. A. (1993). Movement of fatty-acids, fatty-acid analogs, and bile-acids across phospholipid-bilayers – kinetics of fatty acid-mediated proton movement across small unilamellar vesicles. *Biochemistry* **32**, 11074–11086.

Kanduser, M., Fosnaric, M., Sentjurc, M., Kralj-Iglic, V., Hagerstrand, H., Iglic, A. & Miklavcic, D. (2003). Effect of surfactant polyoxyethylene glycol (C12E8) on electroporation of cell line DC3F. *Colloids and Surfaces A: Physicochemical and Engineering Aspects* **214**, 205–217.

Karatekin, E., Sandre, O. & Brochard-Wyart, F. (2003). Transient pores in vesicles. *Polymer International* **52**, 486–493.

Karlovska, J., Lohner, K., Degovics, G., Lacko, I., Devinsky, F. & Balgavy, P. (2004). Effects of non-ionic surfactants *N*-alkyl-*N*,*N*-dimethylamine-*N*-oxides on the structure of a phospholipid bilayer: small-angle X-ray diffraction study. *Chemistry and Physics of Lipids* **129**, 31–41.

Kaufmann, T. C., Engel, A. & Remigy, H. W. (2006). A novel method for detergent concentration determination. *Biophysical Journal* **90**, 310–317.

Keller, M., Kerth, A. & Blume, A. (1997). Thermodynamics of interaction of octyl glucoside with phosphatidylcholine vesicles: partitioning and solubilization

https://doi.org/10.1017/S0033583508004721 Published online by Cambridge University Press

as studied by high sensitivity titration calorimetry. *Biochimica et Biophysica Acta* **1326**, 178–192.

Keller, S., Bothe, M., Bienert, M., Dathe, M. & Blume, A. (2007). A simple fluorescence-spectroscopic membrane translocation assay. *ChemBioChem* **8**, 546–552.

Keller, S., Heerklotz, H. & Blume, A. (2006a). Monitoring lipid membrane translocation of sodium dodecyl sulfate by isothermal titration calorimetry. *Journal of the American Chemical Society* **128**, 1279–1286.

Keller, S., Heerklotz, H., Jahnke, N. & Blume, A. (2006b). Thermodynamics of lipid membrane solubilization by sodium dodecyl sulfate. *Biophysical Journal* **90**, 4509–4521.

Keller, S., Sauer, I., Strauss, H., Gast, K., Dathe, M. & Bienert, M. (2005a). Membrane-mimetic nanocarriers formed by a dipalmitoylated cell-penetrating peptide. *Angewandte Chemie – International Edition* **44**, 5252–5255.

Keller, S., Tsamaloukas, A. & Heerklotz, H. (2005b). A quantitative model describing the selective solubilization of membrane domains. *Journal of the American Chemical Society* **127**, 11469–11476.

Kelly, E., Prive, G. G. & Tieleman, D. P. (2005). Molecular models of lipopeptide detergents: large coiled-coils with hydrocarbon interiors. *Journal of the American Chemical Society* **127**, 13446–13447.

Klose, G., Eisenblatter, S. & Konig, B. (1995). Ternary phase-diagram of mixtures of palmitoyl-oleoyl-phosphatidylcholine, tetraoxyethylene dodecyl ether, and heavy-water as seen by ^{31}P and ^{2}H NMR. *Journal of Colloid and Interface Science* **172**, 438–446.

Klose, G., Islamov, A., Konig, B. & Cherezov, V. (1996). Structure of mixed multilayers of palmitoyloleoylphosphatidylcholine and oligo(oxyethylene glycol) monododecyl ether determined by X-ray and neutron diffraction. *Langmuir* **12**, 409–415.

Klose, G. & Levine, Y. K. (2000). Membranes of palmitoyloleoylphosphatidylcholine and $C_{12}E_4$ – a lattice model simulation. *Langmuir* **16**, 671–676.

Klose, G., Madler, B., Schafer, H. & Schneider, K. P. (1999). Structural characterization of POPC, and $C_{12}E_4$ in their mixed membranes at reduced hydration by solid state ^{2}H NMR. *Journal of Physical Chemistry B* **103**, 3022–3029.

Kluge, S., Gawrisch, K. & Nuhn, P. (1987). Loss of infectivity of red clover mottle virus by lysolecithin. *Acta Virology* **31**, 185–188.

Koltover, I., Salditt, T., Radler, J. O. & Safinya, C. R. (1998). An inverted hexagonal phase of cationic liposome–DNA complexes related to DNA release and delivery. *Science* **281**, 78–81.

Konig, B., Dietrich, U. & Klose, G. (1997). Hydration and structural properties of mixed lipid/surfactant model membranes. *Langmuir* **13**, 525–532.

Kozlov, M. M., Lichtenberg, D. & Andelman, D. (1997). Shape of phospholipid/surfactant mixed micelles: cylinders or disks? Theoretical analysis. *Journal of Physical Chemistry B* **101**, 6600–6606.

Kragh-Hansen, U., le Maire, M. & Moller, J. V. (1998). The mechanism of detergent solubilization of liposomes and protein-containing membranes. *Biophysical Journal* **75**, 2932–2946.

Kresheck, G. C. & Mihelich, J. (2003). Observation of complex thermal transitions for mixed micelle solutions containing alkyldimethylphosphine oxides and phospholipids and the accompanying cloud points. *Chemistry and Physics of Lipids* **123**, 45–62.

Kresheck, G. C. & Nimsgern, R. A. (1983). Unusual enthalpy changes which accompany the titration of dimyristoylphosphatidylcholine vesicles with Triton X-100. *Chemistry and Physics of Lipids* **33**, 55–65.

Ladokhin, A. S., Selsted, M. E. & White, S. H. (1997). Sizing membrane pores in lipid vesicles by leakage of co-encapsulated markers: pore formation by melittin. *Biophysical Journal* **72**, 1762–1766.

Ladokhin, A. S. & White, S. H. (2001). 'Detergent-like' permeabilization of anionic lipid vesicles by melittin. *Biochimica et Biophysica Acta* **1514**, 253–260.

Ladokhin, A. S., Wimley, W. C. & White, S. H. (1995). Leakage of membrane vesicle contents: determination of mechanism using fluorescence requenching. *Biophysical Journal* **69**, 1964–1971.

Landau, E. M. & Rosenbusch, J. P. (1996). Lipidic cubic phases: a novel concept for the crystallization of membrane proteins. *Proceedings of the National Academy of Sciences USA* **93**, 14532–14535.

Lantzsch, G., Binder, H., Heerklotz, H., Wendling, M. & Klose, G. (1996). Surface areas and packing constraints in POPC/$C_{12}EO_n$ membranes. A time-resolved fluorescence study. *Biophysical Chemistry* **58**, 289–302.

Lasch, J. (1995). Interaction of detergents with lipid vesicles. *Biochimica et Biophysica Acta* **1241**, 269–292.

Lasch, J., Hoffmann, J., Omelyanenko, W. G., Klibanov, A. A., Torchilin, V. P., Binder, H. & Gawrisch, K. (1990). Interaction of Triton X-100 and octyl glucoside with liposomal membranes at sublytic and lytic concentrations. Spectroscopic studies. *Biochimica et Biophysica Acta* **1022**, 171–180.

le Maire, M., Champeil, P. & Moller, J. V. (2000). Interaction of membrane proteins and lipids with solubilizing detergents. *Biochimica et Biophysica Acta* **1508**, 86–111.

le Maire, M., Moller, J. V. & Champeil, P. (1987). Binding of a nonionic detergent to membranes: flip-flop rate and location on the bilayer. *Biochemistry* **26**, 4803–4810.

Lemmich, J., Richter, F. & Callisen, T. H. (1998). Structural studies on equimolar suspensions of palmitic acid and 1-lyso-palmitoyl-phosphatidylcholine. *Material Research Society Symposium Proceedings* **489**, 125–130.

Leng, J., Egelhaaf, S. U. & Cates, M. E. (2003). Kinetics of the micelle-to-vesicle transition: aqueous

https://doi.org/10.1017/S0033583508004721 Published online by Cambridge University Press

lecithin–bile salt mixtures. *Biophysical Journal* **85**, 1624–1646.

Lesieur, S., Grabielle-Madelmont, C., Menager, C., Cabuil, V., Dadhi, D., Pierrot, P. & Edwards, K. (2003). Evidence of surfactant-induced formation of transient pores in lipid bilayers by using magnetic-fluid-loaded liposomes. *Journal of American Chemical Society* **125**, 5266–5267.

Lichtenberg, D. (1985). Characterization of the solubilization of lipid bilayers by surfactants. *Biochimica et Biophysica Acta* **821**, 470–478.

Lichtenberg, D. (1993). Micelles and liposomes. In *Biomembranes – Physical Aspects* (ed. M. Shinitzky), pp. 63–96. Weinheim: VCH.

Lichtenberg, D., Goni, F. M. & Heerklotz, H. (2005). Detergent-resistant membranes should not be identified with membrane rafts. *Trends in Biochemical Sciences* **30**, 430–436.

Lichtenberg, D., Opatowski, E. & Kozlov, M. M. (2000). Phase boundaries in mixtures of membrane-forming amphiphiles and micelle-forming amphiphiles. *Biochimica et Biophysica Acta* **1508**, 1–19.

Lichtenberg, D., Robson, R. J. & Dennis, E. A. (1983). Solubilization of phospholipids by detergents. Structural and kinetic aspects. *Biochimica et Biophysica Acta* **737**, 285–304.

London, E. (2005). How principles of domain formation in model membranes may explain ambiguities concerning lipid raft formation in cells. *Biochimica et Biophysica Acta – Molecular Cell Research* **1746**, 203–220.

Long, M. A., Kaler, E. W. & Lee, S. P. (1994). Structural characterization of the micelle–vesicle transition in lecithin–bile salt solutions. *Biophysical Journal* **67**, 1733–1742.

Lopez, O., Cocera, M., de la Maza, A., Coderch, L. & Parra, J. L. (2000). Different stratum corneum lipid liposomes as models to evaluate the effect of the sodium dodecyl sulfate. *Biochimica et Biophysica Acta* **1508**, 196–209.

Lopez, O., de la Maza, A., Coderch, L., Lopez-Iglesias, C., Wehrli, E. & Parra, J. L. (1998). Direct formation of mixed micelles in the solubilization of phospholipid liposomes by Triton X-100. *FEBS Letters* **426**, 314–318.

Loudet, C., Khemtemourian, L., Aussenac, F., Gineste, S., Achard, M. F. & Dufourc, E. J. (2005). Bicelle membranes and their use for hydrophobic peptide studies by circular dichroism and solid state NMR. *Biochimica et Biophysica Acta – General Subjects* **1724**, 315–323.

Luchette, P. A., Vetman, T. N., Prosser, R. S., Hancock, R. E., Nieh, M. P., Glinka, C. J., Krueger, S. & Katsaras, J. (2001). Morphology of fast-tumbling bicelles: a small angle neutron scattering and NMR study. *Biochimica et Biophysica Acta* **1513**, 83–94.

Madler, B., Binder, H. & Klose, G. (1998). Compound complex formation in phospholipid membranes induced by a nonionic surfactant of the oligo(ethylene oxide) alkyl ether type: a comparative DSC and FTIR study. *Journal of Colloid and Interface Science* **202**, 124–138.

Madler, B., Klose, G., Mops, A., Richter, W. & Tschierske, C. (1994). Thermotropic phase behaviour of the pseudobinary mixture DPPC/$C_{12}E_4$ at excess water. *Chemistry and Physics of Lipids* **71**, 1–12.

Majhi, P. R. & Blume, A. (2001). Thermodynamic characterization of temperature-induced micellization and demicellization of detergents studied by differential scanning calorimetry. *Langmuir* **17**, 3844–3851.

Majhi, P. R. & Blume, A. (2002). Temperature-induced micelle–vesicle transitions in DMPC–SDS and DMPC–DTAB mixtures studied by calorimetry and dynamic light scattering. *Journal of Physical Chemistry B* **106**, 10753–10763.

Manceva, S. D., Pusztai-Carey, M., Russo, P. S. & Butko, P. (2005). A detergent-like mechanism of action of the cytolytic toxin Cyt1A from *Bacillus thuringiensis* var. *israelensis*. *Biochemistry* **44**, 589–597.

Marcelino, J., Lima, J. L. F. C., Reis, S. & Matos, C. (2007). Assessing the effects of surfactants on the physical properties of liposome membranes. *Chemistry and Physics of Lipids* **146**, 94–103.

Marcotte, L., Barbeau, J., Edwards, K., Karlsson, G. & Lafleur, M. (2005a). Influence of the lipid composition on the membrane affinity, and the membrane-perturbing ability of cetylpyridinium chloride. *Colloids and Surfaces A: Physicochemical and Engineering Aspects* **266**, 51–61.

Marcotte, L., Barbeau, J. & Lafleur, M. (2005b). Permeability and thermodynamics study of quaternary ammonium surfactants – phosphocholine vesicle system. *Journal of Colloid and Interface Science* **292**, 219–227.

Martin, I., Dubois, M. C., Saermark, T., Epand, R. M. & Ruysschaert, J. M. (1993). Lysophosphatidylcholine mediates the mode of insertion of the NH_2-terminal SIV fusion peptide into the lipid bilayer. *FEBS Letters* **333**, 325–330.

Matsuzaki, K., Murase, O., Fujii, N. & Miyajima, K. (1996). An antimicrobial peptide, magainin 2, induced rapid flip-flop of phospholipids coupled with pore formation and peptide translocation. *Biochemistry* **35**, 11361–11368.

Matsuzaki, K., Sugishita, K., Ishibe, N., Ueha, M., Nakata, S., Miyajima, K. & Epand, R. M. (1998). Relationship of membrane curvature to the formation of pores by magainin 2. *Biochemistry* **37**, 11856–11863.

May, S. & Ben-Shaul, A. (2001). Molecular theory of the sphere-to-rod transition and the second CMC in aqueous micellar solutions. *Journal of Physical Chemistry B* **105**, 630–640.

Mazer, N. A., Benedek, G. B. & Carey, M. C. (1980). Quasi-elastic light-scattering-studies of aqueous biliary lipid systems – mixed micelle formation in bile-salt lecithin solutions. *Biochemistry* **19**, 601–615.

https://doi.org/10.1017/S0033583508004721 Published online by Cambridge University Press

McGregor, C. L., Chen, L., Pomroy, N. C., Hwang, P., Go, S., Chakrabartty, A. & Prive, G. G. (2003). Lipopeptide detergents designed for the structural study of membrane proteins. *Nature Biotechnology* **21**, 171–176.

McLaughlin, S. (1989). The electrostatic properties of membranes. *Annual Review of Biophysics and Biophysical Chemistry* **18**, 113–136.

McMullen, T. P. W., Lewis, R. N. A. H. & McElhaney, R. N. (2004). Cholesterol–phospholipid interactions, the liquid-ordered phase and lipid rafts in model and biological membranes. *Current Opinion in Colloid and Interface Science* **8**, 459–468.

Meagher, R. J. & Hatton, T. A. (1998). Enthalpy measurements in aqueous SDS/DTAB solutions using isothermal titration microcalorimetry. *Langmuir* **14**, 4081–4087.

Meister, A. & Blume, A. (2004). Solubilization of DMPC-d54 and DMPG-d54 vesicles with octylglucoside and sodium dodecyl sulfate studied by FT-IR spectroscopy. *Physical Chemistry Chemical Physics* **6**, 1551–1556.

Meister, A., Kerth, A. & Blume, A. (2004a). The interaction of *n*-nonyl-beta-D-glucopyranoside and sodium dodecyl sulfate with DMPC and DMPG monolayers studied by infrared reflection absorption spectroscopy. *Physical Chemistry Chemical Physics* **6**, 5543–5550.

Meister, A., Kerth, A. & Blume, A. (2004b). Interaction of sodium dodecyl sulfate with dimyristoyl-*sn*-glycero-3-phosphocholine monolayers studied by infrared reflection absorption spectroscopy. A new method for the determination of surface partition coefficients. *Journal of Physical Chemistry B* **108**, 8371–8378.

Moschetta, A., Frederik, P. M., Portincasa, P., VanBerge-Henegouwen, G. P. & Van Erpecum, K. J. (2002). Incorporation of cholesterol in sphingomyelin–phosphatidylcholine vesicles has profound effects on detergent-induced phase transitions. *Journal of Lipid Research* **43**, 1046–1053.

Mui, B. L., Dobereiner, H. G., Madden, T. D. & Cullis, P. R. (1995). Influence of transbilayer area asymmetry on the morphology of large unilamellar vesicles. *Biophysical Journal* **69**, 930–941.

Munro, S. (2003). Lipid rafts: elusive or illusive? *Cell* **115**, 377–388.

Nagle, J. F. & Tristram-Nagle, S. (2000). Structure of lipid bilayers. *Biochimica et Biophysica Acta* **1469**, 159–195.

Nernst, W. (1891). Verteilung eines Stoffes zwischen zwei Lösungsmitteln und zwischen Lösungsmittel und Dampfraum. *Zeitschrift Physikalische Chemie* **8**, 110.

Nibbering, C. P., Frederik, P. M., Van Berge-Henegouwen, G. P., Van Veen, H. A., Van Marle, J. & Van Erpecum, K. J. (2002). Different interactions of egg-yolk phosphatidylcholine and sphingomyelin with detergent bile salts. *Biochimica et Biophysica Acta – Molecular and Cell Biology of Lipids* **1583**, 213–220.

Nicolini, C., Thiyagarajan, P. & Winter, R. (2004). Small-scale composition fluctuations and microdomain formation in lipid raft models as revealed by small-angle neutron scattering. *Physical Chemistry Chemical Physics* **6**, 5531–5534.

Nilsson, P. G., Wennerstrom, H. & Lindman, B. (1983). Structure of micellar solutions of non-ionic surfactants – nuclear magnetic-resonance self-diffusion and proton relaxation studies of poly(ethylene oxide) alkyl ethers. *Journal of Physical Chemistry* **87**, 1377–1385.

Nyholm, T. & Slotte, J. P. (2001). Comparison of Triton X-100 penetration into phosphatidylcholine and sphingomyelin mono- and bilayers. *Langmuir* **17**, 4724–4730.

Ollila, F. & Slotte, J. P. (2002). Partitioning of Triton X-100, deoxycholate and $C_{10}EO_8$ into bilayers composed of native and hydrogenated egg yolk sphingomyelin. *Biochimica et Biophysica Acta* **1564**, 281–288.

Ollivon, M., Eidelman, O., Blumenthal, R. & Walter, A. (1988). Micelle–vesicle transition of egg phosphatidylcholine and octyl glucoside. *Biochemistry* **27**, 1695–1703.

Ollivon, M., Lesieur, S., Grabielle-Madelmont, C. & Paternostre, M. (2000). Vesicle reconstitution from lipid–detergent mixed micelles. *Biochimica et Biophysica Acta* **1508**, 34–50.

Opatowski, E., Kozlov, M. M. & Lichtenberg, D. (1997a). Partitioning of octyl glucoside between octyl glucoside/phosphatidylcholine mixed aggregates and aqueous media as studied by isothermal titration calorimetry. *Biophysical Journal* **73**, 1448–1457.

Opatowski, E., Lichtenberg, D. & Kozlov, M. M. (1997b). The heat of transfer of lipid and surfactant from vesicles into micelles in mixtures of phospholipid and surfactant. *Biophysical Journal* **73**, 1458–1467.

Otten, D., Brown, M. F. & Beyer, K. (2000). Softening of membrane bilayers by detergents elucidated by deuterium NMR spectroscopy. *Journal of Physical Chemistry B* **104**, 12119–12129.

Otten, D., Lobbecke, L. & Beyer, K. (1995). Stages of the bilayer–micelle transition in the system phosphatidylcholine-C(12)E(8) as studied by deuterium-NMR and phosphorus-NMR, light-scattering, and calorimetry. *Biophysical Journal* **68**, 584–597.

Pantaler, E., Kamp, D. & Haest, C. W. (2000). Acceleration of phospholipid flip-flop in the erythrocyte membrane by detergents differing in polar head group and alkyl chain length. *Biochimica et Biophysica Acta* **1509**, 397–408.

Partearroyo, M. A., Alonso, A., Goni, F. M., Tribout, M. & Paredes, S. (1996). Solubilization of phospholipid bilayers by surfactants belonging to the Triton X series: effect of polar group size. *Journal of Colloid and Interface Science* **178**, 156–159.

Paternostre, M., Meyer, O., Grabielle-Madelmont, C., Lesieur, S., Ghanam, M. & Ollivon, M. (1995). Partition coefficient of a surfactant between aggregates and solution: application to the micelle–vesicle

https://doi.org/10.1017/S0033583508004721 Published online by Cambridge University Press

transition of egg phosphatidylcholine and octyl beta-D-glucopyranoside. *Biophysical Journal* **69**, 2476–2488.

Paternostre, M. T., Roux, M. & Rigaud, J. L. (1988). Mechanisms of membrane protein insertion into liposomes during reconstitution procedures involving the use of detergents. 1. Solubilization of large unilamellar liposomes (prepared by reverse-phase evaporation) by triton X-100, octyl glucoside, and sodium cholate. *Biochemistry* **27**, 2668–2677.

Patra, S. K., Alonso, A., Arrondo, J. L. R. & Goni, F. M. (1999). Liposomes containing sphingomyelin and cholesterol: detergent solubilization and infrared spectroscopic studies. *Journal of Liposome Research* **9**, 247–260.

Patra, S. K., Alonso, A. & Goni, F. M. (1998). Detergent solubilisation of phospholipid bilayers in the gel state: the role of polar and hydrophobic forces. *Biochimica et Biophysica Acta* **1373**, 112–118.

Pfeiffer, H., Klose, G., Heremans, K. & Glorieux, C. (2006). Thermotropic phase behaviour of the pseudo-binary mixtures of DPPC/$C_{12}E_5$ and DMPC/$C_{12}E_5$ determined by differential scanning calorimetry and ultrasonic velocimetry. *Chemistry and Physics of Lipids* **139**, 54–67.

Pike, L. J. (2006). Rafts defined: a report on the Keystone symposium on lipid rafts and cell function. *Journal of Lipid Research* **47**, 1597–1598.

Prenner, E. J., Lewis, R. N., Jelokhani-Niaraki, M., Hodges, R. S. & McElhaney, R. N. (2001). Cholesterol attenuates the interaction of the antimicrobial peptide gramicidin S with phospholipid bilayer membranes. *Biochimica et Biophysica Acta* **1510**, 83–92.

Prive, G. G. (2007). Detergents for the stabilization and crystallization of membrane proteins. *Methods* **41**, 388–397.

Radler, J. O., Koltover, I., Salditt, T. & Safinya, C. R. (1997). Structure of DNA–cationic liposome complexes: DNA intercalation in multilamellar membranes in distinct interhelical packing regimes. *Science* **275**, 810–814.

Rakotomanga, M., Loiseau, P. M. & Saint-Pierre-Chazalet, M. (2004). Hexadecylphosphocholine interaction with lipid monolayers. *Biochimica et Biophysica Acta – Biomembranes* **1661**, 212–218.

Rand, P., Fuller, N. & Chen, Z. S. (1998). Measuring spontaneous curvature and bending moduli of membrane lipid layers. *Biophysical Journal* **74**, A27–A27.

Rauch, C. & Farge, E. (2000). Endocytosis switch controlled by transmembrane osmotic pressure and phospholipid number asymmetry. *Biophysical Journal* **78**, 3036–3047.

Record Jr., M. T., Anderson, C. F. & Lohman, T. M. (1978). Thermodynamic analysis of ion effects on the binding and conformational equilibria of proteins and nucleic acids: the roles of ion association or release, screening, and ion effects on water activity. *Quarterly Reviews of Biophysics* **11**, 103–178.

Redlich, O. & Kister, A. (1948). Algebraic representation of thermodynamic properties and the classification of solutions. *Industrial and Engineering Chemistry* **40**, 345–348.

Ribeiro, A. A. & Dennis, E. A. (1975). Proton magnetic resonance relaxation studies on the structure of mixed micelles of Triton X-100 and dimyristoylphosphatidylcholine. *Biochemistry* **14**, 3746–3755.

Rieber, K., Sykora, J., Olzynska, A., Jelinek, R., Cevc, G. & Hof, M. (2007). The use of solvent relaxation technique to investigate head group hydration and protein binding of simple and mixed phosphatidylcholine/surfactant bilayer membranes. *Biochimica et Biophysica Acta – Biomembranes* **1768**, 1050–1058.

Rietveld, T. G., Chupin, V. V., Koorengevel, M. C., Wienk, H. L. J., Dowhan, W. & De Kruijff, B. (1994). Regulation of lipid polymorphism is essential for the viability of phosphatidylethanolamine-deficient *Escherichia coli* cells. *Journal of Biological Chemistry* **269**, 28670–28675.

Rigaud, J. L. & Levy, D. (2003). Reconstitution of membrane proteins into liposomes. *Methods in Enzymology* **372**, 65–86.

Rosenberg, E. & Ron, E. Z. (1999). High- and low-molecular-mass microbial surfactants. *Applied Microbiology and Biotechnology* **52**, 154–162.

Roth, Y., Opatowski, E., Lichtenberg, D. & Kozlov, M. M. (2000). Phase behavior of dilute aqueous solutions of lipid–surfactant mixtures: effects of finite size of micelles. *Langmuir* **16**, 2052–2061.

Rowe, E. S., Zhang, F., Leung, T. W., Parr, J. S. & Guy, P. T. (1998). Thermodynamics of membrane partitioning for a series on *n*-alcohols determined by titration calorimetry: role of hydrophobic effects. *Biochemistry* **37**, 2430–2440.

Ruiz, J., Goni, F. M. & Alonso, A. (1988). Surfactant-induced release of liposomal contents – a survey of methods and results. *Biochimica et Biophysica Acta* **937**, 127–134.

Sadaghiani, A. S., Khan, A. & Lindman, B. (1989). Liquid crystallinity of lecithin systems. Ternary phase diagrams of lecithin–water with Triton X-100 and decanol. *Journal of Colloid and Interface Science* **132**, 352–363.

Saez-Cirion, A., Alonso, A., Goni, F. M., McMullen, T. P. W., McElhaney, R. N. & Rivas, E. A. (2000). Equilibrium and kinetic studies of the solubilization of phospholipid–cholesterol bilayers by $C_{12}E_8$. The influence of the lipid phase structure. *Langmuir* **16**, 1960–1968.

Saitoh, A., Takiguchi, K., Tanaka, Y. & Hotani, H. (1998). Opening-up of liposomal membranes by talin. *Proceedings of the National Academy of Sciences USA* **95**, 1026–1031.

Sanchez, L., Martinez, V., Infante, M. R., Mitjans, M. & Vinardell, M. P. (2007). Hemolysis and antihemolysis

https://doi.org/10.1017/S0033583508004721 Published online by Cambridge University Press

induced by amino acid-based surfactants. *Toxicology Letters* **169**, 177–184.

Sanders, C. R. & Landis, G. C. (1995). Reconstitution of membrane proteins into lipid-rich bilayered mixed micelles for NMR studies. *Biochemistry* **34**, 4030–4040.

Sanders, C. R. & Oxenoid, K. (2000). Customizing model membranes and samples for NMR spectroscopic studies of complex membrane proteins. *Biochimica et Biophysica Acta* **1508**, 129–145.

Schneider, M. J. & Feller, S. E. (2001). Molecular dynamics simulations of a phospholipid–detergent mixture. *Journal of Physical Chemistry B* **105**, 1331–1337.

Schnitzer, E., Kozlov, M. M. & Lichtenberg, D. (2005). The effect of cholesterol on the solubilization of phosphatidylcholine bilayers by the non-ionic surfactant Triton X-100. *Chemistry and Physics of Lipids* **135**, 69–82.

Schubert, R. (2003). Liposome preparation by detergent removal. *Methods in Enzymology* **367**, 46–70.

Schubert, R., Wolburg, H., Schmidt, K. H. & Roth, H. J. (1991). Loading of preformed liposomes with high trapping efficiency by detergent-induced formation of transient membrane holes. *Chemistry and Physics of Lipids* **58**, 121–129.

Schurholz, T. (1996). Critical dependence of the solubilization of lipid vesicles by the detergent CHAPS on the lipid composition. Functional reconstitution of the nicotinic acetylcholine receptor into preformed vesicles above the critical micellization concentration. *Biophysical Chemistry* **58**, 87–96.

Schurtenberger, P., Mazer, N. & Känzig, W. (1985). Micelle to vesicle transition in aqueous solutions of bile salt and lecithin. *Journal of Physical Chemistry* **89**, 1042–1049.

Schwarz, S., Haest, C. W. & Deuticke, B. (1999). Extensive electroporation abolishes experimentally induced shape transformations of erythrocytes: a consequence of phospholipid symmetrization? *Biochimica et Biophysica Acta* **1421**, 361–379.

Seelig, A. & Gerebtzoff, G. (2006). Enhancement of drug absorption by noncharged detergents through membrane and P-glycoprotein binding. *Expert Opinion on Drug Metabolism and Toxicology* **2**, 733–752.

Seelig, J. (1997). Titration calorimetry of lipid–peptide interactions. *Biochimica et Biophysica Acta* **1331**, 103–116.

Seelig, J. & Ganz, P. (1991). Non-classical hydrophobic effect in membrane binding equilibria. *Biochemistry* **30**, 9354–9359.

Seifert, M., Breitenstein, D., Klenz, U., Meyer, M. C. & Galla, H. J. (2007). Solubility *versus* electrostatics: what determines lipid/protein interaction in lung surfactant. *Biophysical Journal* **93**, 1192–1203.

Sharp, K. A., Nicholls, A., Fine, R. F. & Honig, B. (1991). Reconciling the magnitude of the microscopic and macroscopic hydrophobic effects. *Science* **252**, 106–109.

Sheetz, M. P. & Singer, S. J. (1974). Biological membranes as bilayer couples. A molecular mechanism of drug–erythrocyte interactions. *Proceedings of the National Academy of Sciences USA* **71**, 4457–4461.

Simes, S. I., Marques, C. M., Cruz, M. E. M., Cevc, G. & Martins, M. B. F. (2004). The effect of cholate on solubilisation and permeability of simple and protein-loaded phosphatidylcholine/sodium cholate mixed aggregates designed to mediate transdermal delivery of macromolecules. *European Journal of Pharmaceutics and Biopharmaceutics* **58**, 509–519.

Simons, K. & Ikonen, E. (1997). Functional rafts in cell membranes. *Nature* **387**, 569–572.

Simons, K. & Vaz, W. L. (2004). Model systems, lipid rafts, and cell membranes. *Annual Review of Biophysics and Biomolecular Structures* **33**, 269–295.

Small, D. M. (1970). Surface and bulk interactions of lipids and water with a classification of biologically active lipids based on these interactions. *Federation Proceedings* **29**, 1320–1326.

Small, D. M. (1986). *The Physical Chemistry of Lipids*. New York: Plenum Press.

Sot, J., Bagatolli, L. A., Goni, F. M. & Alonso, A. (2006). Detergent-resistant, ceramide-enriched domains in sphingomyelin/ceramide bilayers. *Biophysical Journal* **90**, 903–914.

Sot, J., Collado, M. I., Arrondo, J. L. R., Alonso, A. & Goni, F. M. (2002). Triton X-100-resistant bilayers: effect of lipid composition and relevance to the raft phenomenon. *Langmuir* **18**, 2828–2835.

Spolar, R. S., Ha, J. H. & Record Jr., M. T. (1989). Hydrophobic effect in protein folding and other noncovalent processes involving proteins. *Proceedings of the National Academy of Sciences USA* **86**, 8382–8385.

Staneva, G., Seigneuret, M., Koumanov, K., Trugnan, G. & Angelova, M. I. (2005). Detergents induce raft-like domains budding and fission from giant unilamellar heterogeneous vesicles: a direct microscopy observation. *Chemistry and Physics of Lipids* **136**, 55–66.

Tamba, Y., Tanaka, T., Yahagi, T., Yamashita, Y. & Yamazaki, M. (2004). Stability of giant unilamellar vesicles and large unilamellar vesicles of liquid-ordered phase membranes in the presence of Triton X-100. *Biochimica et Biophysica Acta – Biomembranes* **1667**, 1–6.

Tan, A. M., Ziegler, A., Steinbauer, B. & Seelig, J. (2002). Thermodynamics of sodium dodecyl sulfate partitioning into lipid membranes. *Biophysical Journal* **83**, 1547–1556.

Tanford, C. (1980). *The Hydrophobic Effect: Formation of Micelles and Biological Membranes*, 2nd edn. New York: Wiley.

Taranto, M. P., Fernandez Murga, M. L., Lorca, G. & De Valdez, G. F. (2003). Bile salts and cholesterol induce changes in the lipid cell membrane of *Lactobacillus reuteri*. *Journal of Applied Microbiology* **95**, 86–91.

https://doi.org/10.1017/S0033583508004721 Published online by Cambridge University Press

THURMOND, R. L., OTTEN, D., BROWN, M. F. & BEYER, K. (1994). Structure and packing of phosphatidylcholines in lamellar and hexagonal liquid–crystalline mixtures with a nonionic detergent – a wide-line deuterium and P-31 NMR-study. *Journal of Physical Chemistry* **98**, 972–983.

TREYER, M., WALDE, P. & OBERHOLZER, T. (2002). Permeability enhancement of lipid vesicles to nucleotides by use of sodium cholate: basic studies and application to an enzyme-catalyzed reaction occurring inside the vesicles. *Langmuir* **18**, 1043–1050.

TSAMALOUKAS, A., SZADKOWSKA, H. & HEERKLOTZ, H. (2006). Nonideal mixing in multicomponent lipid/detergent systems. *Journal of Physics Condensed Matter* **18**, S1125–S1138.

TSAMALOUKAS, A., SZADKOWSKA, H., SLOTTE, P. J. & HEERKLOTZ, H. (2005). Interactions of cholesterol with lipid membranes and cyclodextrin characterized by calorimetry. *Biophysical Journal* **89**, 1109–1119.

TSAMALOUKAS, A. D., KELLER, S. & HEERKLOTZ, H. (2007). Uptake and release protocol for assessing membrane binding and permeation by way of isothermal titration calorimetry. *Nature Protocols* **2**, 695–704.

TSUZUKI, W., UE, A., NAGAO, A., ENDO, M. & ABE, M. (2004). Inhibitory effect of lysophosphatidylcholine on pancreatic lipase-mediated hydrolysis in lipid emulsion. *Biochimica et Biophysica Acta – Molecular and Cell Biology of Lipids* **1684**, 1–7.

UENO, M. (1989). Partition behavior of a nonionic detergent, octyl glucoside, between membrane and water phases, and its effect on membrane permeability. *Biochemistry* **28**, 5631–5634.

UENO, M., HIROTA, N., KASHIWAGI, H. & SAGASAKI, S. (2003). Process of destruction of large unilamellar vesicles by a nonionic detergent, octylglucoside, and size growth factor in vesicle formation from phospholipid–detergent mixed micelles. *Colloid and Polymer Science* **282**, 69–75.

VALPUESTA, J. M., ARRONDO, J. L., BARBERO, M. C., PONS, M. & GONI, F. M. (1986). Membrane-surfactant interactions. The role of surfactant in mitochondrial complex III–phospholipid–Triton X-100 mixed micelles. *Journal of Biological Chemistry* **261**, 6578–6584.

VAN DAM, L., KARLSSON, G. & EDWARDS, K. (2004). Direct observation and characterization of DMPC/DHPC aggregates under conditions relevant for biological solution NMR. *Biochimica et Biophysica Acta – Biomembranes* **1664**, 241–256.

VAN DEN BRINK-VAN DER LAAN, E., ANTOINETTE KILLIAN, J. & DE KRUIJFF, B. (2004). Nonbilayer lipids affect peripheral and integral membrane proteins via changes in the lateral pressure profile. *Biochimica et Biophysica Acta – Biomembranes* **1666**, 275–288.

VAN RHEENEN, J., MULUGETA ACHAME, E., JANSSEN, H., CALAFAT, J. & JALINK, K. (2005). PIP(2) signaling in lipid domains: a critical re-evaluation. *EMBO Journal* **24**, 1664–1673.

VANDERKOOI, G., SENIOR, A. E., CAPALDI, R. A. & HAYASHI, H. (1972). Biological membrane structure. 3. The lattice structure of membranous cytochrome oxidase. *Biochimica et Biophysica Acta* **274**, 38–48.

VIGUERA, A. R., GONZALEZMANAS, J. M., TANEVA, S. & GONI, F. M. (1994). Early and delayed stages in the solubilization of purple membrane by a polyoxyethylenic surfactant. *Biochimica et Biophysica Acta – Biomembranes* **1196**, 76–80.

VINSON, P. K., TALMON, Y. & WALTER, A. (1989). Vesicle–micelle transition of phosphatidylcholine and octyl glucoside elucidated by cryo-transmission electron-microscopy. *Biophysical Journal* **56**, 669–681.

VIRIYAROJ, A., KASHIWAGI, H. & UENO, M. (2005). Process of destruction of large unilamellar vesicles by a zwitterionic detergent, CHAPS: partition behavior between membrane and water phases. *Chemical and Pharmaceutical Bulletin* **53**, 1140–1146.

VOGEL, S. S., LEIKINA, E. A. & CHERNOMORDIK, L. V. (1993). Lysophosphatidylcholine reversibly arrests exocytosis and viral fusion at a stage between triggering and membrane merger. *Journal of Biological Chemistry* **268**, 25764–25768.

VOLKE, F. & PAMPEL, A. (1995). Membrane hydration and structure on a subnanometer scale as seen by high resolution solid state nuclear magnetic resonance: POPC and POPC/$C_{12}EO_4$ model membranes. *Biophysical Journal* **68**, 1960–1965.

WALTER, A., KUEHL, G., BARNES, K. & VANDERWAERDT, G. (2000). The vesicle-to-micelle transition of phosphatidylcholine vesicles induced by nonionic detergents: effects of sodium chloride, sucrose and urea. *Biochimica et Biophysica Acta* **1508**, 20–33.

WALTER, A., VINSON, P. K., KAPLUN, A. & TALMON, Y. (1991). Intermediate structures in the cholate–phosphatidylcholine vesicle micelle transition. *Biophysical Journal* **60**, 1315–1325.

WALTER, A., VINSON, P. K. & TALMON, Y. (1990). Cryo-TEM reveals structural transitions of egg pc and sodium cholate mixtures. *Biophysical Journal* **57**, A476–A476.

WANG, H., NIEH, M. P., HOBBIE, E. K., GLINKA, C. J. & KATSARAS, J. (2003). Kinetic pathway of the bilayered-micelle to perforated-lamellae transition. *Physical Review E* **67**, art. no.-060902.

WASSALL, S. R., BRZUSTOWICZ, M. R., SHAIKH, S. R., CHEREZOV, V., CAFFREY, M. & STILLWELL, W. (2004). Order from disorder, corralling cholesterol with chaotic lipids: the role of polyunsaturated lipids in membrane raft formation. *Chemistry and Physics of Lipids* **132**, 79–88.

WEI, T., GEIJER, S., LINDBERG, M., BERNE, B. & TORMA, H. (2006). Detergents with different chemical properties induce variable degree of cytotoxicity and mRNA expression of lipid-metabolizing enzymes and

https://doi.org/10.1017/S0033583508004721 Published online by Cambridge University Press

differentiation markers in cultured keratinocytes. *Toxicology in Vitro* **20**, 1387–1394.

Wenk, M. & Seelig, J. (1997a). Vesicle–micelle transformation of phosphatidylcholine/octyl-β-D-glucopyranoside mixtures as detected with titration calorimetry. *Journal of Physical Chemistry B* **101**, 5224–5231.

Wenk, M. R., Alt, T., Seelig, A. & Seelig, J. (1997). Octyl-beta-D-glucopyranoside partitioning into lipid bilayers: thermodynamics of binding and structural changes of the bilayer. *Biophysical Journal* **72**, 1719–1731.

Wenk, M. R. & Seelig, J. (1997b). Interaction of octyl-beta-thioglucopyranoside with lipid membranes. *Biophysical Journal* **73**, 2565–2574.

Wieprecht, T., Apostolov, O., Beyermann, M. & Seelig, J. (2000). Membrane binding and pore formation of the antibacterial peptide PGLa: thermodynamic and mechanistic aspects. *Biochemistry* **39**, 442–452.

Wieprecht, T., Beyermann, M. & Seelig, J. (1999). Binding of antibacterial magainin peptides to electrically neutral membranes: thermodynamics and structure. *Biochemistry* **38**, 10377–10387.

Wieprecht, T., Beyermann, M. & Seelig, J. (2002). Thermodynamics of the coil-alpha-helix transition of amphipathic peptides in a membrane environment: the role of vesicle curvature. *Biophysical Chemistry* **96**, 191–201.

Wieslander, A., Christiansson, A., Rilfors, L. & Lindblom, G. (1980). Lipid bilayer stability in membranes. Regulation of lipid composition in *Acholeplasma laidlawii* as governed by molecular shape. *Biochemistry* **19**, 3650–3655.

Wieslander, A., Rilfors, L. & Lindblom, G. (1986). Metabolic changes of membrane lipid composition in *Acholeplasma laidlawii* by hydrocarbons, alcohols, and detergents: arguments for effects on lipid packing. *Biochemistry* **25**, 7511–7517.

Williams, A. C. & Barry, B. W. (2004). Penetration enhancers. *Advanced Drug Delivery Reviews* **56**, 603–618.

Wimley, W. C. & White, S. H. (1993). Membrane partitioning: distinguishing effects from the hydrophobic effect. *Biochemistry* **32**, 6307–6312.

Winter, R., Erbes, J., Templer, R. H., Seddon, J. M., Syrykh, A., Warrender, N. A. & Rapp, G. (1999). Inverse bicontinuous cubic phases in fatty acid/phosphatidylcholine mixtures: the effects of pressure and lipid composition. *Physical Chemistry Chemical Physics* **1**, 887–893.

Wrenn, S. P., Gudheti, M., Veleva, A. N., Kaler, E. W. & Lee, S. P. (2001). Characterization of model bile using fluorescence energy transfer from dehydroergosterol to dansylated lecithin. *Journal of Lipid Research* **42**, 923–934.

Yandek, L. E., Pokorny, A., Floren, A., Knoelke, K., Langel, U. & Almeida, P. F. F. (2007). Mechanism of the cell-penetrating peptide transportan 10 permeation of lipid bilayers. *Biophysical Journal* **92**, 2434–2444.

Yang, L., Harroun, T. A., Weiss, T. M., Ding, L. & Huang, H. W. (2001). Barrel-stave model or toroidal model? A case study on melittin pores. *Biophysical Journal* **81**, 1475–1485.

Yegutkin, G. G. (1997). Effect of increasing concentrations of non-ionic detergent Triton X-100 on solubilization and structure of rat liver and adipose plasma membranes. *Membrane and Cell Biology* **10**, 515–520.

Yeliseev, A. A., Wong, K. K., Soubias, O. & Gawrisch, K. (2005). Expression of human peripheral cannabinoid receptor for structural studies. *Protein Science* **14**, 2638–2653.

Yu, J., Fishman, D. A. & Steck, T. L. (1973). Selective solubilization of proteins and phospholipids from red blood cell membranes by nonionic detergents. *Journal of Supramolecular Structures* **3**, 233–247.

https://doi.org/10.1017/S0033583508004721 Published online by Cambridge University Press